Opportunistic Spectrum Utilization for Vehicular Communication Networks

by

Nan Cheng

A thesis
presented to the University of Waterloo
in fulfillment of the
thesis requirement for the degree of
Doctor of Philosophy
in
Electrical and Computer Engineering

Waterloo, Ontario, Canada, 2016

I hereby declare that I am the sole author of this thesis. This is a true copy of the thesis, including any required final revisions, as accepted by my examiners.

I understand that my thesis may be made electronically available to the public.

Abstract

Recently, vehicular networks (VANETs), has become the key technology of the next-generation intelligent transportation systems (ITS). By incorporating wireless communication and networking capabilities into automobiles, information can be efficiently and reliably disseminated among vehicles, road side units, and infrastructure, which enables a number of novel applications enhancing the road safety and providing the drivers/passengers with an information-rich environment.

With the development of mobile Internet, people want to enjoy the Internet access in vehicles just as anywhere else. This fact, along with the soaring number of connected vehicles and the emerging data-craving applications and services, has led to a problem of spectrum scarcity, as the current spectrum bands for VANETs are difficult to accommodate the increasing mobile data demands. In this thesis, we aim to solve this problem by utilizing extra spectrum bands, which are not originally allocated for vehicular communications. In this case, the spectrum usage is based on an opportunistic manner, where the spectrum is not available if the primary system is active, or the vehicle is outside the service coverage due to the high mobility. We will analyze the features of such *opportunistic spectrum*, and design efficient protocols to utilize the spectrum for VANETs.

Firstly, the application of cognitive radio technologies in VANETs, termed CR-VANETs, is proposed and analyzed. In CR-VANETs, the channel availability is severely affected by the street patterns and the mobility features of vehicles. Therefore, we theoretically analyze the channel availability in urban scenario, and obtain its statistics. Based on the knowledge of channel availability, an efficient channel access scheme for CR-VANETs is then designed and evaluated. Secondly, using WiFi to deliver mobile data, named WiFi offloading, is employed to deliver the mobile data on the road, in order to relieve the burden of the cellular networks, and provide vehicular users with a cost-effective data pipe. Using queueing theory, we analyze the offloading performance with respect to the vehicle mobility model and the users' QoS preferences. Thirdly, we employ device-to-device (D2D) communications in VANETs to further improve the spectrum efficiency. In a vehicular D2D (V-D2D) underlaying cellular network, proximate vehicles can directly communicate with each other with a relatively small transmit power, rather than traversing the base station. Therefore, many current transmissions can co-exist on one spectrum resource block. By utilizing the spatial diversity, the spectrum utilization is greatly enhanced. We study the performance of the V-D2D underlaying cellular network, considering the vehicle mobility and the street pattern. We also investigate the impact of the preference of D2D/cellular mode on the interference and network throughput, and obtain the theoretical results.

In summary, the analysis and schemes developed in this thesis are useful to understand the future VANETs with heterogeneous access technologies, and provide important guidelines for designing and deploying such networks.

Acknowledgements

First I would like to express my deep and sincere gratitude to my supervisor Prof. Xuemin Shen for his endless help in my Ph.D. study and life in University of Waterloo. His valuable instructions and patient guides in research, enthusiastic encouragements, and positive philosophy in life and social relationship has offered me great help and benefits during my program, without which this thesis would not be possible. He has dedicated himself for tens of years for mentoring and helping his students to a better career. I feel like to have Professor Shen supervising and guiding me in pursuing a professional career.

I would like to thank Professor Mohamed O. Damen, Professor Catherine Rosenberg, Professor Liping Fu, and Professor Ben Liang, for serving my thesis/oral defence committee. Their valuable comments and insightful questions have significantly improved the presentation of my work. I would also like to thank Professor Weihua Zhuang for helping me to build the knowledge base from her courses, which greatly benefits my research in this thesis.

In the past four years, the precious friendship, help, and support from BBCR members offered me an unforgettable period of life. I am grateful for time spent with Dr. Ning Lu, Dr. Ning Zhang, Dr. Kuan Zhang, Dr. Haibo Zhou, Wenchao Xu, Dr. Hassan Omar, Dr. Hao Liang, Dr. Tom H. Luan, Dr. Miao Wang, Ran Zhang, Dr. Zhongming Zheng, Dr. Yi Zhou, Dr. Xiugang Wu, and many others. I also wish to give my gratitude to Dr. Lei Lei, Dr. Chengzhe Lai, Dr. Tingting Yang, Dr. Yongkang Liu, Dr. Khadige Abboud, Dr. Bong Jun Choi, Dr. Kamal Malekshan, Dr. Zhou Su, and Dr. Kan Zheng, for their advice and help in the Ph.D. pursuit. I would like to specially thank every member in VANET group, for the valuable meetings and discussions we had together, which really benefit my research works a lot.

Finally, I would like to thank my family for all their constant love, support, and encouragement, without whom it would not be possible to finish my Ph.D. study.

Nan Cheneg

June 1, 2016

Waterloo, Ontario, Canada

Table of Contents

List of Tables

List of Figures

Chapter 1

Introduction

Vehicular networks play an increasingly important role in both enhancing the road safety and offering vehicular users mobile data services. However, the exponential growth of the vehicle-related data demand lead to a problem of spectrum scarcity. To solve the problem and accommodate the ever-increasing data demand, more spectrum bands are expected to be utilized for vehicular networks. These spectrum resources, unlike the dedicated spectrum band for vehicular communications, can only be utilized in an opportunistic manner. According to whether the spectrum band is licensed for a certain system or free for use, there are different spectrum utilization technologies. Specifically, the licensed spectrum bands can be utilized for the vehicular users by CR technology and D2D communication, while the free spectrum resource can usually be accessed by the WiFi technologies. In this chapter, we provide an overview of the vehicular networks, followed by the elaboration of the spectrum scarcity problem. Finally, we present the three key enabling technologies for vehicular users to exploit opportunistic spectrum bands.

1.1 Overview of Vehicular Networks

As an indispensable part of modern life, motor vehicles have continued to evolve since people expect more than just vehicle quality and reliability. With the rapid development of information and communication technologies, equipping automobiles with wireless communication capabilities is the frontier in the evolution to the next generation intelligent transportation systems (ITS). In the last decade, the emerging VehiculAr NETworks (VANETs) have attracted much interest from both academia and industry, and significant progress has been made. VANETs are envisioned to improve road safety and efficiency

and provide Internet access on the move, by incorporating wireless communication and informatics technologies into the transportation system. VANETs can facilitate a myriad of attractive applications, which are usually divided into two main categories: safety applications (e.g., collision avoidance, safety warnings, and remote vehicle diagnostic [4,5]) and infotainment applications (e.g., file downloading, web browsing, and audio/video streaming [6,7]). To support these various applications, the U.S. Federal Communication Commission (FCC) has allocated totally 75 MHz in the 5.9 GHz band for Dedicated Short Range Communications (DSRC), based on the legacy of IEEE 802.11 standards (WiFi). On the other hand, the car manufacturers, suppliers and research institutes in Europe have initialed the Car-to-Car Communication Consortium (C2C-CC) with the main objective of utilizing inter-vehicle communication to increase road safety and efficiency. IEEE has also developed IEEE 1609 family, which consists of standards for wireless access in vehicular environments (WAVE).

Unlike most mobile ad hoc networks studied in the literature, VANETs present unique characteristics, which impose distinguished challenges on networking. i) *Potential large scale*: VANETs are extremely large-scale mobile networks, which can extend over the entire road network with a great amount of vehicles and roadside units; ii) *High mobility:* the movement of vehicles make the environment in which the VANET operators extremely dynamic. On highways, vehicle speed of over 150 km/h may occur, while in the city, the speed may exceed 60 km/h while the node density may be very high, especially during rush hour; iii) *Partitioned network:* the high mobility of vehicles may lead to large inter-vehicle distance in sparse scenarios, and thus the network is usually partitioned, consisting of isolated clusters of nodes; iv) *Network topology and connectivity:* the scenario of VANETs is very dynamic because vehicles are constantly moving and changing their position. Therefore, the network topology changes very often and the links between vehicles connect and disconnect frequently. In addition, the links are also affected by the unstable outdoor wireless channels; v) *Varied applications:* applications of VANETs are of a large variety and with different quality of service (QoS) requirements. All these features dramatically complicate network protocol design, implementation and performance evaluation.

VANETs basically consist of three types of communication paradigms, i.e., vehicle-to-vehicle (V2V) communications, vehicle-to-roadside (V2R) communications, and vehicle-to-infrastructure (V2I) communications [8], as shown in Fig. 1.1. Installed with on-board units (OBUs), vehicles can communicate with each other in ad hoc manner without the assistance of any built infrastructure, which is referred to as V2V communications. By disseminating information such as location, speed, and emergency warning messages to nearby vehicles using V2V communications, VANETs can support varied applications such as public safety applications, vehicular traffic coordination, road traffic management [9],

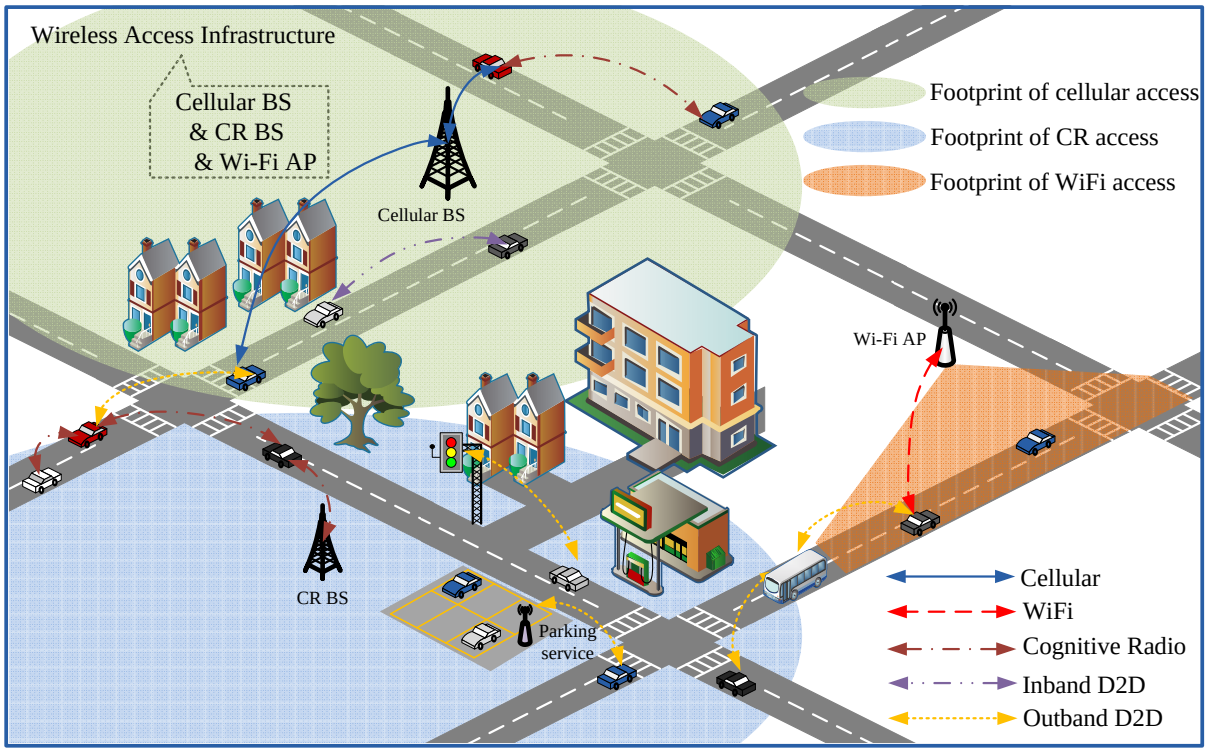

Figure 1.1: An overview of vehicular networks and available communication spectrum bands.

and some comfort applications (e.g., interactive gaming, and file sharing), etc [10, 11]. In February 2014, the U.S. Department of Transportation announced that it would begin to take steps to enable V2V communication technology for light vehicles by early 2017. V2R communication refers to the communication between the road-side units (RSUs) and nearby vehicles, which mainly aims to provide high-rate communication links to enhance the road safety. Communications between vehicles and Internet-access infrastructure are referred to as V2I communications. Internet access has become an essential part of people's daily life, and thus is required anywhere and anytime. It is evidenced that the demand for high-speed mobile Internet services has increased dramatically [12]. Providing high-rate Internet access for vehicles can not only meet the ever-increasing Internet data demand of travelers, such as multi-media services, but also enrich some safety-related applications, such as intelligent anti-theft and tracking [13], online vehicle diagnosis [14], and so forth. We will elaborate the three communication paradigms in the following part.

Motivated by the vision and prospect of VANETs, both the academia, industry and

government institutions have done numerous activities. A review of past and ongoing related programs and projects in USA, Japan and Europe can be seen in [4]. The standards of VANETs is reviewed in [9]. There are also a lot of research works on VANETs, which have been surveyed in papers such as [4] and [15].

1.1.1 V2V, V2R, and V2I Communication

In VANETs, the network connectivity is supported by three categories of communications, i.e., V2V, V2R, and V2I communications, respectively. Each of them has distinctive features, enables the connectivity among different entities, and owns different targets. In the sequel, we will introduce the three communication paradigms, respectively.

V2V Communication

V2V communication refers to the inter-vehicle traffic transmit through single-hop or multi-hop communications. Via V2V communication, the information generated by in-vehicle computers, sensors, controlling system, and passengers can be efficiently disseminated to one or a group of vehicles. Therefore, V2V communication is envisioned as a key technology to the future road transportation system, since it can facilitate a series of important related applications which can enhance road safety and efficiency. For instance, the lane change message can be delivered to the surrounding vehicles as a warning message to avoid potential collision. Other examples include collision warning, approaching emergency vehicle notice, work zone warning, and so forth. In addition, V2V wireless link can also enable infotainment applications among vehicles, such as video/audio streaming, interactive gaming, file sharing, etc.

Almost all the applications rely on the reliable data transmissions among vehicles. Unfortunately, establishing an efficient and reliable wireless V2V link is a challenging topic in VANETs, and has attracted much attention. This is due to the following reasons. First, the high mobility of vehicles leads to fast-changing network topology. Since usually the range of V2V links is small due to the power limitation, V2V communication may suffer from frequent link breakage. Second, the high mobility also results in a more complex fading environment, such as fast fading and Doppler effects [16]. Plus, the V2V line-of-sight (LOS) path is often blocked by buildings and large vehicles. These factors will lead to severe wireless loss. Last but not least, due to the social-behavior based mobility, network dynamic, and limited V2V communication range, network partition may happen, resulting in data traffic disconnections among partitions of the network. In the literature, many

related work analyzing and enhancing the connectivity of V2V communications can be found [17–20].

V2R Communication

V2R communication refers to a communication paradigm where the RSUs and nearby vehicles communicate with each other through one-hop high rate transmission links. V2R connectivity is important to maintain high-rate communication in heavy traffic, mitigate the road accidents, and improve the road efficiency. The RSUs can be ITS infrastructure which provides ITS services. For example, traffic lights, roadside sensors, and street signs can be equipped with transmitters and carry out ITS functions such as traffic monitoring, traffic information collection, vehicle path planing, etc [21–23]. Alternatively, the RSUs can also be deployed by content providers, which offer the proximate vehicles with rich-information services, such as video-on-demand, store flyer broadcasting, news subscription, and so forth [6]. Different from V2I communication where the communication infrastructure provides Internet access to vehicles, RSUs can also offer local services without Internet access.

V2I Communication

In VANETs, V2I communication is responsible for providing vehicles with Internet access, as the infrastructure, such as cellular based stations and WiFi access points, is connected to the backbone networks. The demand for high-speed mobile Internet services has increased dramatically. A recent survey reveals that Internet access is predicted to be a standard feature of future motor vehicles [12]. Passengers in vehicle want to be connected as at home or office, and may require varied Internet services such as web surfing, email, online game, audio and video streaming, among others.

As two candidates for offering V2I communication, cellular network and WiFi technology have different features. Cellular networks, like most popular LTE and LTE-A networks, is widely deployed to provide seamless Internet connectivity, especially in urban areas. Therefore, through cellular networks, vehicular users can enjoy the Internet services at any time and location. Due to the high availability of cellular networks, many industry solutions choose cellular technology for the vehicular Internet access. Car Connectivity Consortium, an organization aiming to incorporate information and communication technology (ICT) into automobile, has proposed a technology called *MirrorLink* for in-vehicle Internet access [24]. By means of MirrorLink, driver or passengers can connected the smart phone to

the vehicle, such that the vehicle can gain Internet access through the smart phone's cellular services. Besides, using the vehicle built-in cellular modules is an alternative options. The typical products include BMW ConnectedDrive [25] and GM OnStar [26].

A shortcoming of cellular network is the prohibit usage cost, which is not feasible for very data-incentive VANETs applications, such as smart vehicle data upload and software update. An alternative option for vehicular Internet is through WiFi wireless access technologies, which can provides high rate access at low cost. The feasibility of outdoor Internet access through WiFi at vehicular speeds has been demonstrated in [27], which is referred to as *drive-thru Internet*. We will elaborate drive-thru Internet in Chapter 2 and Chapter 4.

1.1.2 Wireless Access Standards in VANETs

In VANETs, there are two main standards for wireless access, which are Dedicated Short-Range Communication (DSRC) and Wireless Access in Vehicular Environments (WAVE). In the sequel, we will introduce the two standards.

Dedicated Short-Range Communications (DSRC)

DSRC is a short-range communication technology designed to support V2V and V2R communications. The aim of DSRC is to provide high-rate and low latency communication for vehicles to support a wide range of VANETs applications, including the dissemination of V2V safety message, traffic information, toll information, and so forth. In 1999, Federal Communications Commission (FCC) allocated a 75 MHz spectrum band at 5.9 GHz for DSRC. In 2003, The American Society for Testing and Materials (ASTM) approved ASTM-DSRC standard [28], which is based on IEEE 802.11a standard. In 2004, FCC established the rules governing the use of DSRC band. The spectrum band is divided into seven channels, each with 10 MHz. Among them, one channel is reserved for safety message transmission only, while the others channels can transmit both safety messages and non-safety messages. On these channels, safety messages have a higher priority over non-safety messages in order to guarantee the reliability of safety applications. A more detailed discussion on DSRC can be found in [28, 29].

IEEE 802.11p/WAVE

DRSC standard specified by ASTM in 2003 is based on IEEE 802.11a protocol, with traditional MAC operations not well suited to vehicular environment. For example, the multiple handshakes required to establish connections will bring unacceptable overhead and latency in VANETs, since the encountering time of vehicles may be very short due to the high mobility [30]. To address the issues, the IEEE 802.11 working group modified the DSRC standard, and renamed it to IEEE 802.11p Wireless Access in Vehicular Environments (WAVE). In WAVE, the MAC and physical layer protocols are defined in 802.11p, while the upper layer functions are defined in IEEE 1609 standards.

The standardization of wireless access in VANETs has received wide attention from government, industry and academia. Many efforts have been made to bring the promising technology to fruition. The study of characterizing and enhancing the performance of DSRC/WAVE can be found in [5, 16, 29, 31, 32].

1.1.3 Initiatives and Projects of VANETs

Motivated by the potentials of VANETs, many countries, organizations, and companies have taken various efforts to develop the protocols and standardization, conduct extensive simulations and practical measurements, and demonstrate the real-life deployment of VANETs. Most of the efforts were taken in US, European Union, and Japan. In US, the DSRC/WAVE standards were defined in 2004, which specifies the MAC/PHY layer protocols and upper layer operations of wireless access in VANETs. In Intelligent Vehicle Initiative (IVI), technologies were developed to help reduce the severity of traffic accident. In EU, the C2C-CC aimed to contribute to the EU VANETs standards, i.e., European Telecommunications Standards Institute: Technical Committee: Intelligent Transport Systems (ETSI TC ITS), and validate the V2V and V2I communications. Cooperative Vehicles and Infrastructure Systems (CVIS) tested the V2V and V2I technologies, and develop standards, in order to increase the road safety. In Japan, the Advanced Safety Vehicle Program, supported by the Japan government and automobile manufacturers, took initials to enhance the road safety from the perspective of both active safety and passive safety. A more comprehensive study of such efforts can be found in [33].

1.2 Spectrum Scarcity in VANETs

As introduced above, FCC has allocated 75 MHz spectrum to DSRC, and wireless wide area network (WWAN) can be a practical and seamless way to provide Internet connectivity to vehicles [34], such as off-the-shelf 3G and 4G-LTE cellular networks. However, VANETs still face the problem of spectrum scarcity, which has been demonstrated in [35]. The primary reasons of spectrum scarcity might be: 1) the ever-increasing data intensive applications, such as high-quality video streaming and user generated content (UGC), require a large amount of spectrum resources, and thereby the quality of service (QoS) is difficult to satisfy merely by the dedicated bandwidth; 2) the number of connected vehicles and devices is soaring, and thus the requirement for communication bandwidth increases dramatically. In urban environments, the spectrum scarcity is more severe due to high vehicle density, especially in some places where the vehicle density is much higher than normal [11, 36].

Mobile data demands: People tend to require richer contents when they are static as well as on the road. The types of services required by people in the car have turned from simple GPS, navigation, in-car phone and email to more various services, featuring multimedia applications such as video/audio streaming, UGC upload and sharing, online gaming, web surfing, etc. It is predicted that over two-third of the global mobile data traffic will be video by 2018. These multimedia applications often require heavy communication bandwidth, for example, the size of a typical high definition movie is 5.93 GB while an Android game may need 1.8 GB download/upload to play [37]. In addition, it is reported that the average speed of mobile connection will surpass 2 Mbps by 2016, and the smartphones will generate 2.7 GB of data traffic on average per month.

Connected vehicles and devices: There are two types of entities in VANETs that generate and consume data. The first type is connected vehicles that integrated with Internet access capability and services. It is predicted that the percentage of Internet-integrated vehicle services will jump from 10% today to 90% by 2020 [38]. The connected vehicles can offer a number of integrated services to drivers (e.g., real-time navigation, driver assistance, online diagnosis, etc.) as well as to passengers (e.g., e-mails, video on demand, etc.). The other type of entities are the mobile terminals of in-vehicle passengers. It is reported that the connected mobile devices have become more than the world's population by the end of 2013. Mobile users expect to be connected anywhere and anytime, even when they are traveling in vehicles.

Cellular communication technologies can provide reliable and ubiquitous Internet access services and deliver data traffic for VANETs. Although 4G cellular technologies such as

LTE-A have extremely efficient physical and MAC layer protocols, the cellular network nowadays is straining to meet the current mobile data demand [39]; on the other hand, the explosive growth of mobile data traffic is no end in sight, resulting in an increasingly severe overload problem. Consequently, simply using cellular infrastructure for vehicle Internet access may worsen the overload problem, and degrade the service performance of both non-vehicular and vehicular users. In summary, the dedicated 75 MHz spectrum and the cellular network may not be sufficient to provide a huge number of vehicular users (VUs) with high-quality services, and thus other solutions are required.

1.3 Opportunistic Spectrum Utilization for VANETs

Since the spectrum bands of DSRC and the cellular network are not sufficient to support the ever-increasing vehicular mobile data demand, one intuitive way to solve the problem is seeking for other available spectrum bands. In fact, through certain technologies, many other spectrum bands can be utilized for VANETs. Since these bands are not originally allocated to VANETs, they are utilized in an opportunistic manner, and therefore we can these spectrum bands as "*opportunistic spectrum bands*" for VANETs. In the thesis, we focus on utilizing these opportunistic spectrum bands for VANETs, and the key enabling technologies correspondingly.

The three enabling technologies we study in the thesis are cognitive radio, WiFi, and device-to-device communications. Employing these technologies, both licensed spectrum bands (e.g., TV broadcasting bands) and unlicensed spectrum bands (e.g., ISM bands) can then be exploited for VANETs data services. The available opportunistic spectrum bands and enabling technologies are shown in Fig. 1.1.

Cognitive radio (CR) is envisioned as a promising spectrum-sharing technology which enables unlicensed users opportunistically exploit spatially and/or temporally vacant licensed radio spectrum bands which are allocated to licensed systems. As an example, the IEEE 802.11af [40] and the IEEE 802.22 [41] standards take advantage of the TV white spaces to support wireless local area networks (WLANs) and wireless regional area networks (WRANs), respectively. Although opportunistic spectrum access for CR Networks (CRNs) has been extensively studied [42–45], the results may not be directly applied to VANETs due to the high mobility of vehicles. There have been a few efforts investigating the topic of incorporating CR in VANETs. In [46], Urgaonkar *et al.* exploited Markovian random walk model of SUs and proposed an opportunistic scheduling policy for secondary networks. The objective is to maximize the throughput of SUs by using the technique of Lyapunov optimization. In [47], Niyato *et al.* investigated the optimal channel access

in CR-enabled VANETs to maximize the utility of vehicles under certain QoS constraints for a grid-like urban street layout. The limitation of [47] is that the authors assume the channel availability statistics are known to vehicles. However, in VANETs, the channel availability can be very different from static networks, since vehicular users can exploit both spatial and temporal spectrum opportunities when moving along the road. In [48], the channel availability in CR-enabled VANETs is theoretically analyzed, based on which an efficient spectrum access scheme is proposed. We will elaborate this work in Chapter 3.

WiFi, operating on unlicensed spectrum, is a popular solution to deliver data content at low cost. The feasibility of WiFi for outdoor Internet access at vehicular mobility, referred to as *drive-thru Internet*, has been demonstrated in [27]. Different from the fully covered cellular network, WiFi only provides intermittent small coverage areas along the road. Therefore, although WiFi operates on unlicensed spectrum, it is spatially/temporal opportunistic for vehicles to use due to the vehicle mobility. There are extensive research works in the literature on the evaluation of the practical performance of drive-thru Internet [27,49], and design of data delivery protocols in the context of drive-thru Internet [1,50,51]. However, as far as we know, there are no related works addressing the issue of theoretically analyzing the data delivery performance of vehicular-WiFi network composed of multiple drive-thru Internet along the road. In [52], a theoretical analysis of the performance of vehicular WiFi offloading is provided, considering the intermittent WiFi accessibility due to vehicle mobility, and the QoS requirements of vehicular users. We will elaborate the work in Chapter 4.

Device-to-device (D2D) communication technology, as a promising solution to offload the cellular networks, has gained much attention recently [53]. By utilizing the proximity, mobile users can communicate directly with each other using the cellular spectrum (or other spectrum bands) without traversing the base station or the backhaul networks. Therefore, D2D communications can increase the overall spectral efficiency and reduce communication delay for mobile users [54], which may be applied to many VANETs applications such as video streaming, location-aware advertisement, safety related applications, and so forth. However, D2D communication is opportunistic since D2D communication should avoid interfering the uplink/downlink cellular communication and the D2D communications of neighboring devices. In other words, a D2D communication is not permitted if it would introduce unacceptable interference to other cellular transmissions. While the D2D communication has been extensively studied [39, 55, 56], applying such a proximate communication paradigm on cellular bands in VANETs is still in its initial phase. Admittedly, incorporating D2D communication in vehicular environment introduces several new challenges. For example, a full channel state information, which is usually needed in resource allocation schemes for D2D communication, is hard to track and easy to be

outdated in VANETs. In addition, the topology of VANETs makes the interference pattern more difficult to model than a general cellular network where a Poison point process (P.P.P.) can be applied to model the user spatial distribution. In [57], the performance of underlaid vehicular device-to-device (V-D2D) communications is studied, considering the characteristics of the VANETs. We will elaborate the work in Chapter 5.

1.4 Thesis Outline

The rest of this thesis is organized as follows: Chapter 2 presents a comprehensive overview of opportunistic spectrum bands and the key enabling technologies. Chapter 3 investigates the channel availability and spectrum access scheme when CR is used in VANETs for utilizing licensed spectrum. Chapter 4 analyzes the performance of vehicular WiFi offloading based on queueing theory, and the relation between offloading performance and the average delay is obtained. Chapter 5 investigates the performance of the vehicular D2D communication underlaying cellular network, considering the impact of the spatial distribution of vehicular users on the D2D performance. Finally, Chapter 6 concludes the thesis, and points out the future research directions.

Chapter 2

Background

Heterogeneous network has been considered as one of the most important ways to enhance the network performance, improve the resource utilization, and reduce the network cost, by sharing the idle resource of different networks [58]. In this chapter, we aim to provide a comprehensive overview of potential wireless technologies for spectrum utilization in VANETs, including cognitive radio, WiFi, and device-to-device communications. For each technology, we will introduce the concepts and elaborate the features, followed by the state of the art. Then, we focus on employing these wireless technologies for VANETs, where the challenges resulted from the distinctive features of VANETs are described, and a literature survey is provided.

2.1 Cognitive Radio Networks

Since first proposed by Motila in 1999, cognitive radio has been considered as a promising approach to deal with the problem of spectrum scarcity in wireless networks [59, 60]. By means of opportunistically exploiting the idle wireless spectrum, the overall spectrum utilization can be greatly improved, which means that more users and data connections can be supported without increasing the amount of spectrum resources. In this section, we first introduce the background knowledge of cognitive radio networks, including the concepts, research issues, and state of the arts. Then, as one of the potential spectrum bands, the TV white spaces and related CR technology, *super WiFi*, are depicted. Last, we introduce CR-VANETs, which are vehicular networks with the capability of accessing spectrum resources of other networks opportunistically using CR technology. The distinc-

tive challenges of CR-VANETs are represented, followed by a survey of existing research works on this topic.

2.1.1 Cognitive Radio Ad-hoc Networks

The licensing of wireless spectrum is allocated to different services, organizations, and companies on a long-term basis. However, this static allocation of spectrum resources results in a low utilization of the resources. As shown in Fig. 2.1, the usable radio frequencies have been nearly ran out, and a great amount of low-frequency spectrum bands have been allocated to systems currently less active or less important compared to the modern wireless communication systems, such as the commercial cellular networks, and WiFi networks. The examples are AM radio broadcasting bands taking a vast part of 300 kHz to 3 MHz spectrum band, and TV broadcasting bands mainly residing in 30 MHz to 300 MHz bands. Besides, such systems are usually not capable of efficiently utilizing the spectrum resources. For instance, the spectrum efficiency of digital radio and digital TV is 0.08 bit/s/Hz and 0.55 bit/s/Hz, which are way less than that of LTE-A system, 30 bit/s/Hz. To solve the problem, the best solution may be reallocating the spectrum resources in a more efficient way. However, it is impractical since it will introduce too much cost to change the existing networks. Therefore, based on the fact of spectrum underutilization, FCC has approved the use of licensed bands by unlicensed devices. According to the concept, a new research area called dynamic spectrum access (DSA) has attracted much attention in both academia and industry [61].

DSA allows unlicensed users (secondary users) to use the licensed spectrum when interference to the licensed users (primary users) is limited. In DSA, two approaches to share spectrum between primary and secondary users are considered, i.e., spectrum underlay and spectrum overlay. In spectrum underlay, a severe constraint is imposed on the transmission power of secondary users in order for them to work below the noise floor of the primary users. By utilizing the ultra-wide frequency band (UWB), a short-range high data rate can be achieved by secondary users with very low transmit power. On the other hand, in spectrum overlay, secondary users transmit in an opportunistic manner only when the primary users' signal is not presented. Therefore, rather than limiting the transmit power, the spectrum overlay DSA tends to determine when and where to transmit, and targets at utilizing spatial and temporal spectrum white spaces.

The spectrum overlay sharing in DSA can be considered as an important application of CR. In CRNs, licensed users and unlicensed users are typically referred to as primary users (PUs) and secondary users (SUs), respectively. The basic idea of CRNs is that the

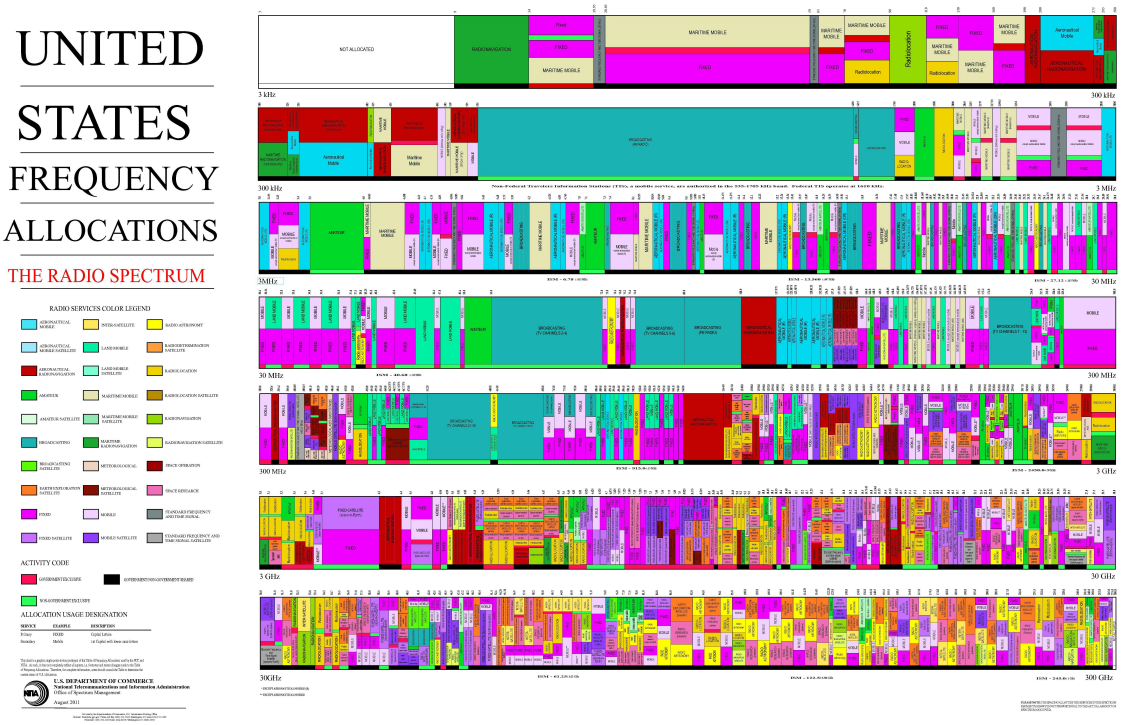

Figure 2.1: United States frequency allocations [2].

secondary users transmit only when primary users are idle, and need to vacate the band once the primary users' signal is detected. The formal definition of the term cognitive radio can be found in [62]:

A "Cognitive Radio" is a radio that can change its transmitter parameters based on interaction with the environment in which it operates.

The target of cognitive radio is to find and use the best available spectrum through changing the transmitter parameters. However, due to the static spectrum allocation, the most important challenge is to utilizing the spectrum without severely interfering the transmissions of primary systems. CR enables devices to detect the spectrum holes, and move among different spectrum holes, as depicted in Fig. 2.2. To this end, CR should be able to carry out certain functionalities, i.e., spectrum sensing and spectrum decision [63]. In the sequel, we introduce the CR functionalities respectively. The literature surveys for general CR networks and technologies can be found in [63–65].

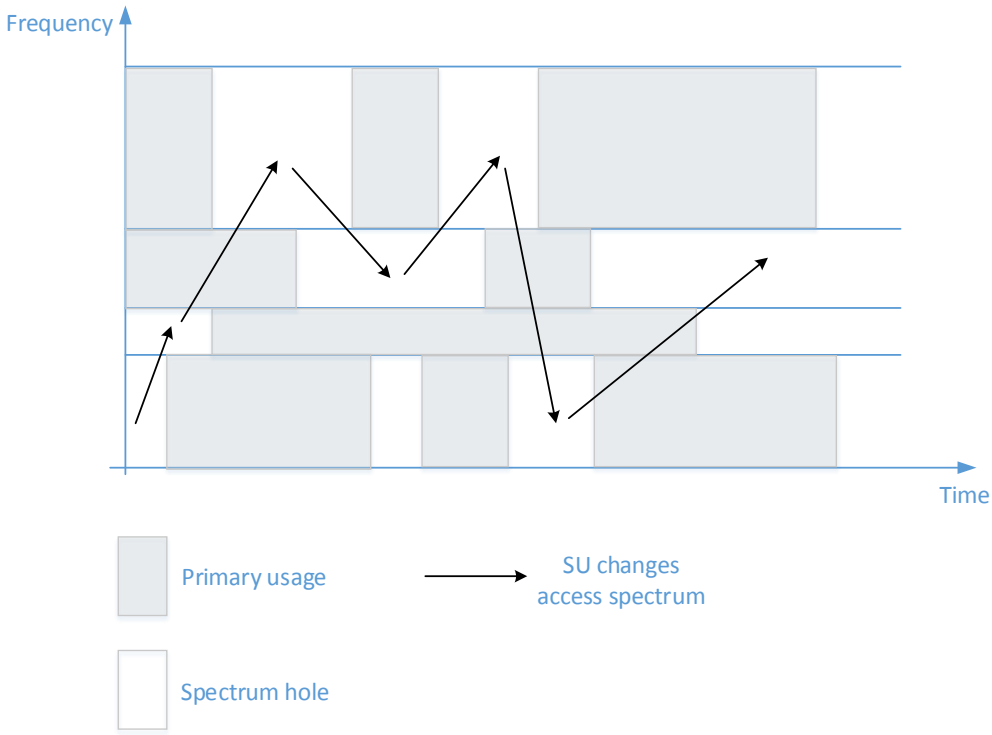

Figure 2.2: CR devices can utilize spectrum holes.

Spectrum Sensing

Since CR users can only utilize the idle spectrum resources, they should be able to monitor the spectrum bands and detect the spectrum holes through the function of *spectrum sensing*. As a basic functionality of CRNs, spectrum sensing provides information about the spectrum occupancy to other spectrum management functionalities. Generally, CR spectrum sensing can be divided into three categories, i.e., primary transmitter detection, primary receiver detection, and interference temperature management, as shown in Fig. 2.3. However, due to the difficulties and technical limitations of receiver detection and interference temperature management, current research works mainly focused on primary transmitter detection.

In transmitter detection, the spectrum sensing problem can be formulated as a binary hypothesis test H_0 and H_1, where H_0 and H_1 indicate that the spectrum is available and

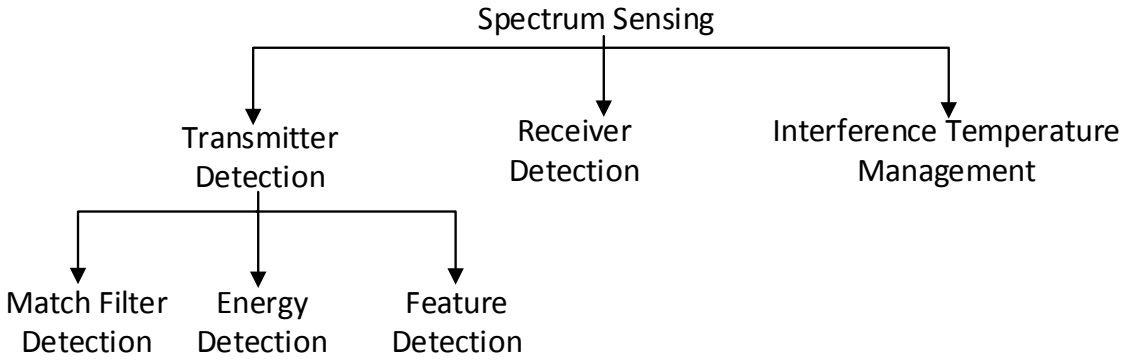

Figure 2.3: Categories of spectrum sensing.

unavailable, respectively. The hypothesis model can be represented as

$$r_t = \begin{cases} n(t) & H_0, \\ hs(t) + n(t) & H_1, \end{cases} \tag{2.1}$$

where $r(t)$ is the received signal of the SU, $n(t)$ is zero-mean additive white Guassian noise, $s(t)$ is transmit signal of the PU, and h is the channel gain. For any spectrum sensing scheme, there are three important metrics, i.e., the false alarm probability P_f, the detection probability P_d, and the missing probability P_m. With the above hypothesis model, the three probabilities can be obtained by

$$P_f = \mathbb{P}(H_1|H_0) \tag{2.2}$$
$$P_d = \mathbb{P}(H_1|H_1) \tag{2.3}$$
$$P_m = \mathbb{P}(H_0|H_1) = 1 - P_d \tag{2.4}$$

In the literature, there are mainly three schemes for primary transmitter detection in spectrum sensing, which are matched filter detection, energy detection, and feature detection, respectively [66].

Spectrum Decision

Given the spectrum availability obtained from spectrum sensing, SUs should make a decision to choose the best spectrum band among all the available bands based on the QoS requirements, the procedure of which is called spectrum decision. In general, spectrum de-

cision consists of two steps. First, the spectrum bands are characterized by the spectrum availability (through spectrum sensing) and the statistic information of the primary networks (known in advance). Then, a decision on the best spectrum band is made according to the information and the QoS requirements of the applications.

According to [63], the spectrum availability or spectrum holes can be characterized by parameters which reflect the time-varying radio environment, such as interference, path loss, wireless link errors, and link layer delay. For the statistic information of the primary networks, most of the related research works on CRNs assumes that PU activities can be modeled by exponential distributions [67–69]. In this model, a two-state mapping is applied to the PU behaviors, where "ON" sate indicates that the PU is active in transmitting, and "OFF" state indicates the opposite. The time durations of ON and OFF states are exponentially distributed with mean α and β. After all the spectrum bands are characterized, the best available spectrum band can be selected based on certain spectrum selection rules, e.g., error rate, data rate, delay bound, etc.

In CRNs, one important characteristic of cognitive radio users is the cognitive intelligence, which enables them to intelligently determine the access spectrum and corresponding communication parameters according to the spectrum sensing results and other users' spectrum access strategies [70]. Therefore, it is natural to employ **game theory** to study the CRN users' behaviors and interactions in the spectrum access and sharing issues. The game theory not only provides a fair and efficient solution for distributed spectrum access, but can also offer equilibrium criteria to study the performance of the game outcomes. Game theory based spectrum access and spectrum sharing have been extensively studied in the literature. In [71], a bargaining approach is used where users self-organize into bargaining groups and adapt their channel assignment to approximate the optimal assignment. A fairness bargaining method is proposed to improve the fairness among users, and derive the lower bound of the minimum assignment of each user. The performance of the proposed method is shown to be similar to topology-based optimization scheme, but with complexity reduced by a half. In [72], two auction based methods are proposed for the spectrum sharing among a group of users, who access the channel and interfere with each other, and thus the utility of a user is a function of received signal-to-interference plus noise ratio. A distributed algorithm is also formulated, and the condition for the auction to achieve the Nash equilibrium using the algorithm is also specified.

2.1.2 TV White Spaces and Super WiFi

As an application of CR technology, the under-utilized TV white spaces (TVWS), which include VHF/UHF frequencies, have been approved for non-TV communications in many

countries such as USA and Canada, using an emerging technology named Super WiFi. TV broadcasting spectrum bands, also known as TV white spaces (TVWS), have been suggested for wireless broadband access due to the abundant and currently underutilized spectrum resources at VHF/UHF bands and its better penetration property, with new standards introduced, such as IEEE 802.11af [40] and IEEE 802.22 [73]. Due to the license-exempt (unlicensed) technologies, i.e., the sharing of radio spectrum among users and Internet service providers, wireless access over TVWS is named "super WiFi". However, compared to WiFi technologies, such as IEEE 802.11g/n/ac, super WiFi has many distinct features. The lower frequency bands have better propagation properties than the 2.4 GHz and 5 GHz ISM bands which stock WiFi uses, and can thus provide much wider coverage with relatively high capacity. It is shown that a super WiFi AP can provide at least 1200 m coverage with 80 Mbps capacity, with a 6 MHz wide TVWS channel and 4 W transmit power [40]. In addition, since TVWS are the licensed spectrum bands for TV broadcasting system, super WiFi should use it in a "cognitive" manner, in order not to affect the operation of the licensed system. To this end, super WiFi transmissions are "allowed" only when no primary transmissions (TV broadcasting) are present. Therefore, two ways can be employed, i.e., cognitive radio technologies and geolocation database server (GDB). For the former, there have been many research works on spectrum sensing-based TVWS utilization [74–76]. However, spectrum sensing can consume a considerable amount of energy and the sensing results might be inaccurate. Fortunately, unlike other licensed system, the spectrum usage of TV broadcasting system is highly stable and predictable, which indicates that the occupancy of TVWS channels do not change frequently and can be known in advance. Therefore, it is recommended that super WiFi users access the GDB to obtain the availability and power constraint of TVWS channels before transmit, such as in IEEE 802.11af.

2.1.3 Spectrum Sensing in CR-VANETs

Since CR can improve the spectrum efficiency through utilizing the spectrum holes, a natural question then rises: whether CR can be applied to solve the problem of spectrum scarcity in VANETs? Recent researches in the literature demonstrate its feasibility [47, 77–79]. With CR technology, VANETs have been coined as CR-VANETs, whereby vehicles can opportunistically access licensed spectrum owned by other systems, outside the IEEE 802.11p specified standard 5.9-GHz band, such as TV broadcasting system and cellular networks. Considering the highly dynamic mobility, vehicles are expected to exploit more spatial and temporal spectrum opportunities along the road than stationary SUs. Other than simply placing a CR in vehicles, CR-VANETs has many unique features which should

be considered. Different from static CR networks in which the spectrum availability is only affected by the spectrum usage patterns of the primary network, in CR-VANETs, the spectrum availability perceived by vehicles is also a function of the mobility of vehicles. Therefore, spectrum sensing should be conducted over the movement path of vehicles, leading to a spatiotemporal distribution, rather than temporal only. In addition, the constrained nature of vehicle mobility according to street patterns can be utilized. For example, the spectrum information in other locations can be obtained by a vehicle through information exchange with vehicles moving from those locations. And a vehicle can adapt its operations in advance using such information and its predicted movement. In the sequel, we introduce two important aspects in CR-VANETs, i.e., spectrum sensing and spectrum access, respectively.

Per-Vehicle Sensing

In per-vehicle sensing, vehicles sense the primary spectrum using the traditional sensing techniques in the literature of CR system, i.e., matched filter detection, energy detection, and cyclostationary feature detection [63]. The advantage of per-vehicle sensing is that the implementation complexity and network support is minimal since each vehicle senses the spectrum and makes decision on its own. However, the accuracy of this method might be low given the high mobility of vehicles and the obstructed environments that may cause fading or shadowing effects. In [80], a mechanism is proposed to improve the accuracy of spectrum sensing via exploring the signal correlation between TV and 2G channels. It is proven that when the signals from adjacent TV and cellular transmitters are received in a common place, a strong Received Signal Strength Indicator (RSSI) can be detected. Therefore, a sudden change in the TV band can be verified by comparing the signal with the fluctuations of cellular channels.

Infrastructured BS Based Sensing

A sensing coordination framework which utilizes road side units (RSUs) is proposed in [81]. Unlike centralized sensing schemes in which a centralized controller gathers sensing reports from all users and allocates the channels for users to access, in [81], RSUs are responsible to assist and coordinate the spectrum sensing and access for nearby vehicles. RSUs continuously detect the occupancy of PUs at its location. The coarse detection results are sent to vehicles, and the vehicles conduct the fine-grained sensing and access the channel correspondingly. The results show that the sensing coordination framework outperforms the stand-alone sensing scheme in terms of successful sensing rate, sensing

overhead, probability of sensing conflict, etc. One advantage of such schemes is that the change of government policies and PU parameters can be easily loaded in RSUs, which can further adapt the operation.

Cooperative Sensing Among Vehicles

A major concern about centralized sensing in CR-VANETs is discussed in [82] that vehicles may have different views of spectrum occupancy, especially near the edge of the range of primary systems, and thus it is difficult to set a BS or data fusion center. Instead, in [82], a distributed collaborative sensing scheme is proposed. Vehicles send the message about the belief on the existence of primary users to neighboring vehicles, which is called belief propagation (BP). Upon receiving the belief messages, vehicles combine the belief with their local observation to create new belief messages. After several iterations, each vehicle is envisaged to have a stable belief, and can conduct spectrum sensing accordingly. However, several issues of this work could be further discussed, such as the convergence speed of the iterations, the extent of belier propagation, etc.

Cooperative sensing between selected neighboring vehicles can be more efficient than cooperation among all neighboring vehicles due to less message exchanges. A light-weight cooperative sensing scheme can be seen in [83]. Roads are divided into segments, and vehicles are allowed to gather spectrum information of h segments ahead from vehicles in front, which is a priori spectrum availability detection. Therefore, vehicles can decide the channel to use in advance so that spectrum opportunities can be better utilized.

Geolocation-Based Sensing

FCC has suggested to use the location information and spectrum database for CR users. Spectrum database provides information about the bands, including the types, locations and specific protection requirements of PUs, the availability of the bands, etc. With the assistance of spectrum database, vehicles can adjust the transmission parameters to avoid interfering PUs without sensing. Geolocation-based sensing is suitable for vehicles because most vehicles are equipped with localization systems (e.g., GPS). Such spectrum databases are already available for users to access, for example, the TV query service in the United States [84] and Google spectrum database (shown in Fig. 2.4). In [85], spectrum database assisted CR-VANETs are proposed, in which fixed BSs are deployed along the road and provide spectrum database access to vehicles in proximity. The deployment density of BSs is optimized to minimize the average cost of VUs accessing spectrum information while

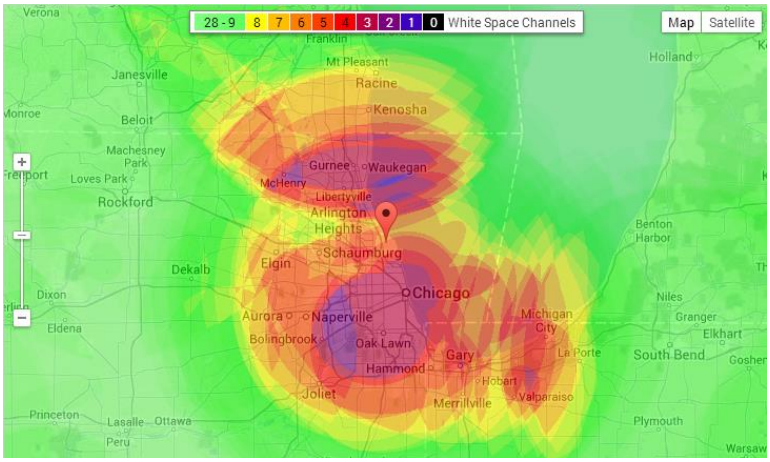

Figure 2.4: TV white bands usage around Chicago from Google spectrum database. Colored areas correspond to channels that are used.

guarantee a low level of error of estimating available spectrum. The simulation results show that the cost of accessing spectrum information increases with the BS density since more vehicles are querying the spectrum database via BSs, which is a more expensive and accuracy way than obtaining the spectrum database information from nearby vehicles and spectrum sensing. In [86], a geo-location database approach is used to create a map of spectrum availability on I-90 in the state of MA. A discussion on the number of available channels, the number of non-contiguous blocks, and design of transceivers is followed.

However, there are several concerns about the spectrum database, e.g., the cost of building and maintaining the database, the coverage area of the service, significant query overhead, etc. The authors in [80] proposed to jointly use the spectrum database and spectrum sensing. In [80], the signal correlation between 2G and TV channels and the mobility of vehicles are utilized to reduce the number of queries to spectrum database in order to save the cost in terms of both money and overhead. A vehicle can send the channel measurements to nearby vehicles, which contains the degree of correlation between TV and cellular channels. When other vehicles arrive the same location, they can conduct spectrum sensing, and make a decision on whether spectrum information update is necessary based on the correlation between TV and cellular channels obtained from measurements sent by former vehicles in the location. The results show that about 23% queries are reduced, which is attractive to spectrum database deployment.

2.1.4 Dynamic Spectrum Access in CR-VANETs

The sensing results should be utilized to correctly choose the spectrum band to access. This can be done through different approaches, which can be categorized into PU protection and QoS support, in terms of the target of the approaches.

Spectrum Access Approaches with PU Protection

In these approaches, vehicles access the spectrum with the goal of avoiding harmful interference to licensed system and PUs. In [87], a learning structure is proposed for channel selection in CR-VANETs. PU channel usage is modeled as "ON/OFF" pattern, where in ON period, the channel usage follows "busy/idle" pattern, and in OFF period, the PU does not transmit. The authors claimed that an instant spectrum sensing is difficult to differentiate OFF periods from idle periods, while longer sensing time reduces the utilization of OFF periods. Based on the fact that samples of spectrum usage during the same time slot of days at the same location keep high consistency, a channel selection is proposed jointly considering the past channel selection experience and current channel conditions. Stored channel profiles are used to select good channel candidates to sense and access, avoiding wasting limited sensing time on other channels. In [88], some metrics for dynamic channel selection are proposed and discussed. These metrics include: 1) channel data rate; 2) product of channel utilization and data rate; 3) product of expected OFF period and data rate.

Spectrum Access with QoS support

QoS support is important for VANETs, such as the delay constraint for safety applications and bandwidth requirement of nonsafety applications. Therefore, QoS support is a crucial consideration in dynamic spectrum access schemes. In [89], a dynamic spectrum access scheme for vehicle-infrastructure uplink communication is proposed to minimize the energy consumptions as well as guarantee the QoS. It is claimed that energy efficient communication is important for VANETs to save energy and reduce greenhouse gas emission, especially for the electric vehicles. A joint optimization algorithm is proposed to minimize the energy consumption while maintain the throughput requirement with the delay constraint of vehicular communications. In [47], a dynamic channel selection scheme is proposed for vehicle clusters, involving dynamic access to shared-use channels, reservation of exclusive-used channels, and control of cluster size. Shared-use channel, i.e., licensed channels, can be accessed by vehicles in an opportunistic manner, while exclusive-use channels

are reserved for vehicle data transmission exclusively, such as DSRC spectrum. Channel selection is modeled as an optimization problem under the constraints of QoS specifications and PU protection, which is solved by constrained Markov decision process.

2.2 WiFi

As one of the most successful wireless access technologies, IEEE 802.11-based WiFi technologies provide cost-effective Internet access that can satisfy the communication requirements of most current wireless services and applications. Due to the high data rate, low deployment complexity, and low price, WiFi infrastructure has been widely deployed around the world and experienced tremendous growth in the recent years. Like many other wireless technologies, since the first standard IEEE 802.11a-1999, WiFi technologies have evolved and integrated the latest technologies, in order to continue to improve the spectrum utilization and network performance. In IEEE 802.11n-2009, single-user multiple-input multiple-output antennas (SU-MIMO) is added to support a maximum data rate from 54 Mbps to 600 Mbps. In addition, frame aggregation is employed to reduce the protocol overhead. IEEE 802.11ac-2013 further extends the features, including multi-user MIMO (MU-MIMO), extending the channel bandwidth to 160 MHz, and high-density modulation (up to 256-QAM). With these feature, IEEE-802.11ac based WiFi can support maximum 866 Mbps data rate. IEEE 802.11af and 802.11ah extend the WiFi spectrum bands to the TV white spaces and sub 1G bands with cognitive radio technologies, so as to support long-range and power saving applications such as machine-to-machine (M2M) communications. In IEEE 802.11p is designed on 5.9 GHz to support Intelligent Transportation Systems (ITS) applications, such as toll collection, vehicle safety applications, and high-speed Internet access. The most popular IEEE 802.11 amendments are shown in Table. 2.1.

Through WiFi, data originally targeted for cellular networks can be delivered, which is referred to as ***WiFi offloading*** of the mobile data. Hereafter, we use the term WiFi offloading to represent data transmission through WiFi networks. The advantages of WiFi access are summarized in Table 2.2. These advantages make WiFi a cost-effective technology to offload the cellular data traffic and alleviate the congestion of cellular networks. In fact, WiFi is recognized as one of the primary cellular traffic offloading technologies [90]. WiFi offloading has been extensively studied for stationary or slow moving users[1] [90–93]. It is shown that around 65% of the cellular traffic can be offloaded by merely using the

[1]We refer to these users as non-vehicular users.

Table 2.1: Main IEEE 802.11 amendments

Amendment	Frequency (GHz)	Bandwidth (MHz)	Maximum data rate (Mbps)	Responsibility
a	5	20	54	Enable up to 54 Mbps data transmission in 5 GHz unlicensed band by utilizing orthogonal frequency division multiplexing (OFDM)
b	2.4	22	11	Enable up to 11 Mbps data transmission in 2.4 GHz unlicensed band by utilizing Direct-sequence spread spectrum (DSSS)
g	2.4	20	54	Enable up to 54 Mbps data transmission in 2.4 GHz unlicensed band by utilizing OFDM
n	2.4/5	20/40	150	Utilize MIMO to support higher data rates
ac	2.4/5	20/40/ 80/160	866.7	Support MU-MIMO to further enhance data rate

most straightforward way of simply switching the IP connection from the cellular network to WiFi when the WiFi connectivity is available (*on-the-spot offloading*). In addition, significant amount (above 80%) of data can be offloaded by delaying the data application [91] (*delayed offloading*).

For moving vehicles, research works have demonstrated the feasibility of WiFi for outdoor Internet access at vehicular speeds [27, 94]. The built-in WiFi radio or WiFi-enabled mobile devices on board can access the Internet when vehicles are moving in the coverage of WiFi hotspots, which is often referred to as the **drive-thru Internet** access [94]. This kind of access solution is workable to offer a cost-effective data pipe for VUs [95], and with the increasing deployment of the urban-scale WiFi network (e.g., Google WiFi in the city of Mountain View), there would be a rapid growth in vehicular Internet connectivity. WiFi offloading in vehicular communication environments (or *vehicular WiFi offloading*) refers to delivering the data traffic generated by the vehicles or VUs through opportunistic WiFi networks, i.e., the drive-thru Internet access. Natural questions arise that how much data can be offloaded through vehicular WiFi offloading; how to improve the offloading performance, i.e., to offload more cellular traffic and guarantee the QoS of VUs simultaneously? Due to high dynamics of vehicular communication environments, the effectiveness of WiFi offloading for VUs requires careful studies. The overview of vehicular WiFi offloading is shown in Fig. 2.5. We elaborate the unique features and challenges of vehicular WiFi offloading from the following three aspects.

Drive-thru Internet access: Mobility plays a both challenging and distinguishing role in vehicular WiFi offloading. During one drive-thru, i.e., the vehicle passing the coverage area of one WiFi AP, VUs can only obtain a relatively small data volume due to the short connection time with the WiFi AP; VUs may experience multiple drive-thrus in a short time period due to high mobility. This short and intermittent connectivity has great impacts on offloading schemes, such as WiFi offloading potential prediction and network selection (cellular/WiFi), which are discussed later. Fluctuating channels may lead to high and bursty losses, resulting in disruptions to connectivity. Thus, proper handoff schemes and transport protocols are needed to reduce the disruptions and adapt to the wireless losses.

Cellular operators: To ease congestion of cellular networks, cellular operators may adopt certain commercial strategies to encourage data offloading, such as stimulating VUs to transmit their data through WiFi networks. Thus, incentive models, such as variable service prices or reward mechanisms, should be investigated. Moreover, cellular operators may deploy their own commercial or non-commercial WiFi networks to offload mobile data, e.g., the WiFi hotspots operated by AT&T [98]. How to determine the WiFi deployment strategy to attain optimal offloading performance is another research challenge.

Table 2.2: The advantages of WiFi access.

Advantage	**Description**
Widely deployed Infrastructure	WiFi hotspots are widely deployed in many urban areas. It is shown that WiFi access is available 53% of the time while walking around popular sites in some large cities [96].
Low cost	WiFi access is often free of charge or inexpensive. For example, KT Corporation in South Korea offers WiFi services with $ 10 a month for unlimited data usage [97].
High availability of user devices	Most of current mobile devices, such as smart phones, tablets, and laptops are equipped with WiFi interfaces.
Efficient data transmission	Currently WiFi technologies (IEEE 802.11 b/g) can provide data rates of up to 54 Mbps. There are new technologies under development or test, e.g., IEEE 802.11 ac/ad, which can provide data transfer at several Gbps.

Vehicular users: As the mobility pattern of vehicles can be predicted from the mobility model, historic drive information, and driver preferences, the WiFi offloading potential, i.e., data volume offloaded in the future, can be predicted. Based on the prediction and the knowledge of usage cost of cellular and WiFi services, and the QoS requirements, it is possible for VUs to determine when to use WiFi or cellular networks upon a service request emerging, in order to get a good trade-off between the cost and satisfaction level in terms of delay. It is a challenging task to understand the cost-effectiveness of WiFi offloading from the VUs' perspective.

In this section, we focus on the problem of WiFi offloading in vehicular environment. We discuss the challenges and identify the research issues related to drive-thru Internet as well as vehicular WiFi offloading. Moreover, we review the state-of-the-art solutions, providing rapid access to research results scattered over many papers.

2.2.1 Drive-thru Internet Access

Drive-thru Internet refers to the Internet connectivity provided by roadside WiFi APs for moving vehicles within the coverage area. The performance of such a drive-thru access network is different from that of a normal WiFi network which only serves non-vehicular users.

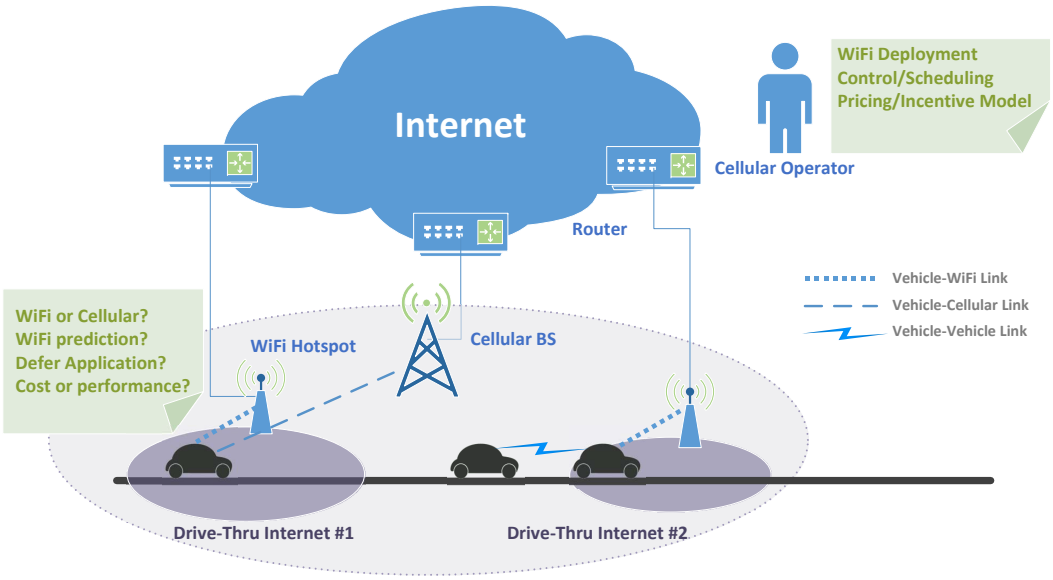

Figure 2.5: WiFi offloading in vehicular communication environments.

The reasons are three-fold. Firstly, high vehicle mobility results in a very short connection time to the WiFi AP, e.g., only several to tens of seconds, which greatly limits the volume of data transferred in one connection time. Moreover, the time spent in WiFi association, authentication, and IP configuration before data transfer cannot be negligible considering the short connection time. Secondly, communications in vehicular environments suffer from the high packet loss rate due to the channel fading and shadowing [50]. Thirdly, the stock WiFi protocol stack is not a specific design for high mobility environments.

Vehicular WiFi offloading mostly relies on the drive-thru Internet access opportunities, provided by open or planed WiFi networks. Therefore, we first review the recent experimental and theoretical studies on drive-thru Internet. After that, we discuss the vehicular WiFi offloading, including the challenges, research issues, and existing and potential solutions.

In the literature, research works of drive-thru Internet mainly focus on performance measurements and network protocol design. Therefore, we also elaborate our discussion on drive-thru Internet from the these two aspects.

Table 2.3: Drive-thru Internet performance measurements - configuration.

	Scenario	WiFi	AP deployment	Antenna
[94]	Highway	802.11b	Planned	External/VU
[99]	Highway	802.11g	Planned	8 dBi/AP; 5dBi/VU
[49]	Traffic free road	802.11b	Planned	N/A
[1]	Highway	802.11a/b/g	Planned	7 dBi/AP
[27]	Urban	802.11b	Unplanned	5.5 dBi/VU
[50]	Urban	802.11b/g	Unplanned	3 dBi/VU

N/A: not applicable.

Characteristics and Performance

To characterize and evaluate the performance of the drive-thru Internet, several real-world measurements have been done based on diverse test bed experiments. The configurations and key results are summarized in Tables 2.3 and 2.4.

In [94] and [99], the drive-thru Internet is evaluated in a planned scenario where two APs are deployed closely along a highway, using IEEE 802.11b and 802.11g, respectively. The performances of User Datagram Protocol (UDP) and Transmission Control Protocol (TCP) at different speeds (80, 120, and 180 km/h) and scenarios (AP to vehicle, vehicle to AP) are evaluated. A very important characteristic observed is that the drive-thru Internet has a three-phase feature, i.e., entry, production, and exit phases. In the entry and exit phases, due to the weak signal, connection establishment delay, rate overestimation, etc., the performance is not as good as when in production phase. In [49], a similar test is conducted on a traffic free road which indicates an interference-free communication environment. It is shown that in such an environment, the performance of the drive-thru Internet suffers most from the backhaul network or application related issues rather than the wireless link problems. For example, with a 1 Mbps bandwidth limitation of backhaul network, the TCP bulk data transferred within a drive-thru reduces from 92 MB to 25 MB. In addition, a backhaul with 100 ms one-way delay greatly degrades the performance of web services due to the time penalty of HTTP requests and responses. The problems that may cause the performance degradation of the drive-thru Internet are thoroughly discussed in [1].

In [27] and [50], large-scale experimental evaluations of the drive-thru Internet with multiple vehicles in urban scenarios have been conducted. Both of the data sets are col-

Table 2.4: Drive-thru Internet performance measurements - results.

	Connection establishment time	Connection time	Inter-connection time	Max rate	Data transfer in once drive-thru
[94]	Max 2.5 s	9 s @ 80	N/A	TCP: 4.5 Mbps UDP: 5 Mbps	TCP: 6 MB @ 80 5 MB @ 120 1.5 MB @ 180 UDP: 8.8 MB @ 80 7.8 MB @ 120 2.7 MB @ 180
[99]	N/A	N/A	N/A	15 Mbps	Max 110 MB
[49]	8 s	217 s @ 8 13.7 s @ 120	N/A	TCP: 5.5 Mbps UDP: 3.5 Mbps	92 MB @ 8 6.5 MB @ 120
[1]	Mean 13.1 s	58 s	N/A	TCP: 27 Mbps	Median 32 MB
[27]	366 ms	13 s	Mean 75 s	30 KBytes/s	Median 216 KB
[50]	8 s	N/A	Median 32 s Mean 126 s	86 Kbps;	Median 32 MB

@ α: at α km/h; N/A: not applicable.

lected from the city of Boston with in situ open WiFi APs. [27] focuses on the TCP upload performance, and shows that with fixed 1 Mbps MAC bit rate, the drive-thru Internet is able to provide an (median) upload throughput of 30 KBytes/s, and the median volume of uploading data in once drive-thru is 216 KB. The average connection and inter-connection time are 13 seconds and 75 seconds, respectively. This demonstrates that although vehicles have short connection time with WiFi APs, they can experience drive-thru access opportunities more frequently, compared with low-mobility scenarios (median connection and inter-connection time 7.4 minutes and 10.5 minutes, respectively [91]). The experiment in [50] shows a 86 kbps long-term average data transfer rate averaged over both connection and inter-connection periods. Moreover, two mechanisms to improve the performance are

proposed, namely Quick WiFi and CTP, to reduce the connection establishment time and deal with the negative impact of packet loss on transportation layer protocols, respectively.

Network Protocol

To improve the performance of the drive-thru Internet, new protocols or modification in existing protocols should be developed. The efforts in the literature include: i) reducing connection establishment time [50]; ii) improving transport protocols to deal with the intermittent connectivity and wireless losses [50]; iii) enhancing MAC protocols for high mobility scenarios [51]; and iv) MAC rate selection schemes [50] and [1].

The AP connection time is typically only seconds to tens of seconds in drive-thru scenarios, and in fact not every second can be used for data transfer. It takes some time to conduct AP association, authentication, IP configuration, etc., before Internet connectivity is available. We call this time as connection establishment time. It is helpful if this time duration can be reduced as much as possible. In [50], a mechanism named Quick WiFi is proposed to reduce the connection establishment time and improve data transfer performance. The main idea of Quick WiFi is to incorporate all processes related to connection establishment into one process, to reduce the timeouts of related processes, and to exploit parallelism as much as possible. It is shown that the connection establishment time can be reduced to less than 400 ms. If the WiFi network is deployed and managed by one operator, a simple yet effective method is presented in [100], in which vehicles are allowed to retain their IP address among different associations, and thus the authentication and IP configuration are carried out only once.

To deal with the high and bursty non-congestion wireless losses in vehicular communication environments, a transport protocol called Cabernet transport protocol (CTP) is proposed in [50]. In CTP, a network-independent identifier is used by both the host and the vehicle user, allowing seamless migration among APs. Large send and receive buffers are also utilized to counter the outages (i.e., the vehicle is out of range of any WiFi AP). More importantly, CTP can distinguish wireless losses from congestion losses, by periodically sending probe packets. Through an experimental evaluation, CTP is demonstrated to achieve twice the throughput of TCP.

The IEEE 802.11 MAC protocols are designed for low-mobility scenarios, and thus require modifications and redesigns for the drive-thru Internet. [51] theoretically studies the performance of IEEE 802.11 distributed coordination function (DCF) of the large-scale drive-thru Internet base on a Markov chain model, and provides some guidelines to enhance the MAC throughput. The impact of vehicle mobility and network size (i.e., vehicle

Table 2.5: Modified MAC bit rate selection scheme in [1].

Parameter	**Original** [101]	**New Value**
Probe Packet	10%	40%
Sample Window	10 s	1 s
Decision Interval	Every 1000 ms	Every 100 ms

traffic density) on the MAC throughput is also discussed. The key observation is that the normal operations of DCF result in a *performance anomaly* phenomenon, i.e., the system performance is deteriorated by the users with the minimum transmission rate. Based on this observation and the analytical model, a contention window optimization is proposed, which is adaptive to variations of transmission rates, vehicle velocity, and network size. The MAC rate selection is discussed in [50] and [1]. In [50], a fixed 11 Mbps IEEE 802.11b bit rate is selected for the drive-thru upload scenario based on the following observations: i) the loss rates for IEEE 802.11b bit rates (1, 2, 5.5, 11 Mbps) are similar; and ii) the IEEE 802.11g bit rates, though may be higher (up to 54 Mbps), all suffer from high loss rate (about 80%). In [1], it is observed that the original bit rate selection algorithm is not responsive enough to the vehicular communication environments, and higher rates are rarely selected. By a simple modification shown in Table 2.5, 75% improvement of TCP goodput can be achieved. However, an optimal MAC bit rate selection scheme which is suitable for the drive-thru Internet is still missing, and will be a challenging research task for future work.

2.2.2 Vehicular WiFi offloading

The roadside WiFi network and vehicles with high mobility constitute a practical solution to offload cellular data traffic, namely, vehicular WiFi offloading. The research issues mainly focus on strategies to improve the offloading performance, especially for non-interactive applications which can tolerate certain delays.

WiFi offloading schemes for non-vehicular users often focus on the availability and offloading performance of the current and next forthcoming AP, since the user is expected to have a relatively stable connection with one AP. This, however, does not apply to vehicular communication environments. Since VUs may meet multiple APs with different quality of connections within a short time period, offloading schemes should incorporate the

prediction of WiFi availability to better exploit multiple data transfer opportunities. Characteristics of data application, e.g., delay requirement, would have considerable impacts on offloading schemes. For example, non-interactive applications, such as email attachments, bulk data transfer, and regular sensing data upload, are often throughput-sensitive, whereas the delay requirements are not very stringent generally. For such applications, a good offloading scheme is to use WiFi as much as possible while guaranteeing that the delay requirement is not violated. On the other hand, interactive applications, such as VoIP and video streaming, are typically delay-sensitive. It is more challenging to design offloading schemes for such applications. We review the literature on vehicular WiFi offloading as follows.

There have been several vehicular offloading schemes proposed in the literature [102–104]. In [102], an offloading scheme called *Wiffler* is proposed to determine whether to defer applications for the WiFi connectivity instead of using cellular networks right away. Wiffler incorporates the prediction of the WiFi throughput potential on vehicles' route and considers delay requirements of different types of applications. An experiment is first conducted to study the availability and performance characteristics of WiFi and 3G networks, and shows that at more than half of the locations in the target city, at least 20% of 3G traffic can be offloaded through drive-thru WiFi networks, although the WiFi temporal availability is low (12% of the time) due to the vehicle mobility. Wiffler enables the delayed offloading and fast switching to 3G for delay-sensitive applications. The delay tolerance of data applications is determined according to VUs' preference or inferred from the application port information or binary names. The effective WiFi throughput, i.e., the volume of datahandled through WiFi APs before the delay period is expired, can be predicted by estimating the number of encountered APs. For the bursty AP encounters, the prediction is done assuming the inter-contact time durations in the future are the same as the history average. Using such a prediction, the traffic is offloaded to WiFi networks when $W > S \cdot c$, where W is the predicted effective WiFi throughput, S is the data size required to be transferred within the delay, and c is called *conservative quotient* to control the tradeoff between the offloading effectiveness and the application completion time. For delay-sensitive applications, a fast switching to 3G is used when the WiFi link-layer fails to deliver a packet within a predefined time threshold.

Motivated by the observation that the mobility and connectivity of vehicles can be well predicted, a prefetching mechanism is proposed in [103], in which APs along the predicted vehicle route cache the contents and deliver them to vehicles when possible. This benefits the WiFi offloading since the vehicle-to-AP bandwidth is often higher than the backhaul bandwidth, and vehicle-to-AP transmissions can use specialized transport protocols which are less sensitive to wireless losses than TCP (e.g., CTP which is discussed in Section 2.2.1).

The prefetching is based on the mobility prediction model, and to deal with the impact of prediction errors, the data is allowed to be redundantly prefetched by subsequent APs. However, as the WiFi backhaul capability has been greatly enhanced in recent years, the advantage of the prefetching solution might be reduced.

In [104], a vehicular WiFi offloading scheme is proposed from a transport layer perspective. A protocol called oSCTP is proposed to offload the 3G traffic via WiFi networks and maximize the user's benefit. The philosophy of oSCTP is to use WiFi and 3G interfaces simultaneously if necessary, and schedule packets transmitted in each interface every schedule interval. By modeling user utility and cost both as a function of the 3G and WiFi network usage, the user's benefit, i.e., the difference between the utility and the cost, is maximized through an optimization problem. The experimental evaluation shows a 63% to 81% offloaded traffic by using oSCTP, validating the effectiveness of the proposed offloading scheme.

It has been shown that merely using in situ WiFi APs cannot provide any performance guarantee of the drive-thru Internet. To achieve a satisfied and stable offloading performance, new and planned WiFi deployment has to be considered and in fact is already an ongoing effort. Since it is cost prohibitive to provide a ubiquitous WiFi coverage, how to deploy a set of WiFi APs to provide a better WiFi availability for vehicles has received many research attentions. For example, WiFi deployment strategies in vehicular communication environments are studied in [105]. A notion call *alpha coverage* is introduced, which guarantees the worse-case interconnection gap, defined as the distance or expected delay between two successive AP contacts experienced by moving vehicles on the road. The metric α is defined in the following way: a WiFi deployment that provides α-Coverage guarantees that there is at least one AP on any path which is of length at least α. Using such a metric to evaluate the AP deployment is reasonable. First, the delay in vehicular WiFi access is usually caused by intermittent connectivities; and second, with such a delay bound, the WiFi offloading potential can be well predicted given the connection time and throughput statistics of one AP connection. As discussed above, predictions of WiFi availability play a vital role in the design of offloading schemes, since such knowledge can facilitate to determine whether and how much to defer applications. Algorithms to achieve budgeted alpha coverage, that is, to find a set of bounded number of APs to provide the alpha coverage with minimum α, are also proposed and evaluated. The limitation of [105] is that the AP deployment is sparse so that the AP coverage radius is negligible compared to the distance between neighboring APs. This is not the case for urban scenarios where a cluster of APs may cover a dense area seamlessly. Optimizing the WiFi deployment for urban scenarios with diverse vehicle densities is a demanding task.

In summary, the drive-thru Internet has been experimentally evaluated, and several

WiFi offloading schemes for VUs have been proposed in the literature to improve the offloading performance. However, there is no related work that can theoretically answer the following questions: 1) how much can WiFi offload in vehicular environment; 2) if the VUs can tolerate certain delay, what is the relation between the offloading performance and the delay tolerance. A theoretical analysis of the performance of vehicular WiFi offloading is of great importance for the following reasons. First, offloading performance of scenarios with different AP deployment and vehicle mobility model can be theoretically analyzed, without the time consuming simulation or even complicated and pricey field test. Second, it can provide network operators with some guidance on WiFi deployment (e.g., the density of WiFi APs), pricing strategies, and incentive mechanisms. Finally, for VUs, the theoretical relation between offloading effectiveness (how much Internet access cost can be saved) and average service delay (how much service degradation the user is willing to tolerate) can provide guidelines for effectively and efficiently making offloading decisions.

2.3 Device-to-Device Communication

To address the intensive mobile data crunch, device-to-device (D2D) communication technology has been proposed as a promising paradigm as a part of next-generation cellular technologies. The basic tenet of D2D communications is that mobile users in proximity can communicate directly with each other on the cellular spectrum (or other spectrum bands) without traversing the base station (BS) or the cellular backhaul networks, as shown in Fig. 2.6. By utilizing the proximity of mobile users and direct data transmission, D2D communications can increase spectral efficiency and throughput, improve overall throughput and performance, improve energy efficiency, and reduce communication delay for mobile users [54]. Due to the advantages of D2D communications technology, it is suitable for many use cases, and can enable novel location-based and peer-to-peer applications and services. In [39], the applications and use cases of D2D communication are summarized, including peer-to-peer communication, content dissemination, multicasting, cellular offloading, machine-to-machine communication, and so forth.

A common taxonomy about D2D communications can be found in the literature [39,55]. In terms of spectrum bands employed, D2D communication can be divided into two categories, i.e., inband D2D communications and outband D2D communications. In the former, D2D communications employ the same spectrum bands of the cellular transmissions, while in the latter, other spectrum bands (WiFi, Blue-tooth) are utilized for data transmission to avoid interference to the cellular network. Note that in outband D2D communications, the cellular BS can still has a certain level of control over the D2D communications in

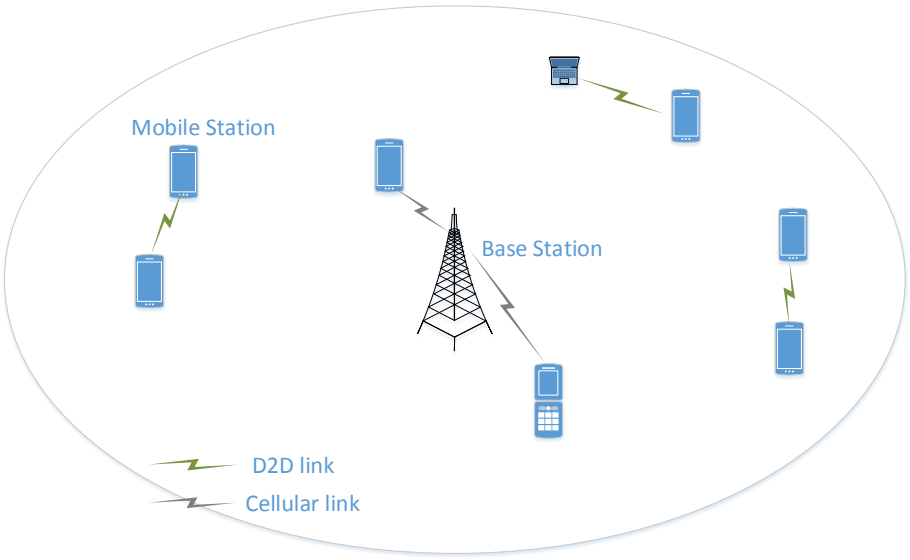

Figure 2.6: D2D communications in a cellular network.

processes such as neighbor discovery, connections setup, etc., leading to a controlled D2D mode. Otherwise, the D2D communications work in an autonomous mode. Inband D2D communications can be further divided into two categories according to the resource reuse pattern. If dedicated resources are allocated to D2D communications for exclusive use, overlay D2D communications are employed, and if D2D communications and conventional cellular transmissions reuse the same resources, it is called underlay D2D communications. In the literature, inband underlay D2D communications attract the most attention since underlay mode can achieve a higher spectrum efficiency.

D2D communication is well studied in the literature, and thus in this section we survey the literature, and discuss the research issues and existing solutions in D2D communication. In [106], D2D communication was first proposed to enable multi-hop communication in the cellular network. The applications and use cases of D2D communication are summarized in [39], including video dissemination, machine-to-machine communication, multicasting, cellular offloading, etc. Although D2D communication may be similar to Ad hoc networks and CRN, the main difference is D2D communication often involves the cellular network in the control panel. In terms of the spectrum resources used, D2D communication can be categorized into inband underlay D2D where D2D and cellular communication share the same spectrum resource [107], inband overlay D2D where part of cellular resources are

dedicated to D2D communications [108], and outband D2D where D2D communication is carried out over ISM spectrum [109]. Among the three, inband underlay D2D is studied by the majority of the literature. It is more spectral efficient than inband overlay D2D since the spectrum resources are reused. On the other hand, inband D2D can provide guaranteed QoS where outband D2D normally cannot due to the uncontrolled nature of the unlicensed spectrum. In the following, we focus on the literature survey of inband underlay D2D communication.

2.3.1 Spectrum Efficiency

Using inband underlay D2D communications, the cellular spectrum efficiency can be increased by exploiting spatial diversity. To achieve this, a series of issues should be addressed, such as interference management, mode selection, resource allocation, etc.

In [56], the authors propose to use the cellular uplink for D2D communications. Received downlink signal power is used for D2D users to determine their pathloss to the cellular base station. Then based on the pathloss, D2D users will adjust their transmit power so that they can communication directly with each other during the uplink frame without causing much interference to the base station. In [107], the mutual interference between cellular and D2D subsystem is addressed when cellular uplink resource is reused for D2D transmissions. Specifically, two interference avoidance mechanisms are proposed to address D2D-cellular and cellular-D2D interference, namely tolerable interference broadcasting approach and interference tracing approach, respectively. In tolerable interference broadcasting approach, the cellular BS calculates and updates the tolerable D2D interference level of each resource unit and broadcasts the table that contains such information. Upon receiving the table, each D2D user equipments (UEs) can calculate the expected interference due to the pathloss to BS and the transmit power. The D2D UEs will prefer to use the resource unit where the expected interference is much lower than tolerable D2D interference level. In interference tracing approach, D2D UEs measure the interference caused by cellular UEs in a certain period and record the average interference. This information is utilized by D2D UEs when choosing communication resource unit to avoid harmful interference from cellular UEs.

In [110], the authors formulate the interference relationships between D2D and cellular links by an interference-aware graph, and propose a near optimal resource allocation algorithm accordingly to obtain the resource assignment solutions at the BS with low computation complexity. In the interference-aware graph, each vertex represents a cellular or D2D link, and each edge has a weight indicating the potential mutual interference between

the two vertices. Simulation results show that the proposed algorithm can achieve the sum rate close to the optimal resource sharing scheme. In [111], a network-assisted method is proposed to intelligently manage resources of devices. Resource units and power are jointly allocated to guarantee the signal quality of all users. In [112], the cellular BS monitors the common control channel and broadcasts the allocated resources. Based on the information, D2D users perform radio resource management to avoid interference to cellular UEs.

2.3.2 Power Efficiency

Power efficiency is very crucial in wireless networks because a higher power efficiency can reduce the power consumption of mobile devices, improve the battery lifetime, and reduce the greenhouse gas emission. Power efficiency enhancement is also a very interesting topic in D2D underlaying cellular networks. In [113], a power optimization scheme with joint resource allocation and mode selection is proposed for OFDMA system with D2D communication integrated. The proposed heuristic algorithm first adopts existing subcarrier allocation and adaptive modulation to allocate subcarriers and bits, and then selects transmission mode for each D2D pair, where if the required transmit power of D2D transmission is higher than a certain threshold, cellular mode is employed to avoid harmful interference. Through simulation, it is shown that 20% power can be saved compared to the traditional OFDMA system without D2D communication.

In [114], a power-efficient mode selection and power allocation scheme are proposed for D2D underlaying cellular networks. First, the optimal power to achieve the maximum power efficiency for all possible modes of each device is calculated by utilizing the concavity of the upper- and lower-bound of power efficiency. Then, the transmission mode sequence is selected by exhaustive search to achieve the maximal power efficiency. The authors show that the proposed joint power allocation and mode selection scheme can perform close to the upper bound in terms of power efficiency. In [115], a joint mode selection, scheduling and power control task for D2D underlaying cellular networks is formulated as an optimization problem and solved. A centralized optimal framework is proposed with the assumption of the availability of a central entity. Then, a sub-optimal distributed with low computational complexity is developed. Via the simulation, the authors show that the proposed method can achieve significant gain of power efficiency over traditional cellular network when the D2D communication distance is no longer than 150 meters.

2.3.3 D2D Communication for VANETs

Due to the advantages of the D2D technology, it is suitable for many vehicular use cases, and can enable novel location-based and peer-to-peer applications and services. For example, considering the huge number of connected smart cars (90% new cars in 2020), the update of smart cars software can put a significant burden on the cellular network, and cost a lot of money of car manufacturers and car owners. Thus, the software update package can be first downloaded by chosen vehicles, and exchanged among other vehicles by vehicular D2D (V-D2D) communications. In the process, the cellular network can apply efficient algorithms to choose downloading vehicles, assist pair devices to reduce delay, and allocate resources (sub-carriers) to mitigate interference, satisfy different QoS requirements, and optimize the performance. In this way, most of the traffic can be offloaded to local V-D2D transmissions, and thus much cellular bandwidth and money can be saved. Moreover, due to the loose delay requirement of software update, the vehicular delay tolerant network (VDTN) can be employed where the package can be disseminated in a store-carry-and-forward manner, which can further offload the cellular network and save the cost. Another type of data service is gaming and video/audio streaming among vehicular users, such as in the vehicular proximity social network [116]. Normally, these services are supported by DSRC or WiFi-direct communication, which may not satisfy the requirements due to the collisions and long device paring time. With V-D2D communication, such services can be better sustained due to cellular-controlled connection setup with shorter delay, and resource (sub-carrier) allocation which can support varied rates.

There are several research works that investigate the issues of applying D2D communications in VANETs. In [117], Cheng *et al.* studied the feasibility of D2D communication for the intelligent transportation systems (ITS), considering the spatial distribution of vehicles, and the channel characteristics given the high mobility of vehicles. Through a simulation study, it is observed that the D2D-underlay mode achieves the highest spectrum efficiency, and the data rate increases with the decrease of D2D distance. In addition, the average spectrum efficiency first increases, then decreases with the increase of V-D2D link density, due to that when V-D2D link density is high, the interference becomes severer. In [118], Sun *et al.* proposed a spectrum resource allocation scheme for both cellular user equipments (CUEs) and vehicular UEs, in order to maximize the CUEs' sum rate while guarantee the strict delay and reliability requirements of VUEs' services. In [119], Ren *et al.* proposed a joint channel selection and power control framework to achieve optimal performance of V-D2D system, where a series simplifications are made to reduce the requirement of full channel state information (CSI).

2.4 Summary

This chapter has surveyed the existing literature for the enabling technologies, CR, WiFi, and D2D communication for opportunistic spectrum utilization. By focusing on the related works on VANETs, we aim to reach a better understanding of the lack and weakness in the current study of this area, and motivate our own contributions.

Chapter 3

Opportunistic Spectrum Utilization for CR-VANETs

In this chapter, we investigate the opportunistic spectrum access for cognitive radio vehicular ad hoc networks (CR-VANETs). The probability distribution of the channel availability is first derived by means of a finite-state continuous-time Markov chain (CTMC), jointly considering the mobility of vehicles, and the spatial distribution and the temporal channel usage pattern of primary transmitters. Utilizing the channel availability statistics, we propose a game theoretic spectrum access scheme for vehicles to opportunistically access licensed channels in a distributed manner. Specifically, the spectrum access process is modeled as a non-cooperative congestion game. The existence of Nash equilibrium is proved and its efficiency is analyzed when employing uniform medium access control (MAC) protocol and slotted ALOHA, respectively. Furthermore, a spectrum access algorithm is devised to achieve a pure Nash equilibrium with high efficiency and fairness. Simulation results validate our analysis and demonstrate that the proposed spectrum access scheme can achieve higher utility and fairness, compared with a random access scheme.

3.1 Introduction

Cognitive radio is a promising approach to deal with the spectrum scarcity, which enables unlicensed users to opportunistically exploit the spectrum owned by licensed users [59,60]. With CR technology, VANETs have been coined as CR-VANETs, whereby vehicles can opportunistically access additional licensed spectrum owned by other systems, such as

digital television (DTV) and 3G/4G cellular networks. Considering the highly dynamic mobility, vehicles are expected to exploit more spatial and temporal spectrum opportunities along the road than stationary SUs.

The opportunistic spectrum access for CRNs has been extensively studied [42–44]. However, the results may not be directly applied to CR-VANETs due to the distinctive features of VANETs. The common assumption in the the study of CRNs is that SUs are stationary and thus the spectrum opportunity is only affected by the spectrum usage patterns of the primary network. However, due to the mobility of vehicles, the spectrum opportunity may vary temporally and spatially, making the opportunistic spectrum access problem more challenging in CR-VANETs. On the other hand, the unique mobility features of vehicles can facilitate the spectrum access if used properly. Since the vehicles move along the roads, and the speeds of vehicles can usually be modeled accurately, the spectrum opportunities for moving vehicles can be tractable. With the assistance of GPS system and digital maps, the spectrum access can be scheduled in advance, in order that the optimal spectrum bands are selected, and the number of switches among selected channels is minimized.

In this chapter, we investigate the efficient utilization of licensed spectrum bands for VANETs using cognitive radio. We first study the channel availability for CR-VANETs in urban scenarios, taking the mobility pattern of vehicles into consideration. Exploiting the statistics of the channel availability, a distributed opportunistic spectrum access scheme based on a non-cooperative congestion game is proposed for vehicles to exploit spatial and temporal access opportunities of the licensed spectrum. Specifically, we consider a grid-like urban street pattern to model the downtown area of a city. Vehicles equipped with a cognitive radio, moving in the grid, opportunistically access the spectrum of the primary network. The probability distribution of the channel availability is obtained by means of a continuous-time Markov chain (CTMC). Then, we employ a non-cooperative congestion game to solve the problem of vehicles accessing multiple channels with different channel availabilities. We prove the existence of the pure Nash equilibrium (NE) and analyze the efficiency of different NEs, when applying uniform MAC and slotted ALOHA, respectively. A distributed spectrum access algorithm is then developed for vehicles to choose an access channel in a distributed manner, so that a pure NE with high efficiency and fairness is achieved. Finally, simulation results validate our analysis and demonstrate that, with the proposed spectrum access scheme, vehicles can achieve higher utility and fairness compared with the random access.

Our contributions are mainly three-fold. First, this work studies the channel availability for CR-VANETs in urban scenarios, which is crucial for devising an efficient spectrum access scheme. Second, based on the statistics of channel availability, a distributed spec-

Table 3.1: The useful notations for Chapter 3

Symbol	Description
$\mathcal{K}$	The set of licensed channels in the network, $\|\mathcal{K}\| = K$
$\lambda_{idle,i}$, $\lambda_{busy,i}$	Parameter of distribution of PTs' usage pattern of channel i
$L_{PH,i}$, $L_{PV,i}$	The horizontal and vertical distance between neighboring PTs on channel i
L_H, L_V	The horizontal and vertical length of the road segments
R_i	The approximate transmission range of PTs on channel i
v	Vehicle speed
$T_{in,i}$, $T_{out,i}$	Time duration in which vehicle remains within/outside the coverage of PTs on channel i
Ψ_i	Effective channel availability (ECA) of channel i
$\mathcal{C}$	Set of available channels in the spectrum access game, $\mathcal{C} \in \mathcal{K}$, $\|\mathcal{C}\| = C$
$\mathcal{N}$	Set of vehicles participating in the game, $\|\mathcal{N}\| = N$
R_v	The transmission range of the vehicle
ρ_v	The vehicle density on the road
U_j^i	The utility vehicle j obtains by choosing channel i
$r(n)$	Resource allocation function. It corresponds to specific MAC scheme
$n(S)$	Congestion vector corresponding to strategy profile S
$\mathcal{E}_S$	Efficiency of strategy profile S
F	Fairness index among vehicles
Φ	Channel diversity

trum access scheme is proposed in CR-VANETs from a game theoretic perspective, and the existence of pure NE is proved. Third, a spectrum access algorithm is introduced to achieve a pure NE with high efficiency and fairness. As the automotive industry gears for supporting high-bandwidth applications, with our proposed scheme applied, the QoS of VANETs applications can be improved by efficiently utilizing the spectrum resource of the licensed band.

The remainder of the chapter is organized as follows. The detailed description of the system model is provided in Section 3.2. In Section 3.3, channel availability is analyzed for CR-VANETs in urban scenarios. A spectrum access scheme based on game theory is presented in Section 3.4. Simulation results are given in Section 3.5. Section 3.6 concludes the chapter.

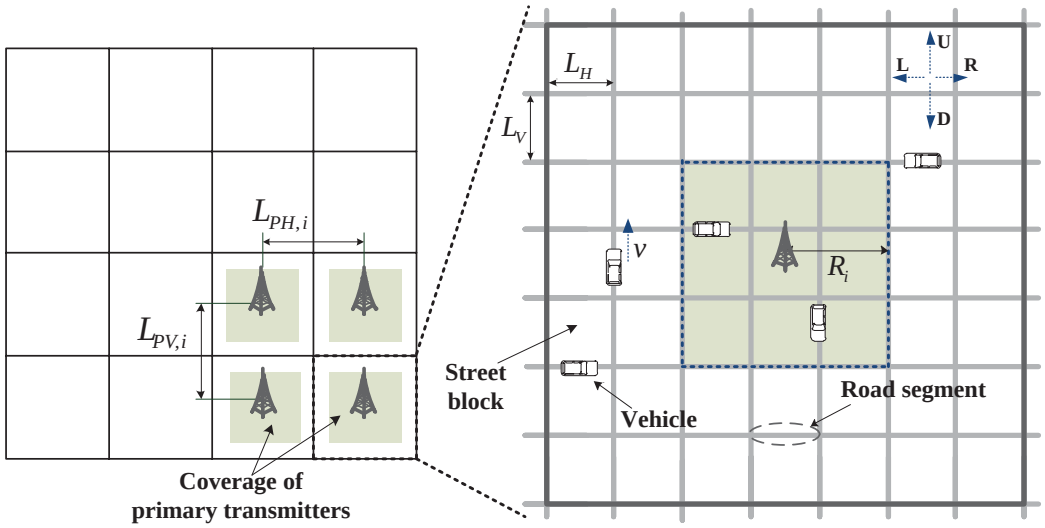

Figure 3.1: Regularly distributed PTs on channel i.

3.2 System Model

In urban scenarios of CR-VANETs, the transmitters of the primary network are referred to as primary transmitters (PTs), such as TV broadcasters and cellular base stations. As SUs, vehicles equipped with a cognitive radio can opportunistically access the licensed spectrum. There is a non-empty set $\mathcal{K}$ of licensed channels that can be accessed by vehicles opportunistically. The channel usage behavior of primary users and vehicle mobility lead to intermittent channel availability for vehicles. The spectrum opportunity is characterized by the *channel availability* experienced by a vehicle, which is defined as the lengths of time duration in which the channel is available or unavailable for that vehicle. The availability of channel $i, i \in \mathcal{K}$, for a vehicle is determined by the spatial distribution and the temporal channel usage pattern of PTs that operate on channel i, as well as the mobility of the vehicle. A summary of the mathematical notations used in this paper is given in Table 3.1.

3.2.1 Urban Street Pattern

A grid-like street layout is considered for analyzing CR-VANETs in urban environments, like the downtown area of many cities, such as Houston and Portland [120]. The network geometry comprises of a set of horizontal roads intersected with another set of vertical

roads. As shown in Fig. 3.1, each line segment represents a road segment (the road section between any two neighboring intersections) with bi-directional vehicle traffic. In addition, all the horizontal segments have the same length L_H, and all the vertical segments have the same length L_V, leading to equal-sized street blocks of $L_H \times L_V$. For example, L_H and L_V are generally from 80 m to 200 m for the downtown area of Toronto [121].

3.2.2 Spatial Distribution of PTs

We consider that PTs operating on a generic channel i are regularly distributed in the grid, as shown in Fig. 3.1. The distance between any two neighboring PTs in the horizontal direction and vertical direction is denoted by $L_{PH,i}$ and $L_{PV,i}$, respectively. Denote by R_i the transmission range of PTs on channel i. The coverage area of the PT is approximated by a square area with side length $2R_i$, where $R_i < \min(L_{PH,i}, L_{PV,i})$ to avoid overlapping of different coverage regions of PTs. The non-overlapping feature of PT coverage areas is common in practice. For example, in the modern cellular system, frequency reuse is employed to reduce inter-cell interference. Therefore, for a give channel, the coverage is only κ of the area, where κ is the frequency reuse factor. The approximate coverage area is larger than the real coverage area to protect the primary transmission. A similar approximation of the PT coverage area can be found in [122].

3.2.3 Temporal Channel Usage Pattern of PTs

The temporal channel usage of PTs operating on a generic channel i is modeled as an alternating busy (the PT is active in transmitting) and idle (the PT does not transmit) process [123] [67]. During the transmission period of a PT, vehicles in the coverage area of the PT are not permitted to use the same channel in order to avoid the interference to the primary network. The length of busy/idle period is modeled as an exponential random variable with parameters $\lambda_{busy}/\lambda_{idle}$, i.e.,

$$T_{busy,i} \sim Exp(\lambda_{busy,i}) \text{ and } T_{idle,i} \sim Exp(\lambda_{idle,i}),$$

where $X \sim Exp(\lambda)$ indicates that variable X follows an exponential distribution with parameter λ. $\varpi_{idle,i} = \frac{\lambda_{busy,i}}{\lambda_{idle,i}+\lambda_{busy,i}}$ and $\varpi_{busy,i} = 1-\varpi_{idle,i}$ are the steady-state probabilities that a PT on channel i is active and inactive, respectively.

3.2.4 Mobility Model

Vehicles move in the grid at a random and slowly changing speed v, where $v \in [v_{min}, v_{max}]$. The average value of v is denoted by $\overline{v}$. At each intersection, vehicles randomly select a direction to move on another road segment. Particularly, a vehicle chooses the direction of north, south, east and west with probability P_n, P_s, P_e, and P_w, respectively, as shown in Fig. 3.1. It holds that $P_n + P_s + P_e + P_w = 1$. Once the vehicle chooses a direction at an intersection, it moves straight until it arrives at the next intersection.

3.3 Channel Availability Analysis

The statistics of channel availability can be utilized to design an efficient spectrum access scheme to improve the QoS of SUs and the spectrum utilization. In this section, we analyze the availability of channel i for vehicles in urban scenarios, jointly considering the spatial distribution and the temporal channel usage pattern of PTs, and the mobility of vehicles. It is assumed that PTs operating on the same channel belong to the same type of system and have the same spatial distribution and temporal channel usage pattern. A similar assumption can be seen in [124]. A continuous-time Markov chain that consists of three states is employed. Denote by S_{Idle}, S_{Busy}, and $S_{\overline{C}}$ the states of a vehicle in the coverage of an idle PT, in the coverage of an active PT, and outside the coverage of any PT that operates on channel i, respectively, as shown in Fig. 3.2. It can be seen that when the vehicle moves along the street, the state transits to one another. Since the channel is unavailable only when the vehicle is in S_{Busy}, we can further merge S_{Idle} and $S_{\overline{C}}$ as one state in which the channel is available for the vehicle, which is denoted by S_A. The state of the channel being unavailable is denoted by S_U, which corresponds to the state S_{Busy}.

Denote the time duration that a vehicle remains in S_A and S_U by $T_{A,i}$ and $T_{U,i}$, respectively. To obtain the channel availability, i.e., the probability distribution of $T_{A,i}$ and $T_{U,i}$, it is necessary to analyze the transition rates among the three states: S_{Idle}, S_{Busy}, and $S_{\overline{C}}$. Denote by $T_{in,i}$ and $T_{out,i}$ the time durations in which the vehicle remains within the coverage area of a PT and outside the coverage area of any PT on channel i, respectively. Therefore, the transition rates are closely related to the probability distribution of $T_{in,i}$ and $T_{out,i}$. In the following, we focus on the analysis of these two time durations in urban scenarios.

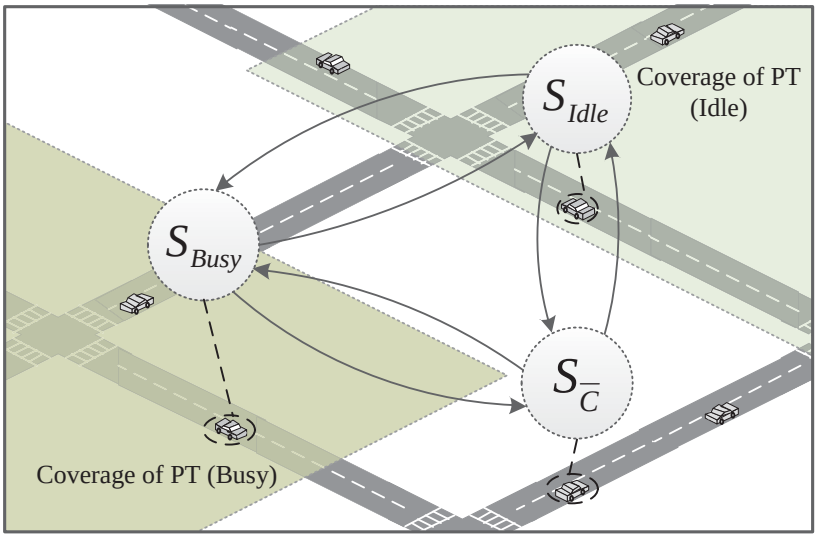

Figure 3.2: The states of a vehicle w.r.t. the mobility.

3.3.1 Analysis of T_{in} in Urban Scenarios

To analyze T_{in}, we consider the case in which vehicles move within the coverage of a PT. Denote by Ω_R the coverage area of the PT. Recall that Ω_R is a square with side length $N_{R,i}$. For ease of the analysis, let $L_V = L_H = L$, and $L_{PH,i} = L_{PV,i} = L_{P,i}$. All lengths are normalized by L, for example, $N_{R,i} = \lceil \frac{2R_i}{L} \rceil$.

In order to analyze T_{in}, a two-dimensional discrete Markov chain is employed, as shown in Fig. 3.3. We index all the intersections within Ω_R, and let each intersection (b, k) be a state $C_{b,k}$. All these states form a Markov chain $\mathbb{C}_{b,k} = \{C_{1,1}, C_{1,2}, \ldots, C_{1,N_{R,i}}, C_{2,1}, C_{2,2}, \ldots, C_{N_{R,i},N_{R,i}}\}$. It is said that a vehicle is in state $C_{b,k}$ if it is moving from intersection (b, k) to a neighboring intersection (b', k'). When the vehicle arrives at intersection (b', k'), the state transits from $C_{b,k}$ to $C_{b',k'}$. The states that lie on the boundary of Ω_R are referred to absorbing states which indicate that the vehicle moves out of the PT coverage area. Let $\mathbf{Q_A}$ be the set of absorbing states. Denote by M the number of transitions it takes before the vehicle leaves Ω_R, i.e., transits to any state in $\mathbf{Q_A}$. T_{in} can be approximated by $M * \Delta t$, where Δt is the time that the vehicle moves through a road segment. To obtain the probability distribution of T_{in}, we need to find the probability distribution of M. To this end, we first

obtain the transition probabilities of $\mathbb{C}_{b,k}$ as follows:

$$\begin{cases} P(C_{b,k-1}|C_{b,k}) = P_l \\ P(C_{b,k+1}|C_{b,k}) = P_r \\ P(C_{b-1,k}|C_{b,k}) = P_u \quad C_{b,k} \notin \mathbf{Q_A} \\ P(C_{b+1,k}|C_{b,k}) = P_d \\ P(other|C_{b,k}) = 0 \end{cases} \tag{3.1}$$

$$\begin{cases} P(C_{b,k}|C_{b,k}) = 1 \qquad C_{b,k} \in \mathbf{Q_A}, \\ P(\text{other}|C_{b,k}) = 0 \end{cases} \tag{3.2}$$

which infers that the transition matrix $\mathbf{P}$ is sparse. Denote by $\pi^{(m)}$ the probability distribution of the states after m transitions. Specifically, $\pi^{(0)}$ is the probability distribution of the initial states. It holds that $\pi^{(m)} = \pi^{(0)}\mathbf{P}^m$. At initial time t_0, it is possible for the vehicle to be in any state in Ω_R except those in $\mathbf{Q_A}$. Denote by $\mathbf{Q_I}$ the set of these possible initial states. Then the cardinality of $\mathbf{Q_I}$, denoted by C_I, can be calculated by $C_I = |\mathbf{Q_I}| = (N_{R,i} - 2)^2$. All possible initial states are considered to be with equal probability, and thus $\pi^{(0)}$ can be obtained as follows:

$$\pi^{(0)}_{(b,k)} = \begin{cases} p_I = \frac{1}{C_I} = \frac{1}{(N_{R,i}-2)^2} & C_{b,k} \in \mathbf{Q_I} \\ 0 & \text{otherwise,} \end{cases}$$

where p_I is the probability of each possible initial state. The probability of the event that M is no more than m is given by

$$\mathbf{Pr}(M \leq m) = \sum_{C_{b,k} \in \mathbf{Q_A}} \pi^{(m)}.$$

Therefore, the probability mass function of M is

$$\begin{aligned} \mathbf{Pr}(M = m) &= \mathbf{Pr}(M \leq m) - \mathbf{Pr}(M \leq m-1) \\ &= \sum_{C_{b,k} \in \mathbf{Q_A}} \pi^{(m)} - \sum_{C_{b,k} \in \mathbf{Q_A}} \pi^{(m-1)}. \end{aligned} \tag{3.3}$$

On the other hand, if all the states in $\mathbf{Q_A}$ are considered as one state S_{End} and all other states as another state S_{Begin}, the two-dimensional Markov chain $\mathbb{C}_{b,k}$ can be reduced to a two-state Markov chain $\{S_{Begin}, S_{End}\}$. The vehicle is in S_{Begin} at the beginning. In

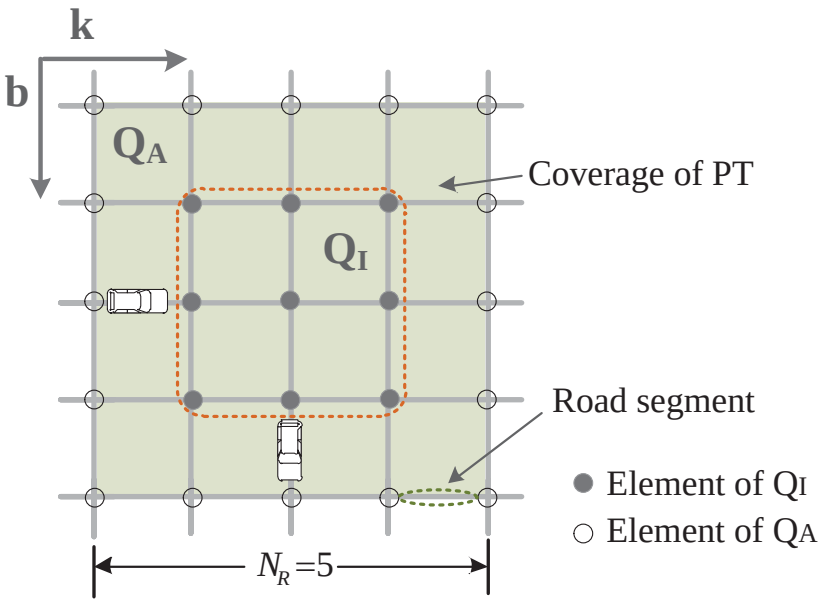

Figure 3.3: Analysis of T_{in}: a two-dimensional Markov chain.

each transition, it either transits to S_{End} with probability p_0 or remains in S_{Begin} with probability $1 - p_0$, where p_0 is as follows:

$$p_0 = \frac{1}{C_I} \sum_{C_{b,k} \in \mathbf{Q_I}} \sum_{C_{b',k'} \in \mathbf{Q_A}} P(C_{b',k'} | C_{b,k}).$$

The vehicle does not stop moving until the state transits to S_{End}. Thus, the number of transitions before the vehicle leaves the PT coverage area can be considered to follow a geometric distribution with $p = p_0$. From this perspective, T_{in} may be approximated by an exponential distribution, which will be discussed later.

3.3.2 Analysis of T_{out} in Urban Scenarios

A two-dimensional Markov chain is also employed to analyze T_{out}. Since PTs operating on the same channel are regularly deployed, we can just take the area around one PT to analyze, as shown in Fig. 3.4. Denote this square area by Ω_D, with side length $N_{D,i} = \lceil \frac{L_{P,i}}{L} \rceil$. We consider that Ω_D is a torus: when a vehicle leaves the boundary of Ω_D, it moves into Ω_D on the same road from the opposite side of the area. In this situation, the

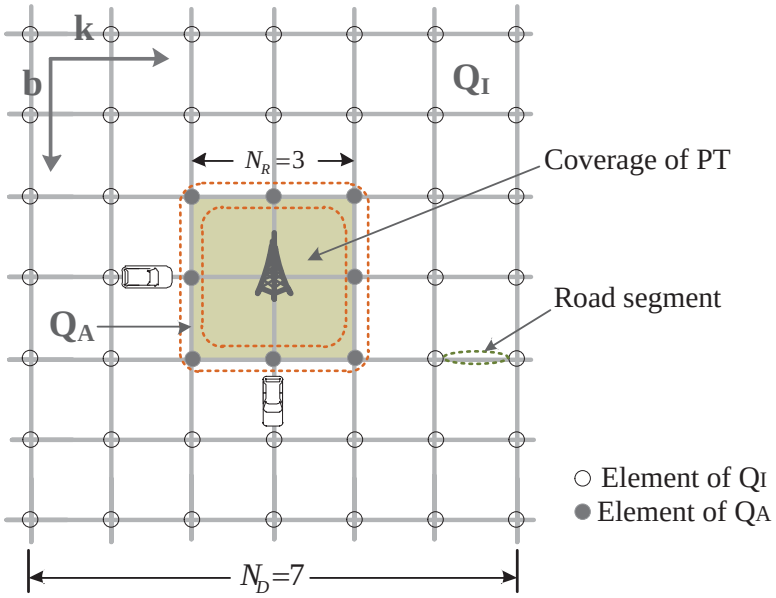

Figure 3.4: Analysis of T_{out}: a two-dimensional Markov chain.

intersections that lie on the boundary of Ω_R are referred to as absorbing states indicating that vehicles in these states move into the coverage of a PT. We can get the transition matrix $\mathbf{P}$, which is similar to (3.1) and (3.2) except

$$\begin{cases} P(C_{b,N_D}|C_{b,1}) = P_l \\ P(C_{b,1}|C_{b,N_D}) = P_r \\ P(C_{N_D,k}|C_{1,k}) = P_u \\ P(C_{1,k}|C_{N_D,k}) = P_d. \end{cases} \tag{3.4}$$

States which are within Ω_D but outside Ω_R are initial states. Similar to the analysis of T_{in}, the possible initial states are with equal probability. Denote by $\mathbf{Q_I}$ the set of possible initial states, and $|\mathbf{Q_I}| = N_{D,i}^2 - N_{R,i}^2$. Then the probability distribution of initial states, denoted by $\pi^{(0)}$, is as follows:

$$\pi_{(b,k)}^{(0)} = \begin{cases} p_I = \frac{1}{N_{D,i}^2 - N_{R,i}^2} & C_{b,k} \in \mathbf{Q_I} \\ 0 & \text{otherwise.} \end{cases}$$

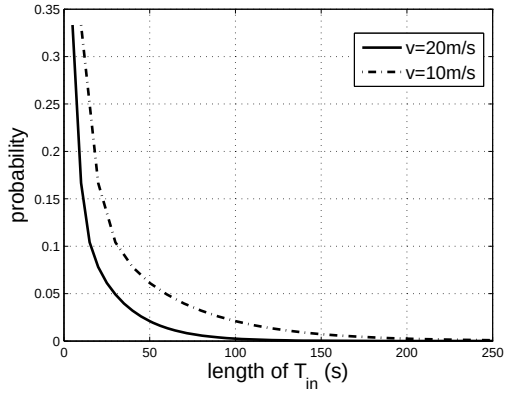

(a) PDF of T_{in}.

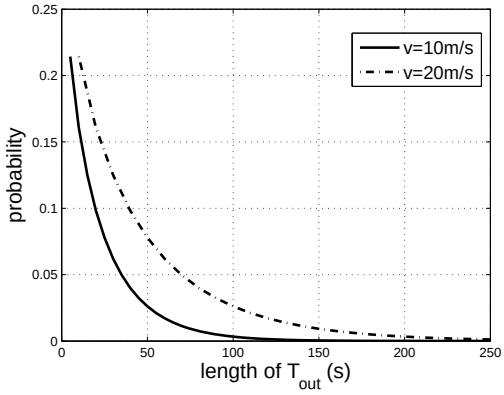

(b) PDF of T_{out}.

Figure 3.5: PDF of T_{in} and T_{out} ($L = 100$ m).

M' denotes the number of transitions before a vehicle moves into the coverage area of a PT. Similar to (3.3), we can get the probability mass function of M' as follows:

$$\begin{aligned}\mathbf{Pr}(M' = m) &= \mathbf{Pr}(M' \leq m) - \mathbf{Pr}(M' \leq m-1) \\ &= \sum_{C_{b,k} \in \mathbf{Q_A}} \pi^{(m)} - \sum_{C_{b,k} \in \mathbf{Q_A}} \pi^{(m-1)}. \end{aligned} \tag{3.5}$$

3.3.3 Estimation of λ_{in} and λ_{out}

The probability density function (PDF) of T_{in} and T_{out} from (3.3) and (3.5) are shown in Fig. 3.5. It can be seen that both T_{in} and T_{out} can be approximated by an exponential distribution. Furthermore, the parameter of the distribution can be estimated by using Maximum Likelihood Estimation (MLE) as follows:

$$\lambda = \frac{1}{\overline{x}},$$

where $\overline{x}$ is the sample mean, and λ is the estimated parameter of the exponential distribution. More interestingly, the expected value of T_{in} and T_{out} (denoted by $\overline{T}_{in}$ and $\overline{T}_{out}$, respectively) change with vehicle speed $\overline{v}$, and the spatial parameters of PTs, i.e., R_i and $L_{P,i}$. Specifically, the parameters of the two exponential distributions can be approximated

Table 3.2: χ^2 tests of T_{in} and T_{out}.

	T_{in}	T_{out}
df	6	7
χ^2	10.799	9.4629
h	0	0

by

$$\lambda_{in} \approx \frac{\overline{v}}{R_i} \text{ and } \lambda_{out} \approx \frac{\overline{v}}{f(L_{P,i} - R_i)}.$$

When $L_{p,i} - R_i < 5L$, $f(\cdot)$ is linear, and we have

$$\lambda_{out} \approx \frac{\overline{v}}{17.4(L_{P,i} - R_i) - 16.4}.$$

Fig. 3.6 shows the comparison of cumulative distribution functions (CDF) of simulation results, analytical results and approximate exponential distribution of T_{in} and T_{out}, respectively. It can be seen that they closely match each other, which validates the accuracy of the estimation. To further show the exponential distribution of T_{in} and T_{out}, we have done chi-square tests, the results of which are shown in Table 3.2. It can be seen that for both T_{in} and T_{out}, the hypothesis is rejected, which shows strong evidence that they follow the exponential distributions. The effect of R_i ($N_{R,i}$) and $L_{P,i}$ ($N_{D,i}$) on $\overline{T}_{in}$ and $\overline{T}_{out}$ is shown in Fig. 3.7(a) and 3.7(b), respectively. A larger value of R_i leads to a larger value of $\overline{T}_{in}$, while a larger value of $L_{P,i}$ leads to a larger value of $\overline{T}_{out}$, which is consistent with our expectation.

3.3.4 Derivation of Channel Availability

From the above analysis, the transition rates among the states in the Markov chain shown in Fig. 3.2 can be obtained, as listed in Table 3.4. Denote by ζ_i the average fraction of the area of PT coverage on channel i, and $\zeta_i = \frac{4R_i^2}{L_{p,i}^2}$. Thus, the average fraction of areas where channel i is available at any given time, denoted by δ_i, can be given by:

$$\delta_i = (1 - \zeta_i) + \zeta_i \varpi_{idle,i} = 1 - \zeta_i \varpi_{busy,i}, \tag{3.6}$$

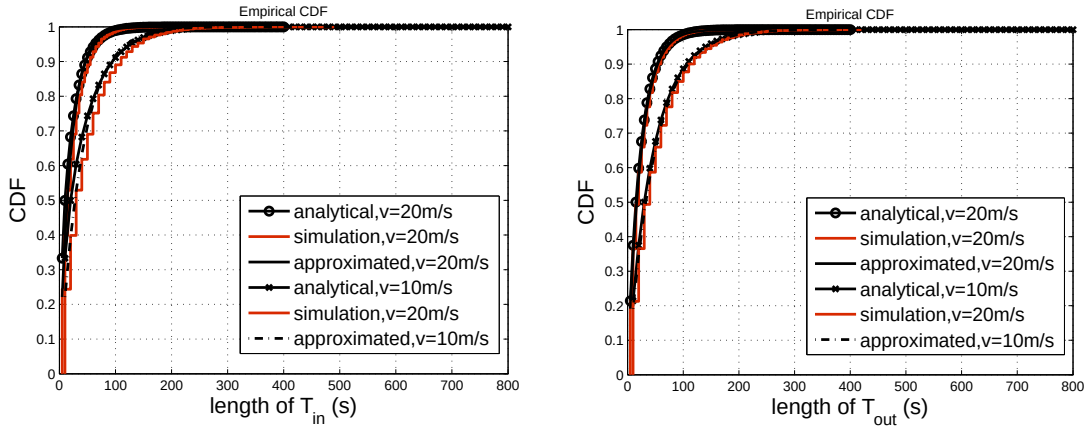

(a) CDF of T_{in}. (b) CDF of T_{out}.

Figure 3.6: Comparison of analytical and approximate results.

The state $S_{U,i}$ ends up when the vehicle moves out of the coverage of the PT or the PT stops transmission. Therefore, $T_{U,i}$ follows an exponential distribution with parameter $\lambda_{U,i}$ where:

$$\lambda_{U,i} = \lambda_{busy,i} + \frac{\overline{v}}{R_i}.$$

Based on the balance condition $\varpi_{A,i}\lambda_{A,i} = \varpi_{U,i}\lambda_{U,i}$, where $\varpi_{A,i} = \delta_i$ and $\varpi_{U,i} = 1 - \delta_i$, we can get the $S_{A,i} \rightarrow S_{U,i}$ transition rate $\lambda_{A,i}$ as follows:

$$\lambda_{A,i} = \frac{\delta_i}{1-\delta_i}\lambda_{U,i} = \frac{\zeta_i \varpi_{busy,i}}{1 - \zeta_i \varpi_{busy,i}}\left(\lambda_{busy,i} + \frac{\overline{v}}{R_i}\right), \tag{3.7}$$

and thus, $T_{A,i} \sim Exp(\lambda_{A,i})$. Fig. 3.8 shows the comparison between analytical and simulation results. The two curves closely match to each other for both $T_{A,i}$ and $T_{U,i}$, which demonstrates the accuracy of the analysis. We have also done chi-square tests for $T_{A,i}$ and $T_{U,i}$, the results of which are shown in Table 3.3.

Define the effective channel availability (ECA) Ψ of channel i as the average time duration in which channel i is available for a vehicle to access, which can be calculated as follows:

$$\Psi_i = \eta_i \cdot \overline{T}_{A,i} = \frac{\eta_i}{\lambda_{A,i}}, \tag{3.8}$$

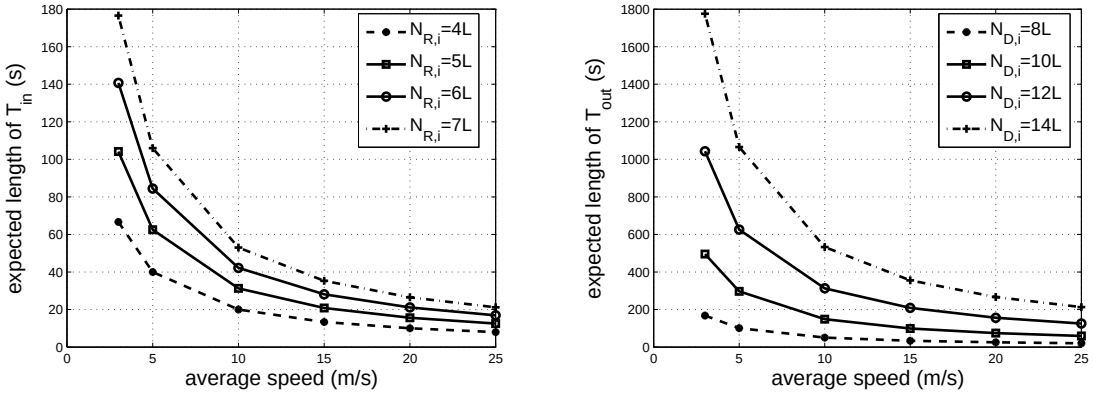

(a) Impact of $N_{R,i}$ on $\overline{T}_{in}$.

(b) Impact of $N_{D,i}$ on $\overline{T}_{out}$.

Figure 3.7: Impact of $N_{R,i}$ and $N_{D,i}$ on $\overline{T}_{in}$ and $\overline{T}_{out}$.

Table 3.3: χ^2 tests of T_A and T_U.

	T_A	T_U
df	3	3
χ^2	7.6257	3.5832
h	0	0

where $\eta_i \in (0, 1)$ is the interference factor representing the tolerance level of interference of primary network. Note that a larger value of η brings more spectrum opportunities, but at the same time results in more interference to the primary network.

Considering a real-world road map can facilitate a more precise analysis of channel availability. This, however, introduces cumbersome challenges. Our approach is based on a simple regular road pattern, which offers a workable approximation.

3.4 Game Theoretic Spectrum Access Scheme

From the previous section, the channel availability statistics, i.e., ECA of each channel, are obtained. Assume that vehicles are aware of the spatial distribution and temporal channel usage pattern of PTs of each channel, i.e., $L_{PH,i}$, $L_{PV,i}$, R_i, $\lambda_{busy,i}$ and $\lambda_{idle,i}$, since the information of primary networks can be obtained from network operators. With such

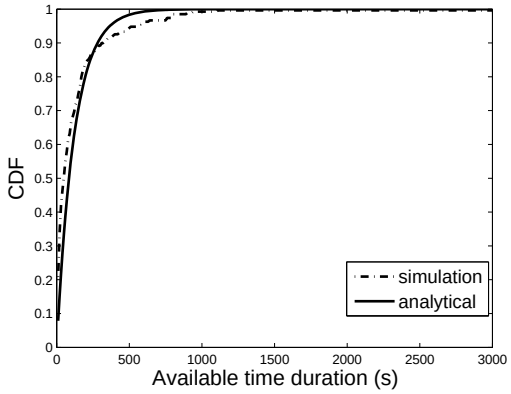

(a) T_A: channel available period.

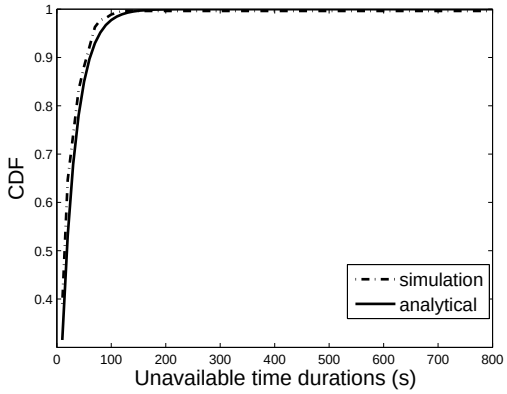

(b) T_U: channel unavailable period.

Figure 3.8: The analytical and simulation results of T_A and T_U.

Table 3.4: State transition rates of a vehicle for channel i

State Transition	Rate
$S_{idle} \rightarrow S_{busy}$	$\lambda_{idle,i}$
$S_{busy} \rightarrow S_{idle}$	$\lambda_{busy,i}$
$S_{busy} \rightarrow S_{\overline{C}}$	$\frac{\overline{v}}{R_i}$
$S_{\overline{C}} \rightarrow S_{busy}$	$\frac{\overline{v}}{f(L_{p,i}-R_i)}\varpi_{busy,i}$
$S_{idle} \rightarrow S_{\overline{C}}$	$\frac{\overline{v}}{R_i}$
$S_{\overline{C}} \rightarrow S_{idle}$	$\frac{\overline{v}}{f(L_{p,i}-R_i)}\varpi_{idle,i}$

information, vehicles can obtain the ECA of each channel, i.e., $\Psi_i, i \in \mathcal{K}$, based on their speed, by using (3.7) and (3.8). Before transmitting, vehicles conduct spectrum sensing, which is assumed to be accurate in this work. Since the channel availability follows the exponential distribution which is memoryless, the channel availability is independent of the situation before the spectrum sensing. Notably, if a channel is unavailable due to primary transmissions, its ECA is zero. We assume that the bandwidth of each channel is identical. Vehicles on the road often maintain relatively stable topology since they follow the same direction and similar speed, and thus they usually form clusters where vehicles within a cluster can communicate with each other [47] [125]. To utilize the licensed spectrum, vehicles should opportunistically access the channels with different ECAs in a distributed manner. Game theory [126] is a well-known tool to analyze the behavior

of distributed players who are considered to be selfish and rational. We apply a non-cooperative congestion game to model the spectrum access process in CR-VANETs, in which vehicles in a cluster choose channels to access in a distributed manner, trying to maximize their own utilities. Then, we analyze the existence and the efficiency of NE using uniform MAC and slotted ALOHA, respectively, and devise a spectrum access algorithm for each vehicle to decide the access channel to achieve an NE with high efficiency.

3.4.1 Formulation of Spectrum Access Game

The spectrum access problem is modeled as a congestion game, where there are multiple players and resources, and the payoff of each player by selecting one resource is related to the number of other players selecting the same resource [127]. In this paper, the spectrum access congestion game is defined as $\Gamma = \{\mathcal{N}, \mathcal{C}, \{S_j\}_{j\in\mathcal{N}}, \{U_j\}_{j\in\mathcal{N}}\}$, where $\mathcal{N} = \{1, \ldots, N\}$ is the finite set of players, i.e., vehicles in a cluster. N is related to the vehicle density, which is denoted by ρ_v; $\mathcal{C} = \{1, \ldots, C\}$ is the set of available channels, where "available" means that they are sensed to be idle, and $\mathcal{C} \subseteq \mathcal{K}$; S_j is the set of pure strategies associated with vehicle j; and U_j is the utility function of vehicle j. Vehicles in the game are aware of the ECA of all channels (Ψ_i) and the number of vehicles in the game (N). The bandwidth (resource) of each channel is identical, and thus we set the bandwidth to one unit.

Since each vehicle is equipped with only one cognitive radio, it can access at most one channel at a time, and thus $S_j = \mathcal{C}$ for all $j \in \mathcal{N}$. In this case, denote by U_j^i the utility of vehicle j by choosing channel i. Note that U_j^i is a function of both s_j and s_{-j}, which are the strategies selected by vehicle j and all of its opponents, respectively. In this game, we define the utility U_j^i as the average total channel resource vehicle j obtains by choosing channel i, before this channel is reoccupied by PTs, i.e.,

$$U_j^i = \Psi_i r(n_i). \tag{3.9}$$

n_i is the total number of vehicles choosing channel i simultaneously, including vehicle j. Resource allocation function $r(n_i)$ indicates the share of channel i obtained by each of the n_i vehicles. For an arbitrary vehicle, Ψ_i is used to measure the average time duration in which channel i is available. Thus, $U_j^i = \Psi_i r(n_i)$ shows the average total amount of channel resource vehicle j can obtain before it must cease transmitting due to the appearance of active PTs. The channel with higher Ψ_i is preferred because choosing it can reduce spectrum sensing and unpredictable channel switching. The form of $r(\cdot)$ is related to the specific MAC scheme. However, based on [128], $r(\cdot)$ should satisfy the following conditions:

- $r(1) = 1$, which means that a user can get all the resource of a channel if it is the only one choosing that channel.
- $r(n)$ is a decreasing function of n.
- Define $f(n) = nr(n)$. $f(n)$ decreases with n and should be convex, i.e., $f'(n) < 0$ and $f''(n) > 0$.
- $n_i r(n_i) \leq 1$. Resource waste may happen when multiple users share the same resource due to contention or collision.

Since vehicles are rational and selfish, they prefer the strategy that can maximize their utilities. To analyze this game, we focus on NE. We will analyze the existence, condition and efficiency ratio (ER) of the pure NE, using uniform MAC and slotted ALOHA, respectively. After that, a spectrum access algorithm to achieve the pure NE with high ER is derived.

3.4.2 Nash Equilibrium in Channel Access Game

Nash equilibrium is a well-known concept to analyze the outcome of the game, which states that in the equilibrium every user can select a utility-maximizing strategy given the strategies of other users.

Definition 1: A strategy profile for the players $S^* = (s_1^*, s_2^*, \ldots, s_N^*)$ is an NE if and only if

$$U_j(s_j^*, s_{-j}^*) \geq U_j(s_j', s_{-j}^*), \forall j \in \mathcal{N}, s_j' \in S_j, \tag{3.10}$$

which means that no one can increase its utility alone by changing its own strategy, given strategies of the other users. If the strategy profile S in (3.10) is deterministic, it is called a pure NE. In this paper, we consider pure NE only, so we use the term NE and pure NE interchangeably.

In the spectrum access game Γ, given a strategy profile, if no vehicle can improve its utility by shifting to another channel alone, the strategy profile is referred to as a pure NE. Denote by $S = (s_1, s_2, \ldots, s_N)$ the strategy profile of all vehicles, where s_i is a specific channel. Denote by $\mathbf{n}(S) = (n_1, n_2, \ldots, n_C)$ the congestion vector, which shows the number of vehicles choosing each channel, corresponding to the strategy profile S. According to

Definition 1, the spectrum access game Γ has pure NE(s) if and only if for each player $j \in \mathcal{N}$,

$$\Psi_{s_j} r(n_{s_j}) \geq \Psi_k r(n_k + 1), \forall k \in \mathcal{C}, k \neq s_j. \tag{3.11}$$

Note that there are typically multiple strategy profiles that correspond to one congestion vector. If a strategy profile S corresponding to congestion vector $\mathbf{n}^*$ is a pure NE, then all strategy profiles corresponding to $\mathbf{n}^*$ are pure NEs according to (3.11). Denote by NE-*set*($\mathbf{n}$) the set of pure NEs corresponding to congestion vector $\mathbf{n}$. The NEs in NE-*set*($\mathbf{n}$) may yield different utilities for each player. However, they yield the same total utility, which is defined as the summation of the utilities of all vehicles, and is given by

$$U_{total,\mathbf{n}} = \sum_{i=1}^{C} \Psi_i n_i r(n_i) = \sum_{i=1}^{C} \Psi_i f(n_i), \tag{3.12}$$

where $\mathbf{n} = (n_1, n_2, \ldots, n_C)$. In the following, the NE of the spectrum access game is analyzed using uniform MAC and slotted ALOHA, respectively.

3.4.3 Uniform MAC

The simplest way to share the channel among multiple users is to make each of them access the channel equally likely, which is referred as to uniform MAC [128]. Each vehicle starts a back-off with the back-off time randomly chosen from a fixed window. If one vehicle finds that its back-off expires and the channel is idle, it can capture the channel during the whole time slot, while others should keep silent. In uniform MAC, the resource allocation function $r(n) = \frac{1}{n}$, thus the utility function:

$$U^i_{j\{\mathbf{uni}\}} = \frac{\Psi_i}{n_i}.$$

Note that $f_{\mathbf{uni}}(n) = 1$. It is shown in [128] that such a game using uniform MAC does have the pure NE. In proposition 1, we obtain the condition of the pure NE when uniform MAC is employed, and show that there may exist multiple NE-*set*s.

Proposition 1 *For the spectrum access game Γ using uniform MAC, if a congestion vector $\mathbf{n} = (n_1, n_2, \ldots, n_C)$ yields NE-set($\mathbf{n}$), the following condition should be satisfied:*

$$\begin{cases} n_i = \lceil \frac{\Psi_i N - \sum_{k \neq i, k \in \mathcal{C}} \Psi_k}{\sum_{k \in \mathcal{C}} \Psi_k} \rceil + W_0, \ i = 1, 2, \ldots, C \\ \sum_{i=1}^{C} n_i = N, \end{cases} \tag{3.13}$$

where $W_0 \in \{0, 1, 2, \ldots, \lceil \frac{\Psi_i |N| + \Psi_i (|\mathcal{C}| - 1)}{\sum_{k \in \mathcal{C}} \Psi_k} \rceil - \lceil \frac{\Psi_i |N| - \sum_{k \neq i, k \in \mathcal{C}} \Psi_k}{\sum_{k \in \mathcal{C}} \Psi_k} \rceil - 1\}$. See the proof in Appendix 3.7.1. From (3.13), it can be seen that there may exist more than one NE-*set*.

3.4.4 Slotted ALOHA

Compared with uniform MAC, slotted ALOHA is a more typical MAC used in ad hoc networks, including VANETs. In slotted ALOHA, vehicles access the channel with probability p, and the throughput of each vehicle is $th(p) = p(1-p)^{n-1}$. To maximize the throughput, let $th'(p) = 0$. Then we get $p = \frac{1}{n}$, and the resource allocation function using slotted ALOHA is:

$$r_{\mathbf{SA}}(n) = \frac{1}{n}(1 - \frac{1}{n})^{n-1}.$$

It can be shown that for slotted ALOHA, $f_{\mathbf{SA}}(n) = (1 - \frac{1}{n})^{n-1}$, with $f'_{\mathbf{SA}}(n) < 0$ and $f''_{\mathbf{SA}}(n) > 0$. (See the proof in [128]). Moreover, if n goes to infinity, the total throughput of slotted ALOHA:

$$\lim_{n \to \infty} f_{\mathbf{SA}}(n) = \frac{1}{e}. \tag{3.14}$$

The utility of vehicle j choosing channel i using slotted ALOHA is given by:

$$U^i_{j\{\mathbf{SA}\}} = \Psi_i \frac{1}{n_i}(1 - \frac{1}{n_i})^{n_i - 1}.$$

Different from uniform MAC, it is more difficult to derive the explicit condition of pure NE using slotted ALOHA. However, we show the existence of the pure NE and propose a scheme to achieve it.

Proposition 2 *In the spectrum access game with vehicle set $\mathcal{N}$ and channel set $\mathcal{C}$, each vehicle sequentially chooses the access channel one by one. In each round, one vehicle chooses the best response to the strategies of the vehicles before it as the channel to access, i.e., its strategy in this game. Then, in each round, the strategy profile of the vehicles who have already made the decision is a pure NE.*

The proof is given in Appendix 3.7.2. Proposition 2 shows the existence of the pure NE in the spectrum access game Γ when using slotted ALOHA and provides a simple way to achieve a pure NE. However, to better understand the utilization of the channel resource, the efficiency of different NEs should be analyzed.

3.4.5 Efficiency Analysis

In the previous subsection, we prove the existence of pure NE(s) in the spectrum access game Γ. Generally speaking, an NE does not achieve global optimality due to the selfish behavior of the players. The efficiency of an NE is analyzed to evaluate the utilization of resources, which is defined as the total utility of all players under this NE. According to (3.12), in the spectrum access game Γ, the efficiency of a pure NE is defined as:

$$\mathcal{E}_S = \sum_{j=1}^{N} U_j^i = \sum_{j=1}^{N} \Psi_{s_j} r(n_{s_j}) = \sum_{i=1}^{C} \Psi_i n_i r(n_i),$$

where S is a strategy profile that is a pure NE.

The social optimality is defined as the maximum total utility of all player among all possible strategy profiles. For a specific game, the social optimality is fixed. It is proved in [128] that the social optimality in Γ is:

$$opt_\Gamma = \begin{cases} \sum_{i=1}^{N} \Psi_i, & \text{if } N \leq C; \\ \sum_{i=1}^{C-1} \Psi_i + \sum_{i=C}^{N} \Psi_C r(N-C+1), & \text{if } N > C, \end{cases}$$

where Ψ_i is ordered such that $\Psi_1 \geq \Psi_2 \geq \cdots \geq \Psi_C$. Thus, to evaluate the efficiency of an NE, we define efficiency ratio (ER) of an NE as the ratio between the efficiency and the social optimality:

$$ER_S = \frac{\mathcal{E}_S}{opt_\Gamma}.$$

Different NE-*set*s may achieve different ERs. For example, in a game using uniform MAC with two channels ($\Psi_1 = 30$ and $\Psi_2 = 10$) and three vehicles, there are two NE-*set*s, as shown in Table 3.5, as well as their efficiency ratios. Obviously, NE-set_2 is better than NE-set_1 because it achieves a higher ER. In the following, the ER of the pure NE using uniform MAC and slotted ALOHA is discussed, respectively.

Uniform MAC

In uniform MAC, $f(n) = 1$. Among multiple NE-*set*s with different congestion vectors, we can easily draw the following conclusions:

- A pure NE in which each channel is chosen by at least one vehicle has ER=1.
- For any two different NE-*set*s NE-set_1 and NE-set_2 in which not all channels are chosen, if

$$\sum_{i=1}^{C} \Psi_i I_i^1 \geq \sum_{i=1}^{C} \Psi_i I_i^2,$$

  where I_i^j is the indicator of whether channel i is chosen in NE-set_j, then $\mathrm{ER}_1 \geq \mathrm{ER}_2$.

The proof is straightforward. When uniform MAC is employed, the efficiency equals the summation of the ESA of all channels that are selected, i.e., $\mathcal{E}_S = \sum_{i=1}^{C} \Psi_i I_i^S$. When all channels are selected, all resource is fully utilized, and therefore, ER=1. Otherwise, the higher efficiency yields higher efficiency ratio since the social optimality is fixed for a specific game.

Slotted ALOHA

In slotted ALOHA, although there is no explicit relation between the congestion vector and ER, Corollary 1 can help to lead a pure NE with high ER.

Corollary 1 *When Slotted ALOHA is used, in the process of composing a pure NE described in Proposition 2, the following rules can yield an NE with the highest efficiency ratio.*

If in a round the new vehicle has two best responses (BE_1 and BE_2),

- *when BE_1 corresponds to a vacant channel (no vehicle chooses it) and BE_2 corresponds to a channel that has been already chosen, then BE_1 is preferred;*
- *when each channel has been selected by at least one vehicle, the channel with* ***higher*** *ECA is preferred.*

See the proof in Appendix 3.7.3.

Table 3.5: Multiple NE-*set*s in a game

	n1	n2	ER
NE-set_1	3	0	0.75
NE-set_2	2	1	1

3.4.6 Distributed Algorithms to Achieve NE with High ER

After spectrum sensing, each vehicle has the knowledge of the available channels $i \in \mathcal{C}$, and the ECA of each channel, i.e., Ψ_i. Vehicles maintain a sorted list of the channels in $\mathcal{C}$ in a decreasing order of Ψ. Then they participate in the distributed spectrum access game Γ. Since vehicles behave in a distributed manner in CR-VANETs, the best solution to the game is a pure NE in which each vehicle has no incentive to change its current choice of the access channel unilaterally. According to Proposition 2, the pure NE can be achieved by each vehicle choosing the best response sequentially. Moreover, based on the analysis of Section 3.4.5 and Corollary 1, a pure NE with high ER can be achieved.

However, in such a process to achieve the NE, the vehicles who choose their strategy before others usually benefit more. For instance, in a game Γ with two channels and two vehicles, and $\Psi_1 = 15$ and $\Psi_2 = 10$, the one making decision first could obtain utility of 15 while the other could only get 10. To solve the problem, and achieve a pure NE with high ER in a distributed manner, we design a distributed cognitive spectrum access algorithm, as shown in Algorithm 1. Each vehicle will randomly select a back-off time and start the back-off. When the back-off timer expires, the vehicle chooses one channel to access according to the best response to the strategies of vehicles that have already chosen the channel. Then the vehicle broadcasts its decision in order for other vehicles to derive their strategies. Since the selection of the back-off time is random, the proposed algorithm is fair for each vehicle.

3.5 Performance Evaluation

In this section, we evaluate the performance of the proposed congestion game based opportunistic spectrum access scheme. We consider an urban scenario with 10 km $\times$ 10 km, where PTs and vehicles coexist. There are five licensed channels each with bandwidth of 1 MHz which vehicles can access in an opportunistic manner. PTs operating on different channels are associated with different parameters, i.e., R, L_P, λ_{idle}, and λ_{busy}. The

Algorithm 1: Distributed Cognitive Spectrum Access Algorithm

// **Initialization**
Get available channels $\mathcal{C}$ by sensing.
Update and order the channel availability $[\Psi_1, \Psi_2, \ldots, \Psi_C]$ decreasingly using (3.7) and (3.8). Consider the current time is t_s.
Each vehicle that seeks for transmission opportunity picks a random back-off time t_b from $(0, t_{b\_max}]$, and starts the back-off.
while current time$\leq (t_s + t_{b_max})$ **do**
  if The back-off timer of vehicle i expires **then**
    if uniform MAC **then**
      Select the best response with free channel considering the strategies that it receives. If all channels have been already chosen, then select any best response.
    end if
    if Slotted ALOHA **then**
      Select the channel according to Corollary 1.
    end if
    Broadcast the channel sequence number that it chooses.
  end if
end while
Each vehicle tunes its radio to its strategic channel, and starts transmission using specific MAC.
return

length of road segment L is set to 100 m. Vehicles move in the area with a constant speed $v \in [10, 30]$ m/s. The probabilities of vehicles selecting a direction at the intersection are given by $P_n = P_s = P_e = P_w = 0.25$. Denote by Th_j the utility of vehicle j by accessing the selected channel before the channel becomes unavailable, and the fairness index is defined as:

$$F = \frac{(\sum_j Th_j)^2}{N \sum_j Th_j^2},$$

which is used to evaluate the fairness among vehicles [129]. Specifically, we compare the proposed spectrum access (denoted by 'NE') with a random channel access (denoted by 'random') in which vehicles uniformly choose a channel from $\mathcal{C}$ to access.

Fig. 3.9 shows the impact of vehicle density on the road (ρ_v) on the NE of the game,

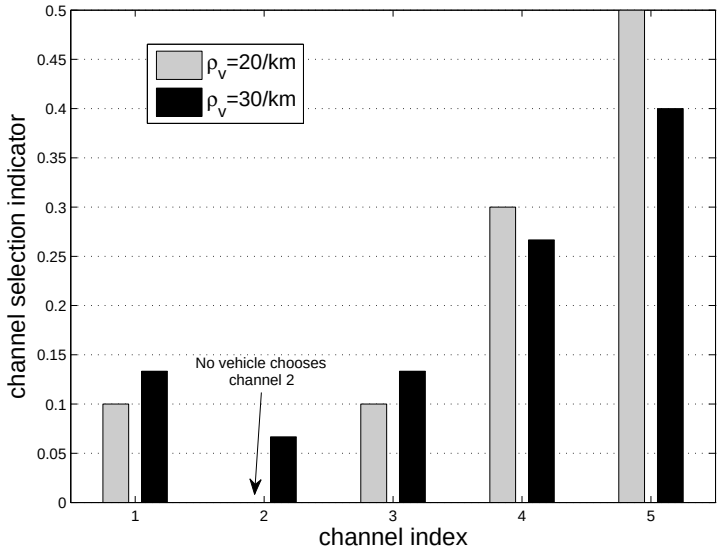

Figure 3.9: Impact of ρ_v on Nash equilibrium.

when uniform MAC is used. ρ_v captures the average number of vehicles on the road with unit length. Define the channel selection indicator of channel i as the ratio between the number of vehicles choosing channel i and the total number of vehicles, i.e., n_i/N, which reflects the popularity of the channel. When the value of ρ_v is small, some channels may not be chosen by any vehicle (e.g., channel 2 in Fig. 3.9 when ρ_v is 20 /km). When the density of vehicles becomes higher, all channels are selected by at least one vehicle and the selection indicator of each channel also changes to satisfy the NE condition (Proposition 1).

Fig. 3.10 shows the performance of the proposed spectrum access scheme with respect to the vehicle speed v, when ρ is set to 20 /km. From Fig. 3.10, it can be seen that 'NE' outperforms 'random' on average utility when using either uniform MAC or slotted ALOHA. This is because for uniform MAC, in 'NE', vehicles access the channels based on a pure NE while in 'random', each vehicle chooses a channel in random manner, which may result in lower average utility since there may exist some channels which are not selected by any vehicle. However, for slotted ALOHA, channels with larger ECA are chosen by more vehicles, resulting in more collisions. When vehicle density is 20 /km, the decrease of resource utilization caused by collisions is less than that caused by random access in which some channels are not utilized, which is the reason for that 'NE' outperforms 'random'

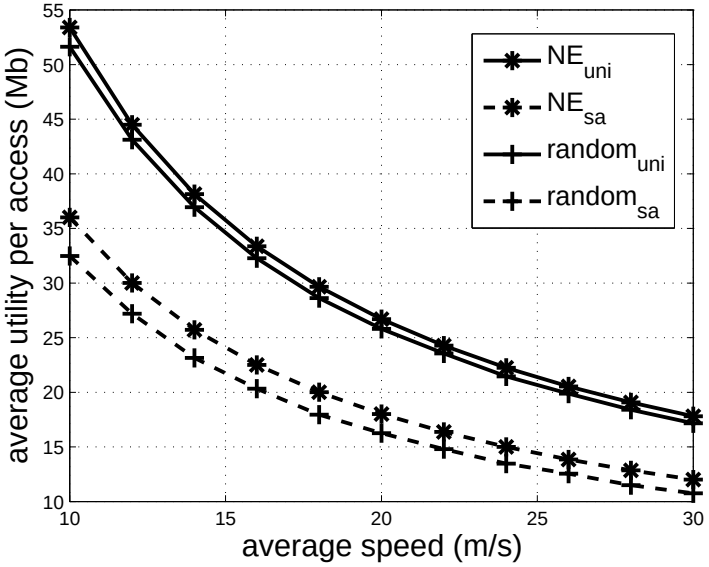

Figure 3.10: Performance w.r.t. speed. Vehicle density $\rho_v = 20/km$.

on average utility when using slotted ALOHA. The utility of both 'NE' and 'random' decreases with the increase of vehicle speed, because a higher speed leads to a smaller channel availability Ψ, and thus a smaller average utility.

Fig. 3.11 shows the performance of the proposed spectrum access scheme with respect to the vehicle density. From Fig. 3.11(a), it can be seen that the average utility decreases with the vehicle density. This is straightforward since the total channel resource is fixed and the resource allocation function $r(n)$ is decreasing with n. For uniform MAC, the reason that 'NE' achieves higher average utility than 'random' is that in 'NE', vehicles always choose channels with higher ECA while in 'random' vehicles randomly choose the access channel. When ρ_v increases, the probability that all channels are chosen by at least one channel increases. Note that if all channels are selected by at least one vehicle, the average utility of 'NE' and 'random' is the same. This fact explains the reason that the difference of average utility between 'NE_{uni}' and '$\text{random}_{\text{uni}}$' becomes smaller when vehicle density increases. For slotted ALOHA, when ρ_v increases, the average utility of 'NE' and 'random' also becomes closer, and the average utility of 'random' is slightly higher than that of 'NE' ($\rho_v > 20$ /km) because in 'NE', the preference to choose channels with higher ECA results in more collisions.

Fig. 3.11(b) shows the fairness index of 'NE' and 'random' in terms of vehicle density.

It can be seen that NE outperforms random access in terms of fairness in both uniform MAC and slotted ALOHA. This is because in a pure NE, the selfish property of vehicles leads to an even share of the spectrum resources. On the other hand, in random access, each vehicle randomly chooses a channel to access, which results in different utilities among vehicles. For 'NE_{sa}', when ρ_v is low, the increase of ρ_v may make vehicles choose channels with different ECA to achieve NE, resulting in the decrease of fairness. For example, two vehicles may both choose the channel with largest ECA, and the fairness index is 1. When ρ_v increases, a third vehicle may choose another channel, which makes the fairness index decrease. However, when ρ_v is high, with all channels selected, the increase of the number of vehicles will make utilities among vehicles closer based on the NE condition. If the density is extremely high, from (3.14), the game using slotted ALOHA turns into a game using uniform MAC, with the channel bandwidth $\frac{1}{e}$ of the original bandwidth.

Fig. 3.12 shows the efficiency ratio of the obtained NE in the proposed spectrum access game Γ. We introduce the channel diversity, which is defined as

$$\Phi = \sum_{i=1}^{C} (\Psi_i - \bar{\Psi})^2.$$

where $\bar{\Psi}$ is the mean ECA of all channels. Channel diversity shows the variance among primary channels due to the properties of PTs, such as the spatial distribution and temporal channel usage pattern. A smaller value of Φ indicates that on average, the channels have relatively similar ECAs, and vice versa. Fig. 3.12(a) shows the ER with respect to vehicle density. It can be seen that 'NE' achieves a higher ER than 'random' by utilizing either uniform MAC or slotted ALOHA, because the total utility of 'NE' is higher, as shown in Fig. 3.11(a). The decrease of ER using random access when ρ_v is low is because with the increase of ρ_v, the social optimality also increases. However, for 'random', more vehicles will not lead to as much increase in total utility as in social optimality. The reason for the increase of the ER of '$\text{random}_{\text{uni}}$' when vehicle density becomes higher ($\rho_v \geq 25$ /km) is that the social optimality will not change (all channels are selected) with the increase of ρ_v, while the total utility increases due to that in expectation, more channels are chosen. In fact, it approaches to the ER of 'NE_{uni}', which is not shown in the figure. The ER of '$\text{random}_{\text{sa}}$' changes slightly when vehicle density is high. This is because when ρ_v is high, $f_{\mathbf{SA}}(n)$ changes very little with ρ_v, and thus the total utility changes little due to (3.12). And with (3.14), when vehicle density is extremely high, we have

$$ER_{\mathbf{SA}} \to \frac{\frac{1}{e}\sum_{i=1}^{C} \Psi_i}{\sum_{i=1}^{C-1} \Psi_i + \frac{1}{e}\Psi_C}, \tag{3.15}$$

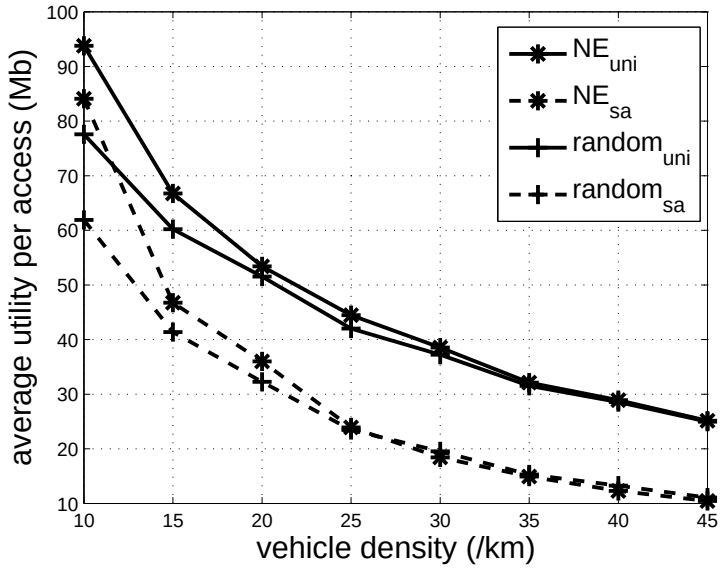

(a) Average utility w.r.t. vehicle density.

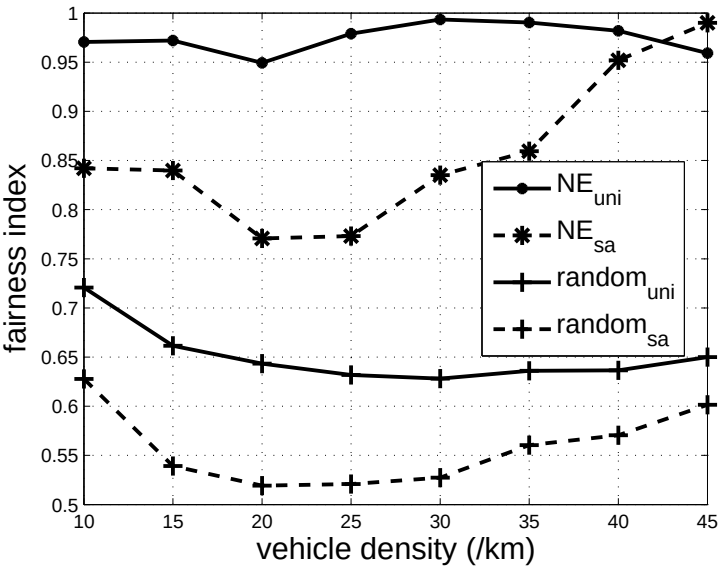

(b) Fairness w.r.t. vehicle density.

Figure 3.11: Performance w.r.t. vehicle density. Vehicle speed $v = 10m/s$.

where (3.15) is the lower bound of $ER_{\mathbf{SA}}$ when vehicle density increases.

Fig. 3.12(b) shows the relationship between ER and the channel diversity Φ. The ER of uniform MAC remains stable when Φ increases, because although the channels with smaller ECA are chosen less often, they have little impact on the ER since their ECA are small. However, for slotted ALOHA, the reason for the decrease of ER is two-fold: first, the channels with smaller ECA are rarely chosen; second, more vehicles choose channels with higher ECA, which results in more contentions and collisions. When Φ increases, more vehicles contend for the channels with high ECA, resulting in more collisions, and smaller value of ER.

3.6 Summary

In this paper, we have analyzed the channel availability for vehicles in urban CR-VANETs, jointly considering the mobility of vehicles, and the spatial distribution and the temporal channel usage pattern of PTs. We have then proposed a game theoretic spectrum access scheme to better exploit the spatial and temporal spectrum resource. Simulation results have demonstrated that the proposed scheme can achieve higher average utility and fairness than the random access scheme, when applying either uniform MAC or slotted ALOHA. The impact of vehicle density and channel diversity on the performance of the proposed scheme has also been studied. The research results can be applied for designing efficient spectrum sensing and access schemes in CR-VANETs. For future works, we will study the effect of sensing errors, and consider other usage patterns of PTs.

3.7 Appendix

3.7.1 NE condition for uniform MAC

First, the situation for two channels is considered. Since $C = 2$ and $N \in \mathbb{Z}^+$, we have

$$\frac{\Psi_1}{n_1} \geq \frac{\Psi_2}{n_2 + 1} \text{ and } \frac{\Psi_2}{n_2} \geq \frac{\Psi_1}{n_1 + 1},$$

which can be rewritten as follows:

$$\frac{\Psi_1}{\Psi_2} n_2 - 1 \leq n_1 \leq \frac{\Psi_1}{\Psi_2} n_2 + \frac{\Psi_1}{\Psi_2}. \tag{3.16}$$

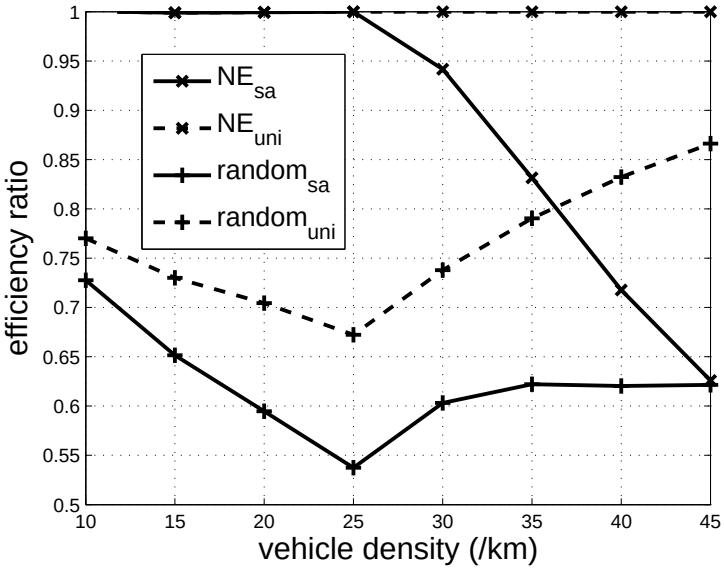

(a) Efficiency ratio w.r.t. vehicle density. $\Omega = 20$.

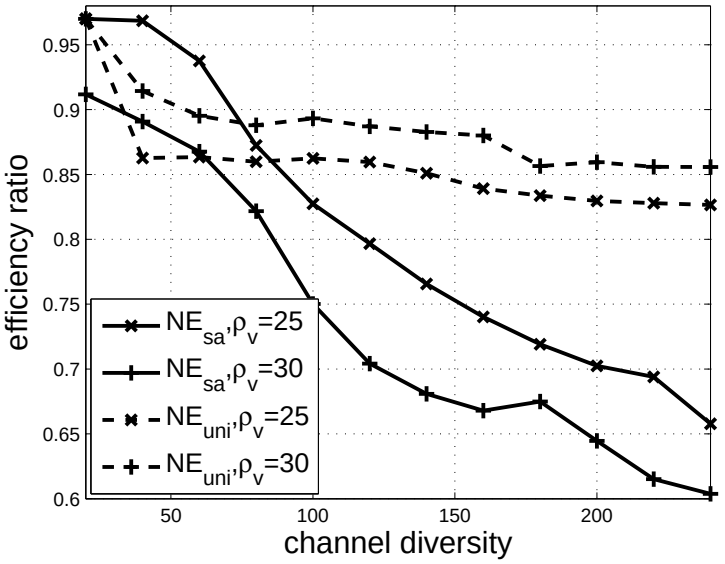

(b) Efficiency ratio w.r.t. channel diversity.

Figure 3.12: Efficiency ratio. $\bar{\Psi} = 20$.

Substitute $n_2 = N - n_1$ into (3.16), we obtain

$$\frac{\Psi_1 N - \Psi_2}{\Psi_1 + \Psi_2} \leq n_1 \leq \frac{\Psi_1 N + \Psi_1}{\Psi_1 + \Psi_2}. \tag{3.17}$$

Since

$$\frac{\Psi_1 N + \Psi_1}{\Psi_1 + \Psi_2} - \frac{\Psi_1 N - \Psi_2}{\Psi_1 + \Psi_2} = 1 \tag{3.18}$$

and

$$-1 < \frac{\Psi_1 N - \Psi_2}{\Psi_1 + \Psi_2} < N \tag{3.19}$$

Γ has at least one pure NE, in which

$$n_1 = \lceil \frac{\Psi_1 N - \Psi_2}{\Psi_1 + \Psi_2} \rceil \text{ and } n_2 = N - n_1. \tag{3.20}$$

Next, we extend this conclusion to the situation where more than two channels are available, i.e., $C > 2$. When $C > 2$, any two arbitrary channels i and k, $i, k \in \mathcal{C}$ should satisfy (3.16) to constitute an NE. Thus,

$$\frac{\Psi_k}{\Psi_i} n_i - 1 \leq n_k \leq \frac{\Psi_k}{\Psi_i} n_i + \frac{\Psi_k}{\Psi_i}. \tag{3.21}$$

Define $F_{L,ki}$ and $F_{U,ki}$ as

$$F_{L,ki} = \frac{\Psi_k}{\Psi_i} n_i - 1 \text{ and } F_{U,ki} = \frac{\Psi_k}{\Psi_i} n_i + \frac{\Psi_k}{\Psi_i}.$$

Then, for channels i and $\forall k \neq i$, $i, k \in \mathcal{C}$, we have

$$F_{L,ki} \leq n_k \leq F_{U,ki}.$$

It holds that

$$\sum_{k \neq i, k \in \mathcal{C}} F_{L,ki} \leq \sum_{k \neq i, k \in \mathcal{C}} n_k \leq \sum_{k \neq i, k \in \mathcal{C}} F_{U,ki}. \tag{3.22}$$

By substituting $\sum_{k\neq i,k\in\mathcal{C}} n_k = N - n_i$ into (3.22), we have

$$\frac{\Psi_i N - \sum_{k\neq i,k\in\mathcal{C}} \Psi_k}{\sum_{k\in\mathcal{C}} \Psi_k} \leq n_i \leq \frac{\Psi_i N + \Psi_i(C-1)}{\sum_{k\in\mathcal{C}} \Psi_k}. \tag{3.23}$$

Similar to (3.18) and (3.19), it can be proved that

$$\frac{\Psi_i N + \Psi_i(C-1)}{\sum_{k\in\mathcal{C}} \Psi_k} - \frac{\Psi_i N - \sum_{k\neq i,k\in\mathcal{C}} \Psi_k}{\sum_{k\in\mathcal{C}} \Psi_k} > 1$$

and

$$-1 < \frac{\Psi_i N - \sum_{k\neq i,k\in\mathcal{C}} \Psi_k}{\sum_{k\in\mathcal{C}} \Psi_k} < N.$$

Then, for any $\mathcal{C}$ and $\mathcal{N}$, (3.8) has at least one solution, which is

$$n_i = \lceil \frac{\Psi_i N - \sum_{k\neq i,k\in\mathcal{C}} \Psi_k}{\sum_{k\in\mathcal{C}} \Psi_k} \rceil + W_0,$$

where $W_0 \in \{0, 1, 2, \ldots, \lceil \frac{\Psi_i N + \Psi_i(C-1)}{\sum_{k\in\mathcal{C}} \Psi_k} \rceil - \lceil \frac{\Psi_i N - \sum_{k\neq i,k\in\mathcal{C}} \Psi_k}{\sum_{k\in\mathcal{C}} \Psi_k} \rceil - 1\}$. With $\sum_{i\in\mathcal{C}} n_i = N$, we have (3.13). Thus, the game Γ has at least one pure NE. (3.13) is called NE condition of the spectrum access game Γ when uniform MAC is used.

3.7.2 Proposition 2

Assume that for a given round R_t, the congestion vector $\mathbf{n}(S_t) = \{n_1, n_2, \ldots, n_C\}$ composes a pure NE. According to (3.8), for each channel $i \in \mathcal{C}$,

$$\Psi_i r(n_i) \geq \Psi_k r(n_k + 1),\ \forall k \in \mathcal{C}, k \neq i.$$

Then for a new round R_{t+1}, a new vehicle joins the game and chooses its best response according to the existing strategy profile, i.e., $\mathbf{n}(S_t)$. Consider its best response is channel m, and thus the new congestion vector is $\mathbf{n}(S_{t+1}) = \{n_1, \ldots, n_m + 1, \ldots, n_C\}$. For the new congestion vector, we have the following observations:

1. For each channel $i \in \mathcal{C}, i \neq m$, $\Psi_i r(n_i) \geq \Psi_k r(n_k + 1),\ \forall k \in \mathcal{C}\backslash\{i, m\}$ holds because the number of vehicles that choose the channels other than channel m does not

change, and $r(n_i), i \neq m$ remains unchanged.

2. $\Psi_m r(n_m+1) \geq \Psi_k r(n_k+1), \forall k \in \mathcal{C}, k \neq m$. This statement holds due to that channel m is the best response for the new vehicle.

3. $\Psi_k r(n_k) \geq \Psi_m r(n_m+1+1), \forall k \in \mathcal{C}, k \neq m$. Remember in round t, $\Psi_k r(n_k) \geq \Psi_m r(n_m+1)$. $r(n)$ is a non-increasing function, and thus $r(n_m+1) \geq r(n_m+1+1)$.

Therefore, $\mathbf{n}(S_{t+1})$ also constitutes a pure NE. For a specific game, the first vehicle chooses the channel with largest ECA and of course composes a pure NE. Then, for each round, the strategies of vehicles which have participated in the game constitute a new pure NE, until all vehicles have chosen their strategies.

3.7.3 Corollary 1

For any round in proposition 2, assume that the congestion vector $\mathbf{n}(S) = \{n_1, n_2, \ldots, n_C\}$ constitutes a pure NE and Ψ_i is sorted so that $\Psi_1 \geq \Psi_2 \geq \cdots \geq \Psi_C$. The efficiency of the NE is

$$\mathcal{E}_S = \sum_{i=1}^{C} f(n_i).$$

Remember that in slotted ALOHA, $f(n) = (1-\frac{1}{n})^{n-1}$. A new vehicle comes and finds there are more than one best response (BR).

1) If BR_1 corresponds to a free channel i when BR_2 corresponds to channel j that has been selected by at least one vehicle, then BR_1 leads to a NE with efficiency:

$$\mathcal{E}_{S1} = \mathcal{E}_S + \Psi_i > \mathcal{E}_S.$$

BR_2 leads to a NE with efficiency:

$$\mathcal{E}_{S2} = \mathcal{E}_S - \Delta < \mathcal{E}_S.$$

where Δ is the loss of $f(n_j)$ since $f(n)$ decreases with n. Obviously, $\mathcal{E}_{S1} > \mathcal{E}_{S2}$.

2) Consider that BR_1 and BR_2 correspond to channel i and j with $n_i \geq 1$ and $n_j \geq 1$, respectively. Without loss of generality, consider $\Psi_i > \Psi_j$. Under this condition, it is clear that $n_i > n_j$, or else channel i and j cannot be the best response simultaneously. Consider only the total utility of users choosing channel i and j since other channels are not affected

in this round. BR_1 will lead to an NE with utility $\mathcal{E}_1 = \Psi_i f(n_i+1) + \Psi_j f(n_j)$, while BE_2 will lead to an NE with utility $\mathcal{E}_2 = \Psi_i f(n_i) + \Psi_j f(n_j+1)$. Using the property of the pure NE, we have $\Psi_i r(n_i+1) \geq \Psi_j r(n_j+1)$ and $\Psi_j r(n_j+1) \geq \Psi_i r(n_i+1)$, and thus $\Psi_i r(n_i+1) = \Psi_j r(n_j+1)$, i.e., $\Psi_i \frac{f(n_i+1)}{n_i+1} = \Psi_j \frac{f(n_j+1)}{n_j+1}$. Let

$$\Psi_i = \frac{\frac{f(n_j+1)}{n_j+1}}{\frac{f(n_i+1)}{n_i+1}} \Psi_j = \alpha \Psi_j.$$

To prove

$$\begin{aligned} & \mathcal{E}_1 - \mathcal{E}_2 \\ =\ & \Psi_i f(n_i+1) + \Psi_j f(n_j) - (\Psi_i f(n_i) + \Psi_j f(n_j+1)) \\ =\ & \Psi_j [\alpha(f(n_i+1) - f(n_i)) + f(n_j) - f(n_j+1)] > 0, \end{aligned}$$

is equivalent to prove

$$\alpha = \frac{\frac{f(n_j+1)}{n_j+1}}{\frac{f(n_i+1)}{n_i+1}} < \frac{f(n_j) - f(n_j+1)}{f(n_i) - f(n_i+1)},$$

since $f(n) - f(n+1) > 0$.

$$\begin{aligned} & \frac{\frac{f(n_j+1)}{n_j+1}}{\frac{f(n_i+1)}{n_i+1}} < \frac{f(n_j) - f(n_j+1)}{f(n_i) - f(n_i+1)} \\ \Leftrightarrow\ & \frac{\frac{f(n_j+1)}{n_j+1}}{f(n_j) - f(n_j+1)} < \frac{\frac{f(n_i+1)}{n_i+1}}{f(n_i) - f(n_i+1)} \\ \Leftrightarrow\ & g(n) = \frac{\frac{f(n+1)}{n+1}}{f(n) - f(n+1)} \text{ increasing with } n \geq 1 \\ \Leftrightarrow\ & g'(n) > 0, \text{ when } n \geq 1. \end{aligned} \tag{3.24}$$

We skip the tedious proof of (3.24) to simplify the exposition. Then, we have $\mathcal{E}_1 > \mathcal{E}_2$.

Chapter 4

Vehicular WiFi Offloading

WiFi is envisioned as a promising solution to the mobile data explosion problem in cellular networks as well as a cost-effective way to provide Internet access to mobile users. In this chapter, we study to utilize WiFi to efficiently deliver data services for vehicular users. WiFi offloading for moving vehicles poses unique characteristics and challenges, due to high mobility, fluctuating mobile channels, etc. We focus on the performance analysis of WiFi offloading in vehicular communication environments through a queueing based analytical framework. Specifically, we consider a generic vehicular user having Poisson data service arrivals to download/upload data from/to the Internet via sparsely deployed WiFi networks (want-to) or the cellular network providing full service coverage (have-to). For this scenario, the WiFi offloading performance, characterized by *offloading effectiveness*, is analyzed under the requirement of a desired *average service delay* which is the time the data services can be deferred for WiFi availability. We establish an explicit relation between offloading effectiveness and average service delay by an M/G/1/K queueing model, and the tradeoff between the two is examined. We validate our analytical framework through simulations based on a VANETs simulation tool VANETMobisim and real map data sets. Our analytical framework is useful for providing offloading guidelines to both vehicular users and network operators.

4.1 Introduction

With millions of hotspots deployed all over the world, WiFi can be a complementary solution to vehicular Internet access with low cost. It has been shown in the literature that in stationary/low-mobility scenarios, the WiFi offloading performance can be very

high (80% of the cellular traffic offloaded through delayed offloading) [52,90,91]. However, the offloading performance in the vehicular environment remains unclear. In a vehicular environment, vehicles signal to nearby WiFi access points (APs) when traveling along a road, so that the cellular traffic can be delivered to vehicles through the drive-thru Internet in an opportunistic manner. Such an opportunistic WiFi offloading has unique features.

- ▷ *A relatively small volume of data can be delivered to a vehicle in each drive-thru, due to the short connection time with WiFi APs*; and
- ▷ *The offloading performance can be significantly improved if the data service can tolerate a certain delay, as vehicles with a high speed can have multiple drive-thru opportunities in a short future.*

In this chapter, we aim at theoretically analyzing the performance of vehicular WiFi offloading with the delayed offloading strategy. We consider a generic vehicular user having randomly arrived data services, either to download data (e.g., E-mail attachment and `YouTube` video clip,) or upload data (e.g., `WeChat` messages and online diagnosis data) from/to the Internet. The data services can be fulfilled via either WiFi networks (want-to) or the cellular network (have-to). The cellular network is considered ubiquitous and WiFi APs are sparsely deployed. The offloading performance is characterized by average service delay and offloading effectiveness. *Average service delay* is defined as the average duration from the arrival of a data service request to the fulfillment of the service via WiFi networks, which is mostly contributed by the waiting time for the WiFi availability and is the "price" of using delayed offloading. *Offloading effectiveness* is defined as the long-term proportion of data services fulfilled via WiFi networks under the requirement of a desired average service delay. Intuitively, if the data services can be deferred for a longer time (i.e., relaxing the requirement on the average service delay), more data services can be offloaded by WiFi networks, yielding a higher offloading effectiveness. From a user's perspective, however, the increased average service delay would somehow reduce the user satisfaction on data services. Our analytical framework provides the relation between these two metrics and the tradeoff is examined.

In more detail, we present a queueing analysis of offloading performance in a vehicular environment. Each VU maintains an M/G/1/K queue, with M characterizing the arrival process of data service requests waiting to be served by drive-thru Internet, and system capacity K controlling the average service delay. If a service request arrives with a full queue, it will be served directly via the cellular network to avoid a longer delay than the expected service delay. As the data transmission with WiFi APs is in an opportunistic

manner, the queue departure process (i.e., the process of data transmission or service fulfillment) is characterized by the *effective service time* (EST) which is the duration from the transmission of the first bit of a data service to the service request is fulfilled. The probability distribution of the EST is theoretically derived using Laplace-Stieltjes transform (LST). Based on the statistics of the EST, the offloading effectiveness and average service delay and their relation are given. We validate our analytical framework through simulations based on a VANET simulation tool VANETMobisim and real map data sets.

Implementation of our analytical framework: For VUs, the explicit relation between offloading effectiveness (how much Internet access cost can be saved) and average service delay (how much service degradation the user is willing to tolerate) can provide offloading guidelines. For example, the on-board smart offloading engine (a mobile App) can do intelligent network selection based on the user's preference on service delay. On the other hand, due to the razor-sharp competition, many network operators are looking for new ways to cut spending and stand out in the market. Network operators, such as AT&T, NTT Docomo and China Mobile, are starting to deploy carrier WiFi to offload cellular networks and profit from the new business model. First of all, our results give the network operators more incentives to deploy outdoor WiFi networks as the offloading effectiveness is notable in vehicular environments. Moreover, our framework can provide network operators with some guidance on WiFi deployment (e.g., the density of WiFi APs) according to the theoretical offloading effectiveness. In a nutshell, our analytical framework can be applied in practice not only for VUs to make offloading decisions, but also for network operators to evaluate AP deployment strategies, make offloading-related pricing models, and so forth.

The remainder of the chapter is organized as follows. Section 4.2 describes the system model. Section 4.3 derives the probability distribution of the EST. Section 4.4 analyzes the queue and the tradeoff between offloading effectiveness and average service delay. Section 4.5 evaluates the analysis by real road map based simulation. Section 4.6 concludes the chapter.

4.2 System Model

In this section, we present the system model, including communication paradigm, mobility of vehicles, and queueing model of VUs. Based on the system model, we can evaluate the performance of vehicular WiFi offloading by analyzing the M/G/1/K queue.

4.2.1 Communication model

In this paper, we consider an urban area as a bounded region with WiFi APs randomly deployed. VUs access drive-thru Internet when possible since it tends to have a higher data rate and less cost than cellular networks. Automatic rate adaptation is widely used in the stock WiFi technology according to the signal strength. However, for simplicity, we consider the communication data rate between APs and vehicles is identical and denoted by R. Assume the idle MAC is employed where channel access time is fairly shared by the nearby VUs. To account for real MAC behaviors, a MAC throughput effective factor η is considered. η indicates the theoretical maximum portion of throughput considering the protocol overhead, e.g., $\eta = 45.5\%$ for bit rate 11 Mbps of IEEE 802.11b [130]. Thus, the data rate of a tagged VU $\mathcal{V}$ can be represented by $r = \frac{\eta R}{n+1}$, where n is the number of neighbor VUs of $\mathcal{V}$ connected to the same AP. With the second order Taylor approximation, the average data rate of an arbitrary VU connected to an AP can be approximated by

$$\bar{r} = r|_{\bar{n}} + \frac{1}{2}\mathrm{Var}(n)\frac{d^2 r}{dn^2}|_{\bar{n}}, \tag{4.1}$$

where $\bar{n}$ and $\mathrm{Var}(n)$ are the mean and variance of n, respectively [6].

4.2.2 Mobility model

The high mobility of vehicles may lead to short and intermittent drive-thru access opportunities. We model the mobility of $\mathcal{V}$ by an on-off process, with on-state and off-state denoting the situation that $\mathcal{V}$ is within and out of the coverage area of an AP. In on-state, $\mathcal{V}$ can transmit data through the AP with an average data rate $\bar{r}$; and in off-state, the transmission rate is assigned to zero, since $\mathcal{V}$ is out of the coverage area of any AP. Due to the random locations and coverage of open APs, we model the sojourn time of both on-state and off-state by the unpredictable and memoryless exponential distribution, with parameter λ and μ, respectively [6], as shown in Fig. 5.1.

4.2.3 Queueing model

Each VU maintains an M/G/1/K queue to store the data service requests about to be served, as shown in Fig. 4.2. A data service request arrives at the queue with a random inter-arrival time which follows the exponential distribution with mean $1/\gamma$. In other words, the arrival process of the queue is Poisson process. We also consider that the sizes

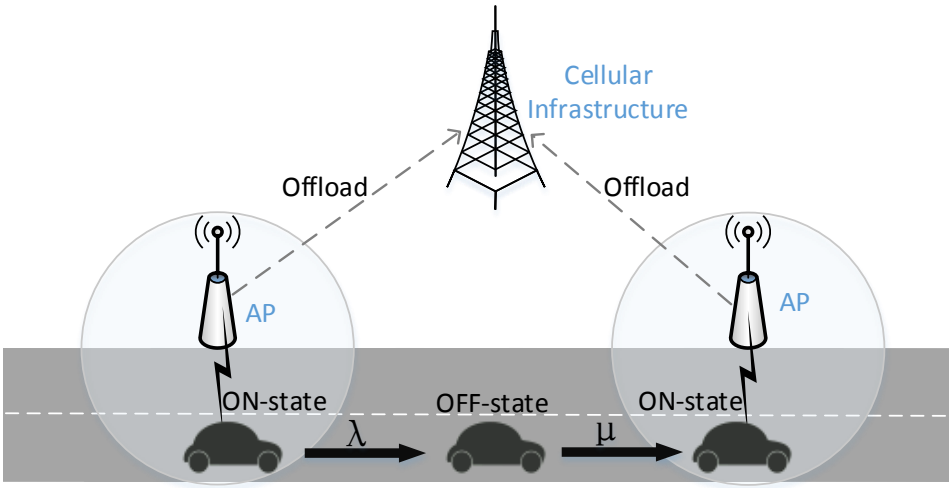

Figure 4.1: System model for vehicular WiFi offloading.

of service requests are identical, denoted by S. The departure process of the queue is not Markovian due to the service interruption. If a service request cannot be fulfilled within one drive-thru, it will wait for more drive-thru opportunities until fulfillment. We model the departure process by the EST which follows a general distribution. The EST t_e composes of the service time x, and time of server interruptions, i.e., when the vehicle is out of the coverage area of any AP. The queue capacity K represents the maximum number of service requests in the system, and thus the queue buffer length is $K-1$. We consider patient customer-type of queue, which means that if one service request enters the queue, it will wait until fulfillment. However, if a service arrives with a full queue, it expects that the delay would exceed the desired service delay. Thus, the service request will be directly served by the cellular network. With the queueing model and probability distribution of the EST which is obtained in the next section, the queue performance can be evaluated, with the average service delay and offloading effectiveness analyzed.

4.3 Derivation of Effective Service Time

We characterize the departure process and derive the probability distribution of the EST in this section.

Since the data transmission cannot happen when a vehicle is outside the coverage area

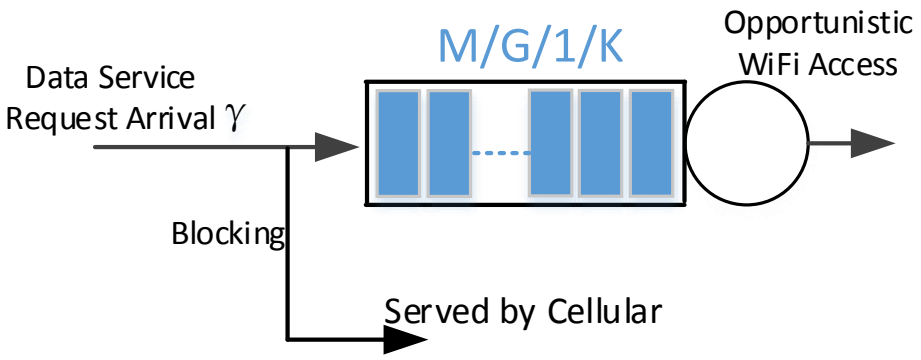

Figure 4.2: Queueing model.

of any WiFi AP, the queue server is subject to intermittent interruptions. Let $t_e(x)$ denote the EST of an arbitrary request with service time x, whereas x is assumed to follow the exponential distribution with parameter $\lambda_s = \frac{\bar{r}}{S}$, as in [6]. Since $t_e(x)$ composes of x and the time of server interruptions, we then have

$$t_e(x) = \begin{cases} x & H_\lambda \geq x \\ H_\lambda + H_\mu + T(x - H_\lambda) & H_\lambda < x, \end{cases} \tag{4.2}$$

where H_λ and H_μ are the length of an arbitrary on-state period and off-state period, which follow the exponential distribution with mean $1/\lambda$ and $1/\mu$, respectively. According to [131], the EST can be analyzed using LST. Let $T_e(\xi)$ be LST of the probability density function (PDF) of $t_e(x)$, and based on [131]:

$$\begin{aligned} T_e(\xi) &= \int_0^\infty f(x) e^{-(\xi+\lambda-\lambda V_\mu(\xi))} dx \\ &= \int_0^\infty \lambda_s e^{-\lambda_s x} e^{-(\xi+\lambda-\lambda V_\mu(\xi))} dx \\ &= \frac{\lambda_s}{\xi + \lambda - \lambda V_\mu(\xi) + \lambda_s}, \end{aligned} \tag{4.3}$$

where $V_\mu(\xi) = \frac{\mu}{\mu+\xi}$ is LST of the PDF of the length of an arbitrary off-state period. We

can then obtain the expectation of the EST by

$$\begin{aligned}\mathbb{E}[t_e] &= -\frac{dT_e(\xi)}{d\xi}\Big|_{\xi=0} \\ &= \frac{\lambda_s(1-\lambda\frac{dV_\mu(\xi)}{d\xi})}{[\xi+\lambda-\lambda V_\mu(\xi)+\lambda_s]^2}\Big|_{\xi=0} \\ &= \frac{1}{\lambda_s}(1+\frac{\lambda}{\mu}). \end{aligned} \tag{4.4}$$

From (4.4), $\mathbb{E}[t_e]$ is affected by server interruptions in the way that $\mathbb{E}[t_e]$ increases with the increase of interruption occurrence rate (λ) and mean interruption duration ($\frac{1}{\mu}$).

To analyze the M/G/1/K queue, we then derive the PDF of the EST, which is denoted by $f_e(t)$. Utilizing the inverse transform of LST, we have

$$f_e(t) = \mathcal{L}^{-1}(T_e(\xi)) = \frac{1}{2\pi i}\lim_{\delta\to\infty}\int_{\theta-i\delta}^{\theta+i\delta} e^{\xi t}T_e(\xi)d\xi, \tag{4.5}$$

where θ is a real number that is greater than the real part of all singularities of $T_e(\xi)$. The singularities of $T_e(\xi)$ can be obtained by making the denominators equal zero, i.e.,

$$\xi_{\mathbf{sin}} = \{\xi|\xi+\mu=0\}\cup\{\xi|\xi+\lambda-\lambda\frac{\mu}{\mu+\xi}+\lambda_s=0\}. \tag{4.6}$$

Simplifying (4.6), we can get $\xi_{sin1} = -\mu$ and $\xi_{sin2} = \frac{1}{2}\big[-(\lambda+\lambda_s+\mu)\pm\sqrt{(\lambda+\lambda_s+\mu)^2-4\lambda_s\mu}\big]$ (if $\xi+\lambda-\lambda\frac{\mu}{\mu+\xi}+\lambda_s=0$ has solution(s).) Since all singularities of $T_e(\xi)$ are smaller than zero, we can set $\theta=0$. Using Bromwich inversion integral [132] and the fact that $\theta=0$, we have

$$\begin{aligned} f_e(t) &= \frac{2e^{\theta t}}{\pi}\int_0^\infty Re(T_e(\theta+iu))\cos(ut)du \\ &= \frac{2}{\pi}\int_0^\infty Re[\frac{\lambda_s(\mu+iu)}{iu(\mu+iu)+(\lambda+\lambda_s)(\mu+iu)-\lambda\mu}]\cos(ut)du \\ &= \frac{2}{\pi}\int_0^\infty \frac{\lambda_s(\lambda_s\mu^2+\lambda u^2+\lambda_s u^2)}{(\lambda_s\mu-u^2)^2+u^2(\lambda+\lambda_s+\mu)^2}\cos(ut)du. \end{aligned} \tag{4.7}$$

Since integration (4.7) is difficult to calculate, we use numerical methods to calculate $f_e(t)$ for any given t_e. We use Fourier-Series method and the trapezoidal rule to obtain the

numerical integration of (4.7) [132].

$$f_e(t) \approx f_e^h(t)$$
$$\equiv \frac{he^{\theta t}}{\pi} T_e(\theta) + \frac{2he^{\theta t}}{\pi} \sum_{k=1}^{\infty} Re(T_e(\theta + ikh))\cos(kht). \tag{4.8}$$

Some results of the EST derivation are shown in Fig. 4.3(a), with the effects of λ_s, λ and μ compared. It can be seen that the EST increases with the decrease of λ_s and μ, and with the increase of λ. Smaller λ_s indicates a larger request service time x, and thus a larger EST with server interruptions. On the other hand, because a larger λ and a smaller μ indicate more frequent and longer interruptions, respectively, the EST then increases. To validate the accuracy of the EST derivation, the theoretical results are compared with the simulation results in Fig. 4.3(b). In the simulation, a virtual queue with exhaustive customer arrivals and server interruptions is considered. From the figure, it can be shown that the curves of theoretical and simulation results closely match each other, which demonstrates the accuracy of the analysis.

4.4 Analysis of Queueing System and Offloading Performance

Given the probability distribution of the EST obtained in (4.8), we can evaluate the performance of offloading by analyzing the M/G/1/K queue. Because the EST is not exponential, we utilize the imbedded Markov chain of system states at the time instant t_{di}, which is the time instance of service request i's fulfillment, to analyze the queue [133].

4.4.1 Queue analysis

Let n_i be the number of requests left in the system seen by the i^{th} request when it leaves the system, and χ_i be the number of arrivals during the EST of request i. We then have

$$n_{i+1} = n_i - U(n_i) + \chi_{i+1}, \tag{4.9}$$

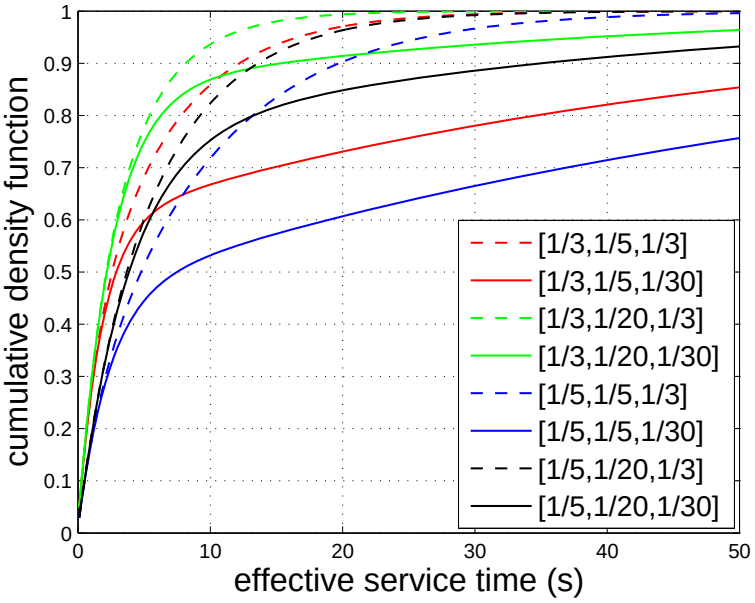

(a) EST w.r.t. λ_s, λ and μ.

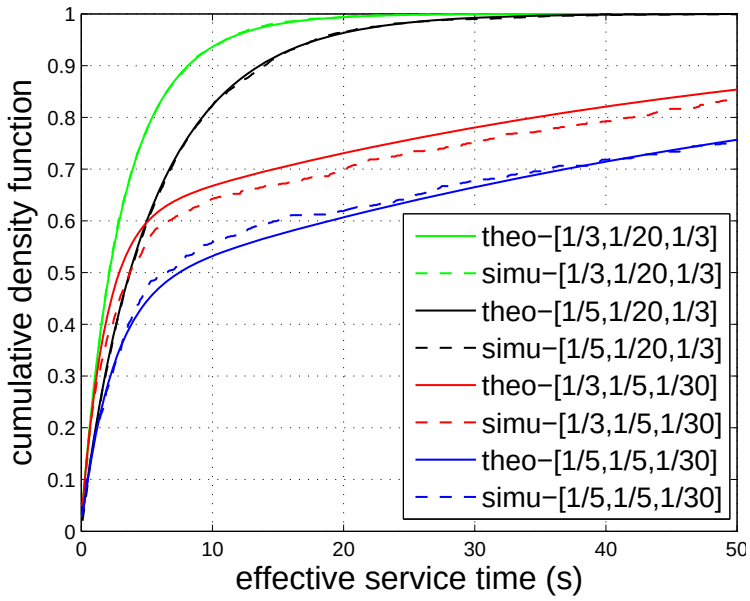

(b) Theoretical and simulation results of EST.

Figure 4.3: Results of the EST. In the legend, $[x,y,z]$ stand for λ_s, λ and μ, respectively.

where $U(n_i)$ is the unit step function where $U(n_i) = 0$ if $n_i = 0$, and $U(n_i) = 1$ otherwise. Then, the transition probabilities at departure instances are defined as

$$p_{d,jk} = P\{n_{i+1} = k | n_i = j\} \quad 0 \leq j, k \leq K-1. \tag{4.10}$$

Let ω_k be the probability of k arrivals during the EST of an arbitrary service request. Using the Poisson arrival property, we can get

$$\omega_k = \int_{t=0}^{\infty} \frac{(\gamma t)^k}{k!} e^{-\gamma t} f_e(t) dt, \tag{4.11}$$

where γ is the arrival rate of service requests and $f_e(t)$ is the PDF of the EST given in (4.8). Thus, we can easily obtain the $K \times K$ transition probability matrix as

$$\mathbf{P_{d,jk}} = \begin{bmatrix} \omega_0 & \omega_1 & \omega_2 & \cdots & \omega_{K-2} & \sum_{m=K-1}^{\infty} \omega_m \\ \omega_0 & \omega_1 & \omega_2 & \cdots & \omega_{K-2} & \sum_{m=K-1}^{\infty} \omega_m \\ 0 & \omega_0 & \omega_1 & \cdots & \omega_{K-3} & \sum_{m=K-2}^{\infty} \omega_m \\ \vdots & \vdots & \vdots & & \vdots & \vdots \\ 0 & 0 & 0 & \cdots & \omega_0 & 1-\omega_0 \end{bmatrix} \tag{4.12}$$

Let $p_{d,k}$ be the equilibrium state probabilities at departure instants, which can be computed by

$$p_{d,k} = \sum_{j=0}^{K-1} p_{d,j} p_{d,jk} \quad k = 0, 1, \cdots, K-1 \tag{4.13}$$

$$\sum_{k=0}^{K-1} p_{d,k} = 1 \quad (Normalisation\ Condition). \tag{4.14}$$

Let $p_k, k = 0, 1, 2, \cdots, K$ be the steady-state probabilities of the system states, and $P_B = p_K$ be the blocking probability. Based on Poisson arrivals see time averages (PASTA) property, p_k can be calculated by (4.15) [133].

$$p_k = (1 - P_B) p_{d,k} \quad k = 0, 1, 2, \cdots, K-1. \tag{4.15}$$

The traffic intensity ρ and the actual traffic intensity ρ_c considering queue blocking are given by $\rho = \gamma \mathbb{E}[t_e]$ and $\rho_c = (1 - P_B)\rho$, respectively. It is straightforward that p_0, the

steady-state probability that the queue is empty, should equal $1 - \rho_c$. Then, we can have

$$P_B = 1 - \frac{1}{p_{d,0} + \rho}, \tag{4.16}$$

by using (4.15) for the case $k = 0$ and the fact that $p_0 = 1 - \rho_c$. Using (4.15) and (4.16), we have

$$p_k = \frac{1}{p_{d,0} + \rho} p_{d,k} \quad k = 0, 1, 2, \cdots, K - 1. \tag{4.17}$$

4.4.2 Offloading performance

Using (4.16) and (4.17), the mean number of customers N in the system can be represented as a function of K:

$$N(K) = \sum_{k=0}^{K} k p_k = \frac{1}{p_{d,0} + \rho} \sum_{k=0}^{K-1} k p_{d,k} + K(1 - \frac{1}{p_{d,0} + \rho}). \tag{4.18}$$

And the average total time in the system, i.e., average service delay, is also a function of K and can be calculated using Little's law:

$$W(K) = \frac{N}{(1 - P_B)\gamma} = \frac{\sum_{k=0}^{K-1} k p_{d,k} + K(p_{d,0} + \rho - 1)}{\gamma}. \tag{4.19}$$

We use unblocked rate $(1 - P_B)$ to measure the offloading effectiveness $\mathcal{E}$. For the system with queue capacity K, request size S, and statistics of on and off periods, λ and μ, the offloading effectiveness can be calculated by

$$\mathcal{E} = 1 - P_B = \frac{1}{p_{d,0} + \rho}. \tag{4.20}$$

Thus, the blocked services requests, with portion P_B of the total traffic, should be transmitted using cellular networks. To show the offloading capability for a given traffic load, define average offloading throughput for traffic load γ as

$$\Omega = \gamma S \mathcal{E} = \frac{\gamma S}{p_{d,0} + \rho}. \tag{4.21}$$

It can be seen that for a given γ, a larger $\mathcal{E}$ generally leads to a larger Ω. However, for an overload queue ($\rho > 1$) due to the heavy traffic, there is an upper bound of the average offloading throughput, denoted by Ω_m. For an overloaded queue, we can calculate Ω_m by setting $p_0 = 0$ since the server keeps busy serving the requests. Because the average service time of a request is its mean EST, calculated by (4.4), we can obtain the upper bound of the average offloading throughput as

$$\Omega_m = \frac{S}{\mathbb{E}[t_e]} = \frac{\bar{r}}{1 + \frac{\lambda}{\mu}}. \tag{4.22}$$

As discussed above, there is a tradeoff between average service delay and the offloading effectiveness. Such a tradeoff is analyzed using the results of the queueing model. There are two cases that VUs and network operators may care about: 1) Given a certain average service delay, how much data can be offloaded; 2) To offload a certain amount of data, how much is the least average delay that the users should tolerate. For 1), assume that the average service delay that users can tolerate is W_U^*. The corresponding K should be

$$K^* = \max\{K | W(K) \leq W_U^*\}. \tag{4.23}$$

Then, the offloading effectiveness $\mathcal{E}^*$ can be calculated by

$$\mathcal{E}^* = 1 - P_B|_{K=K^*} = \frac{1}{p_{d,0} + \rho}|_{K=K^*}. \tag{4.24}$$

For 2), the solution is similar by setting a target offloading effectiveness $\mathcal{E}_U^*$.

4.5 Simulation Results

In this section, we evaluate our proposed queueing model, and demonstrate the performance of vehicular WiFi offloading and the tradeoff between offloading effectiveness and average service delay. The simulation is carried out in a 2.0 km $\times$ 2.0 km region road map of the downtown area of Washinton D.C., USA. WiFi APs are randomly deployed with the coverage radius of 100 meters. There may exist overlapping of WiFi coverage areas. However, we show that low-level overlapping has little impact on the offloading performance. The street layout and AP locations are shown in Fig. 4.4. Each street segment has two lanes with the bidirectional vehicle traffic. VANETMobisim [134] is used to generate the mobility traces of 300 vehicles. With 50 deployed APs, the parameters can be obtained from the simulation, as $1/\lambda = 31.5$ s, $1/\mu = 52.09$ s, $\bar{n} = 1.54$, and $\text{Var}(n) = 7.71$. It is

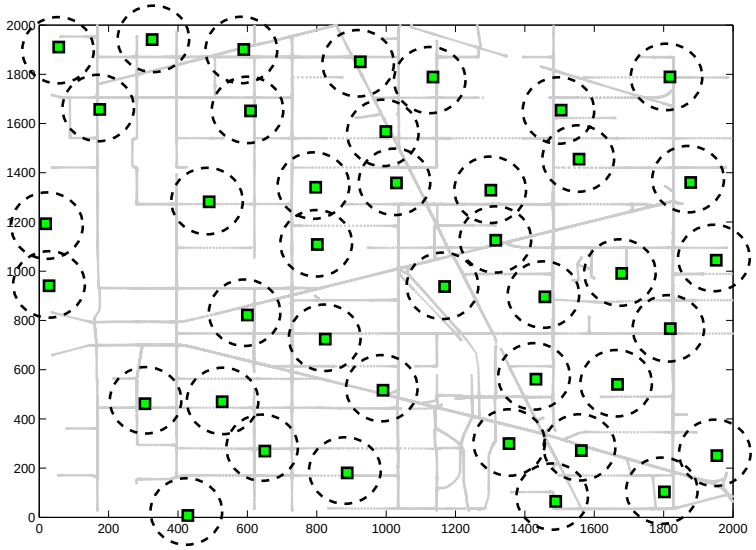

Figure 4.4: Street layout and AP locations. Number of APs is 40. The map data is from TIGER/Line Shapefiles [3].

considered that vehicles can transmit through WiFi immediately when they move into the coverage area, which is already supported by advanced WiFi technologies, e.g., HotSpot 2.0. With 802.11b bit rate 11 Mbps, $\bar{r} = 4.32$ Mbps using (4.1). Note that our proposed analytical model can be applied to other WiFi technologies if the average data rate is known. The service request size S is set to 5 MB, which is the size of a typical MP3 file.

The offloading effectiveness $\mathcal{E} = 1 - P_B$ is shown in Fig. 4.5(a). It can be seen that with a larger queue capacity K, the offloading effectiveness $\mathcal{E}$ increases, which means that a larger portion of mobile data can be offloaded via WiFi networks. Such results are straightforward because with larger K, more requests can be temporarily buffered, and then served when WiFi is available. On the other hand, if K is smaller, more service requests are blocked due to a full queue. However, there is a tradeoff between the offloading effectiveness and the average service delay. The average service delay is shown in Fig. 4.5(b). It can be seen that a larger K leads to larger average service delay, which may decrease the user satisfaction. We can also see that a large value of request arrival rate γ increases the average service delay and decreases the offloading effectiveness due to a larger traffic load. Moreover, the curves of analysis and simulation results match each other well, which validates the theoretical analysis. Fig. 4.5(c) shows the average offloading throughput Ω. It can be seen

Table 4.1: Maximum utility of VUs

$[K, U_m]$	$\gamma = 0.03$	$\gamma = 0.045$	$\gamma = 0.06$
$D_t = 400\ s$	[2, 1.17]	[8, 2.41]	[6, 2.54]
$D_t = 800\ s$	[4, 1.23]	[12, 2.59]	[8, 2.71]

that Ω increases with K, since $\mathcal{E}$ increases. When the queue is overloaded (e.g., $\gamma = 0.11$ in Fig. 4.5(c)), the upper bound of the average offloading throughput in such a scenario is about 1.63 Mbps.

To better depict the tradeoff between service delay and offloading effectiveness, we introduce the concept of user satisfaction level Φ, which reflects the user satisfaction with respect to the average delay W. In this paper, we simply use a linear relationship between Φ and W as $\Phi(W) = 1 - W/D_t$, where D_t is the delay tolerance of a user. Then, we define the utility of a VU as $H = \varpi\Omega + \Phi(W)$ which describes the user utility considering both average service delay and offloading throughput. ϖ is a parameter that accounts for the preference of the VU on the offloading throughput (or cost saved) with respect to the average service delay. Fig. 4.5(d) shows the utility with respect to D_t, with $\varpi = 2.5$. Results of maximum utility and corresponding K are summed in Table 4.1. It can be seen that if the delay constraint is loose (e.g., $D_t = 800$ s), users might care offloading throughput (or cost saved) more than the delay. They may choose larger K for a loose delay constraint to achieve higher offloading throughput and get the maximum utility. On the other hand, if the delay constraint is strict (e.g., $D_t = 400$ s), a smaller K is more likely to be chosen for lower average service delay.

4.6 Summary

In this chapter, we have theoretically investigated the performance of vehicular WiFi offloading. We have modeled the data service requests of VUs as an M/G/1/K queue, derived the probability distribution of the effective service time and analyzed the performance metrics of vehicular WiFi offloading, i.e., average service delay and offloading effectiveness by the queueing analysis. Simulation results have validated the analysis, and shown the relationship between average service delay and offloading effectiveness.

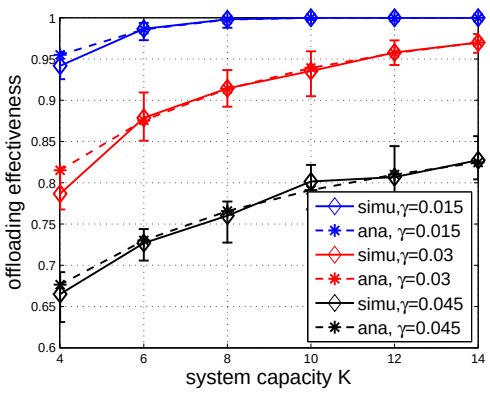

(a) Offloading effectiveness.

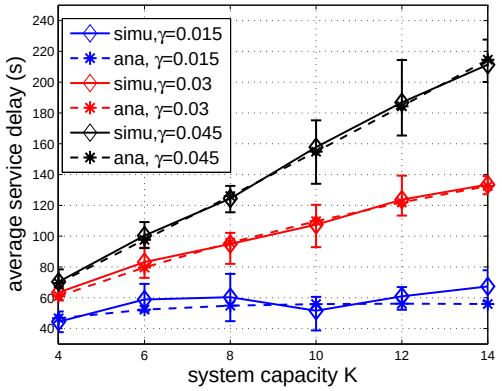

(b) Average service delay.

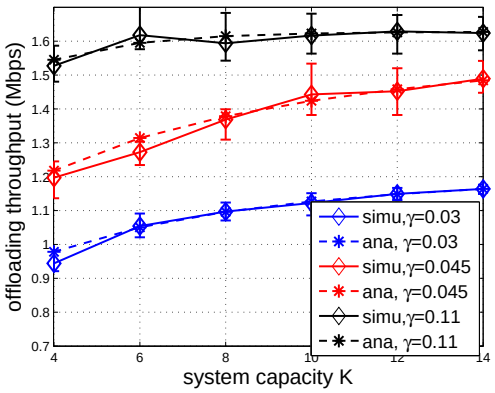

(c) Offloading throughput.

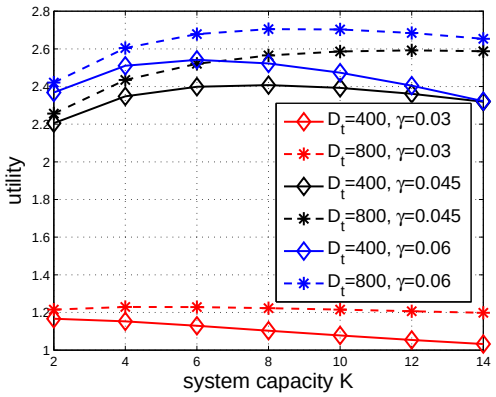

(d) User utility. $\varpi = 2.5$.

Figure 4.5: Simulation and theoretical results. The figures are plotted with 90% confidential intervals.

Chapter 5

Performance Analysis of V-D2D Communications

The demand for vehicular mobile data services has increased exponentially, which necessitates alternative data pipes for vehicular users other than the cellular network and dedicated short-range communication (DSRC). In this chapter, we study the performance of underlaid vehicular device-to-device (V-D2D) communications, where the cellular uplink resources are reused by V-D2D communications, considering the characteristics of the vehicular network. Specifically, we model the considered urban area by a grid-like street layout, with non-homogeneous distribution of vehicle density. We then propose to employ a joint power control and mode selection scheme for the V-D2D communications. In the scheme, we use channel inversion to control the transmit power, in order to determine transmit power based on pathloss rather than instantaneous channel state information, and avoid severe interference due to excessively large transmit power; the transmission mode is selected based on the biased channel quality, where D2D mode is chosen when the biased D2D link quality is no worse than the cellular uplink quality. Under the proposed scheme, two performance metrics of V-D2D underlaid cellular networks, SINR outage probability and link/network throughput, are theoretically analyzed. Simulation results validate our analysis, and show the impacts of design parameters on the network performance.

5.1 Introduction

To address the spectrum scarcity in VANETs, additional data pipes for VUs are desirable, which mitigate the congestion in cellular networks or in DSRC spectrum, and provide data

services to vehicles with QoS guarantee. Device-to-device (D2D) communication is envisioned as a promising solution for next-generation vehicular communication system [117]. By utilizing the proximity of mobile users, concurrent transmissions can reuse the same spectrum band without severely interfering each other, which significantly enhances the spectrum efficiency. In addition to spectrum utilization, vehicular D2D (V-D2D) communication can provide more benefits. Comparing to the transmitter-BS-receiver two-hop cellular transmission, V-D2D communication offers much shorter communication latency due to the one-hop proximate transmission, which facilitates delay-sensitive vehicular data services. Moreover, unlike distributed DSRC, V-D2D communications are controlled by the (centralized) cellular networks, in both control plane functions (e.g., connection setup and maintenance) and data plane functions (e.g., resource allocation). Thus, a better performance is expected thanks to collision avoidance and careful interference mitigation. Also, varied QoS requirements, such as rates, can be satisfied by resource (sub-carrier) allocation mechanisms. Finally, D2D communications could be less expensive than conventional cellular communications because of its inherent nature of spectrum reuse [55].

Due to the advantages of the D2D technology, it is suitable for many vehicular use cases, and can enable novel location-based and peer-to-peer applications and services. For example, considering the huge number of connected smart cars (90% new cars in 2020), the update of smart cars software can put a significant burden on the cellular network, and cost a lot of money of car manufacturers and car owners. Thus, the software update package can be first downloaded by chosen vehicles, and exchanged among other vehicles by vehicular D2D (V-D2D) communications. In the process, the cellular network can apply efficient algorithms to choose downloading vehicles, assist pair devices to reduce delay, and allocate resources (sub-carriers) to mitigate interference, satisfy different QoS requirements, and optimize the performance. In this way, most of the traffic can be offloaded to local V-D2D transmissions, and thus much cellular bandwidth and money can be saved. Moreover, due to the loose delay requirement of software update, the vehicular delay tolerant network (VDTN) can be employed where the package can be disseminated in a store-carry-and-forward manner, which can further offload the cellular network and save the cost. Another type of data service is gaming and video/audio streaming among vehicular users, such as in the vehicular proximity social network [116]. Normally, these services are supported by DSRC or WiFi-direct communication, which may not satisfy the requirements due to the collisions and long device paring time. With V-D2D communication, such services can be better sustained due to cellular-controlled connection setup with shorter delay, and resource (sub-carrier) allocation which can support varied rates.

However, we realize that there lacks a theoretical study that systematically investigates the performance of D2D communication for vehicular network scenarios. Indeed, this

topic is a challenging research problem. First, unique mobility patterns of vehicles impact the network performance differently, when comparing to well-understood human mobility patterns. Second, the grid-like vehicular network topology degrades the spectrum reuse efficiency, since V-D2D communications only happen on roads. Last but not the least, the interference pattern is even more difficult to model than normal D2D communications where the spatial user distribution can be modeled by Poison point process (P.P.P.) [135].

In this chapter, we establish a theoretical framework to analyze the performance of V-D2D communications underlaying cellular networks, by taking the unique characteristics of VANETs into consideration. To the best of our knowledge, our study is first of this kind to look into this emerging topic. Specifically, we model the urban road layout as a grid-like pattern. The cellular coverage areas are thus also considered as a square area, with the capability to extend to any other coverage patterns. The density of vehicles is modeled by non-homogeneous distributions in the considered area, because vehicles are more likely to move around social spots [136]. We then apply D2D communication in the modeled VANETs scenario. A channel inversion transmit power control mechanism is utilized to keep the receive power to be a threshold ρ_0. In addition, we employ a biased channel quality based mode selection strategy, where a biased factor φ explicitly controls the preference on V-D2D mode over cellular mode. Based on these models, two critical performance metrics, signal-to-interference-plus-noise (SINR) outage probability and link/network throughput, are theoretically analyzed, and the relation with the important design parameters ρ_0 and φ is obtained, followed by simulation validation. A counter-intuition observation is found that the network throughput does not always increase with larger φ (more D2D transmissions). Plus, the impact of φ on the network throughput also depends on ρ_0. The contributions of the paper are as follows:

- ▷ Our proposed V-D2D underlay cellular network is governed by simple yet effective mechanisms. In particular, a channel inversion power control scheme avoids high interference level in V-D2D system, and a biased mode selection strategy based on channel quality optimally controls the appropriate portion of vehicular users selecting D2D mode or cellular mode;

- ▷ Our proposed theoretical framework, which takes into account the unique characteristics of VANETs, is able to systematically evaluate the performance of V-D2D underlay cellular networks. We specifically examine the impact of inversion power control mechanism and biased mode selection strategy on such V-D2D networks. Two most critical performance metrics – SINR outage probability and throughput – are thoroughly analyzed and systematically validated via extensive simulations. The

Table 5.1: The useful notations for Chapter 5

Symbol	Description
r_i	Road segment i
L	Length of a road segment
Ω_C	The considered cellular coverage area
Ω_T	Inter-cell interference area of Ω_C
M	Side length of Ω_C
ϵ_i	Vehicle density on r_i
d_D	D2D transmission distance
$d_{C,i}$	Cellular uplink distance of r_i
γ_C, γ_D	Path-loss exponent of cellular transmission and D2D transmission
h	Channel gain
ρ_0	Receive power threshold
φ	Bias factor
$Z_{C,i}$, $Z_{D,i}$	Transmit power given D2D (resp. cellular) mode is selected
$\mathcal{I}$	Interference
η	Signal-to-interference-plus-noise ratio (SINR)
$p_{o,i}(\omega)$	SINR outage probability, where ω is SINR outage threshold
n_0	Noise power
σ	Average link throughput

relation between performance metrics and design parameters offers deep insights on the emerging V-D2D communications underlaying cellular network.

The proposed analytical framework provides theoretical insights into the performance of emerging V-D2D underlaying cellular networks. For cellular network operators, our framework not only offers guidelines to plan and deploy such cellular infrastructures and better utilize cherished spectrum resource, but also obtains the close-form relation between critical performance metrics and major system design parameters that could be used to further optimize the system efficiency of V-D2D networks.

The remainder of the chapter is organized as follows. Section 5.2 describes the system model. Section 5.3 theoretically analyzes the network performance, followed by framework validation via simulation in Section 5.4. Finally, Section 5.5 concludes the chapter.

5.2 System Model

In this section, the system model of the analytical framework is presented. We first describe the street pattern of the considered area, followed by the network model, including the D2D and cellular transmission distances, the transmit power control, and channel characteristics. Then, the mode selection strategy is given, where a bias factor φ is used to reflect the preference of D2D transmissions over cellular transmissions. A summary of the mathematical notations used in this paper is given in Table 5.1.

5.2.1 Street Pattern

We consider an urban area fully covered by the LTE cellular network. The considered area has a grid-like street pattern, as the downtown area of many cities, such as Houston and Portland [120]. The network geometry consists of a set of north-south (vertical) roads intersected with a set of east-west (horizontal) roads, as shown in Fig. 5.1. The lengths of each road segment r_i are identical, which is denoted by L, leading to equal-sized square street blocks with side length L. We further consider the coverage area of an LTE eNB to be a square, with the side length M normalized by L. Also denote the considered cellular coverage area by Ω_C. Note that we consider M is even in the analysis, while the methodology can be easily applied when M is odd. Denote the set of road segments within a cellular coverage area by $\mathcal{M}_\mathcal{C}$ with $|\mathcal{M}_\mathcal{C}| = 2M(M+1)$. There are two things worth to be noted. First, we focus on the urban area because in these areas V-D2D communication is more urgent due to the heavy-loaded data traffic, and we will leave the analysis of suburban and rural areas in the future works; second, the analysis can be easily applied to coverage patterns other than the square pattern, such as hexagon and Vorinoi coverage patterns which are more common coverage patterns of LTE networks.

The density of vehicles in road segments can impact the network performance, since V-D2D communication can happen only when two vehicles are close to each other. According to [137], the vehicle density at a location can be accurately modeled by different heavy-tail distributions, such as Weibull, log-logistic, and log-gamma distribution. We consider that on road segment r_i, the probability density function (PDF) and cumulative density function (CDF) of the vehicle density ϵ_i are $f_{\epsilon,i}(x)$ and $F_{\epsilon,i}(x)$, respectively.

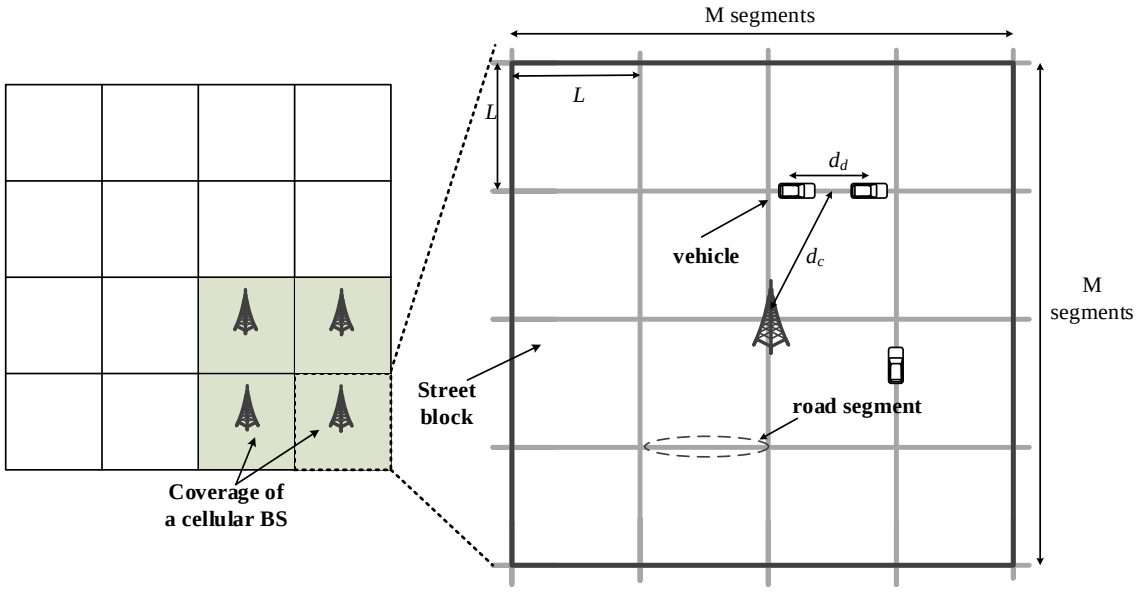

Figure 5.1: System model for V-D2D communications.

5.2.2 Network Model

The FDD LTE network is considered, where uplink and downlink transmissions use orthogonal sets of channels. We consider V-D2D communications for vehicle-to-vehicle data services in this paper, e.g., direct video/audio streaming or Internet contents sharing, while vehicle-to-infrastructure data services can be supported by normal cellular transmissions. Two VUEs can transmit data via the cellular network, and as an alternative, if close to each other, they can transmit directly without going through the LTE, i.e., V-D2D transmissions. Without the loss of generality, V-D2D transmissions can happen only when two VUEs are in the same road segment r_i, for the reasons that V-D2D transmissions are only available for vehicles in proximity, and it is usually difficult for the signal to transmit between two intersected road segments in urban areas due to the block of buildings. In addition, vehicles in the same road segment are more likely to preserve a longer and more reliable connection, which avoids frequent D2D connection set up and tear down. Therefore, the eNB can schedule V-D2D communication only within one road segment. A similar consideration can be found in [136]. Then, the D2D transmission distance $d_D \in [0, L]$ [1].

[1]Since the D2D communication often involves bi-directional communication, we do not differentiate D2D transmitter and receiver in this paper.

Since the existence of a transmission in r_i requires no less than two vehicles in r_i, the probability a transmission request exists in r_i can then be calculated by $p_{T,i} = 1 - F_{\epsilon,i}(2)$. It is further considered that within a road segment r_i, the location of an arbitrary VUE follows a uniform distribution, which means that within r_i, a VUE appears in any location equally likely. Consequently, given that a V-D2D link exists in r_i, the V-D2D transmission distance $d_{D,i}$ follows a triangular distribution, and thus the PDF of $d_{D,i}$ can be expressed by

$$f_{d_{D,i}}(x) = \frac{2}{L}(1 - \frac{x}{L}). \tag{5.1}$$

Since $f_{d_{D,i}}(x)$ does not depend on i, D2D transmission distances in all road segments are independent and identically distributed (*i.i.d.*) random variables with the PDF given in (5.1). Note that the distribution of locations a vehicle may appear in a road segment can be extended to a general model, and the distribution of V-D2D distances can be obtained in a similar way. For cellular uplink transmission, denote by $d_{C,i}$ the cellular uplink distance if the transmitting VUE is in r_i. For the simplicity of analysis, we consider that $d_{C,i}$ is independent of $d_{D,i}$, and is approximated by the distance from the eNB to the middle point of r_i, due to that usually the cellular uplink distance is much larger than the D2D distance. Therefore, due to the symmetry of the road pattern, the probability mass function (PMF) of the cellular uplink distance $d_{C,i}$, denoted by $p_{d_C}(x)$, can be easily obtained as

$$p_{d_C}(x) = \begin{cases} \frac{4}{|\mathcal{M}_C|}, & x = \frac{L}{2} \\ \frac{8}{|\mathcal{M}_C|}, & x = \frac{\sqrt{5}L}{2} \\ \frac{4}{|\mathcal{M}_C|}, & x = \frac{3L}{2} \\ \frac{8}{|\mathcal{M}_C|}, & x = \frac{13L}{2} \\ \dots \end{cases} \tag{5.2}$$

Due to the high mobility of vehicles, the rapid channel variations results in difficulty in obtaining real-time full CSI which contains the actual channel fading parameters. Thus, large-scale fading effects including path loss and shadowing are preferred when designing V-D2D communication protocols [118,119,138]. In [117], a simulation has been conducted, showing that the performance degradation of V-D2D communication is very little when only path loss is considered. Based on these observations, in this paper, we only consider the large-scale fading effects. Following [135] and [139], we consider a general power-law path-loss model with the decay rate $d^{-\gamma}$, where d is the distance between the transmitter and the receiver, and $\gamma > 2$ is the path-loss exponent. The cellular uplink and V-D2D links

may have different path-loss exponents, denoted by γ_C and γ_D, respectively. We consider a Rayleigh fading environment[2], where the channel gain h between any two locations follows *i.i.d.* exponential distribution with unit mean, i.e., $h \sim exp(1)$.

The transmit power is regulated by a channel inversion power control model, in which the path-loss is compensated by the transmit power such that the average received signal power at the intended receiver (i.e., eNB for uplink transmissions and receiving VUE for V-D2D transmission) equals a certain receive power threshold ρ_0. Therefore, the instant received power can be expressed by $\rho_0 h$. In general, if the channel inversion power control is employed, a power truncate outage may happen due to that the required transmit power is larger than the maximum transmit power P_m [135]. However, in the considered urban V-D2D scenario, power truncate outage does not happen since P_m is large enough to compensate the path-loss of a cellular edge transmission, the distance of which is much larger than the maximum D2D transmission distance L. The V-D2D communications underlaying cellular network may have multiple channels. However, since the interference statistics of all channels are similar, we restrict our analysis to one channel, which is shared by V-D2D transmissions and maximum one uplink transmission in the considered cellular coverage area.

5.2.3 Mode Selection Strategy

VUEs can transmit data using either cellular mode or D2D mode. In cellular mode, eNB routed two-hop transmission is employed: the data packet is first transmitted from the transmitting VUE to the eNB through uplink channels, and then from the eNB to the receiving VUE through downlink channels. In D2D mode, two VUEs can directly transmit data reusing the cellular uplink resources. The cellular uplink resources are reused by V-D2D transmissions, since the interference caused at the BS can be efficiently managed [141]. The mode selection greatly impacts the network performance. If more VUEs select D2D mode, the frequency spatial reuse can be improved; however, more interference is introduced to both D2D and cellular uplink transmissions. Therefore, more D2D transmissions do not always enhance the throughput or offloading performance, as demonstrated in [117].

In this paper, we employ a biased channel quality based mode selection strategy to model the tradeoff among SINR, frequency reuse, throughput, and offloading performance. In the biased channel quality based mode selection, a VUE selects D2D mode if the biased

[2]Methods to relax to general fading models can be found in [140]

quality of D2D channel is no worse than the quality of the cellular uplink channel, i.e.,

$$P_{t,D} = \rho_0 d_D^{\gamma_D}; \tag{5.3}$$

otherwise, the cellular mode will be chosen. The bias factor φ reflects the preference on D2D mode over cellular mode, where a larger φ indicates that D2D transmissions are more likely to happen, leading to higher frequency reuse and more interference. With this model, the interference to the cellular uplink transmissions can be controlled. To satisfy (5.3), a D2D transmission closer to the eNB tends to have a smaller transmission distance d_D, and a correspondingly smaller transmit power due to the channel inversion power control. We show that the interference power from any D2D transmission to the eNB can be upper bounded by $\varphi\rho_0$ in Appendix 5.6.1. Fig. 5.2 shows the mode selection results in terms of φ, in a scenario with $L = 100$ m and $M = 10$. A dot in the figures indicates a transmission request between two vehicles within road segment r_i, while blue dot and red dot indicate that the transmission selects cellular and D2D mode, respectively. It can be seen that the number of V-D2D transmissions (shown as red dots) increases when the value of φ becomes larger, since a larger φ indicates D2D mode is more preferred. Moreover, in the area closer to the BS, the D2D transmission is less likely to happen, which protects the cellular uplink transmission from severe interference.

Under the mode selection strategy, we can calculate the probability that D2D/cellular mode is selected. In road segment r_i, the cellular uplink distance $d_{C,i}$ is a constant. Thus, given a transmission request among two VUEs in r_i, the probability that D2D mode is selected can be obtained by

$$\begin{aligned} p_{D,i} &= \mathbb{P}(\varphi d_{D,i}^{-\gamma_D} \geq d_{C,i}^{-\gamma_C}) \\ &= F_{d_D}(\varphi^{\frac{1}{\gamma_D}} d_{C,i}^{\frac{\gamma_C}{\gamma_D}}) \\ &= \frac{\varphi^{\frac{1}{\gamma_D}} d_{C,i}^{\frac{\gamma_C}{\gamma_D}}}{L}(2 - \frac{\varphi^{\frac{1}{\gamma_D}} d_{C,i}^{\frac{\gamma_C}{\gamma_D}}}{L}) \end{aligned} \tag{5.4}$$

where $F_{d_D}(\cdot)$ is the cumulative density function (CDF) of D2D distance d_D. Accordingly, the probability that the cellular mode is selected is $p_{C,i} = 1 - p_{D,i}$.

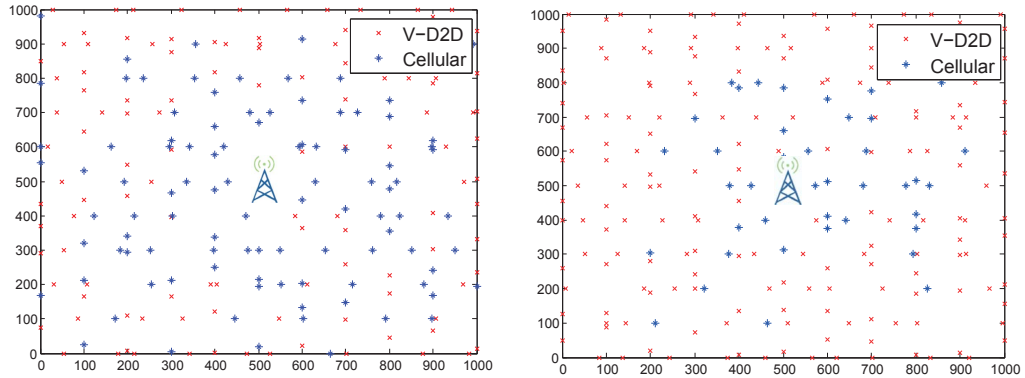

(a) $\varphi = 10^{-4}$.

(b) $\varphi = 5 \times 10^{-4}$.

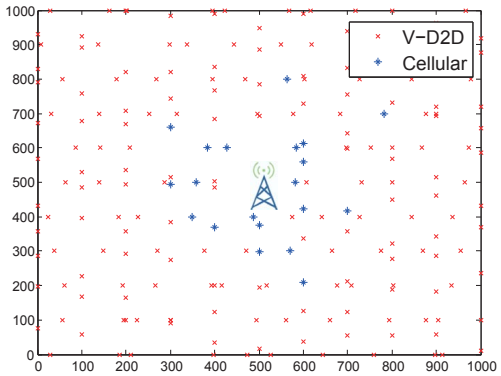

(c) $\varphi = 5 \times 10^{-3}$.

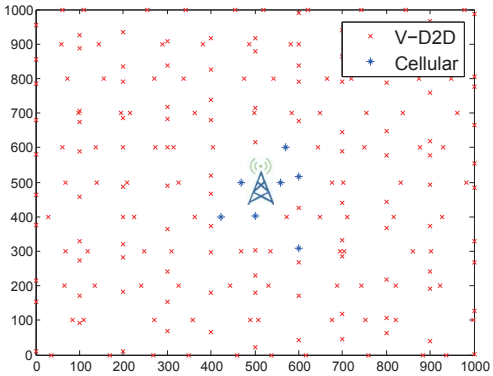

(d) $\varphi = 10^{-2}$.

Figure 5.2: Mode selection result.

5.3 Network Performance Analysis

In this section, we analyze the performance of the V-D2D communications underlaying cellular networks. We start with the probability distribution of the transmit power of an arbitrary V-D2D transmission and cellular uplink transmission. Then, we analyze the interference from both V-D2D transmissions and uplink transmission in the considered cellular coverage area and the first tier around the considered cellular coverage area, based on which the probability distribution of SINR is derived. Then, the performance metrics, the SINR outage probability and throughput, are theoretically obtained. Note that for integer values of path loss exponents, the SINR outage probability can be expressed in closed-form.

5.3.1 Transmit power

In this part, we analyze the transmit power of both D2D mode and cellular mode. According to the channel inversion power control and mode selection model, the maximum D2D transmission power in road segment r_i is $P_{D_{m,i}} = \min\left(P'_{D_m}, \varphi\rho_0 d_{C,i}^{\gamma_C}\right)$, where $P'_{D_m} = \rho_0 L^{\gamma_D}$ is the maximum transmit power due to the maximum V-D2D distance L, and $\varphi\rho_0 d_{C,i}^{\gamma_C}$ is the maximum transmit power due to the mode selection strategy. Given D2D mode is selected, the D2D transmit power $Z_{D,i}$ is the transmit power required to compensate the path-loss conditioned on $\varphi d_{D,i}^{-\gamma_D} \geq d_{C,i}^{-\gamma_C}$, i.e., $Z_{D,i} = \{P_{D,i} : \varphi d_{D,i}^{-\gamma_D} \geq d_{C,i}^{-\gamma_C}\}$, where $P_{D,i}$ is the unconditioned V-D2D transmit power. The PDF of $Z_{D,i}$ is given in Lemma 1.

Lemma 1 *In the urban V-D2D communication underlaying cellular network with channel inversion power control and biased channel quality based mode selection, the PDF of the D2D transmit power in r_i, denoted by $Z_{D,i}$, is given by*

$$f_{Z_{D,i}}(x) = \frac{1}{p_{D,i}}\left(\frac{2x^{\frac{1}{\gamma_D}-1}}{\gamma_D L \rho_0^{\frac{1}{\gamma_D}}} - \frac{2x^{\frac{2}{\gamma_D}-1}}{\gamma_D L^2 \rho_0^{\frac{2}{\gamma_D}}}\right), Z_{D,i} \leq P_{D_{m,i}}, \tag{5.5}$$

where $P_{D_{m,i}} = \min\left(P'_{D_m}, \varphi\rho_0 d_{C,i}^{\gamma_C}\right)$.

Proof. See Appendix 5.6.2. □

For cellular mode, the transmit power $Z_{C,i}$ is the transmit power from the VUE to the eNB (denoted by $P_{C,i}$) conditioned on $\varphi d_{D,i}^{-\gamma_D} < d_{C,i}^{-\gamma_C}$. Since $P_{C,i} = \rho_0 d_{C_i}^{\gamma_C}$ is a constant, $Z_{C,i} = P_{C,i} = \rho_0 d_{C_i}^{\gamma_C}$ is a constant.

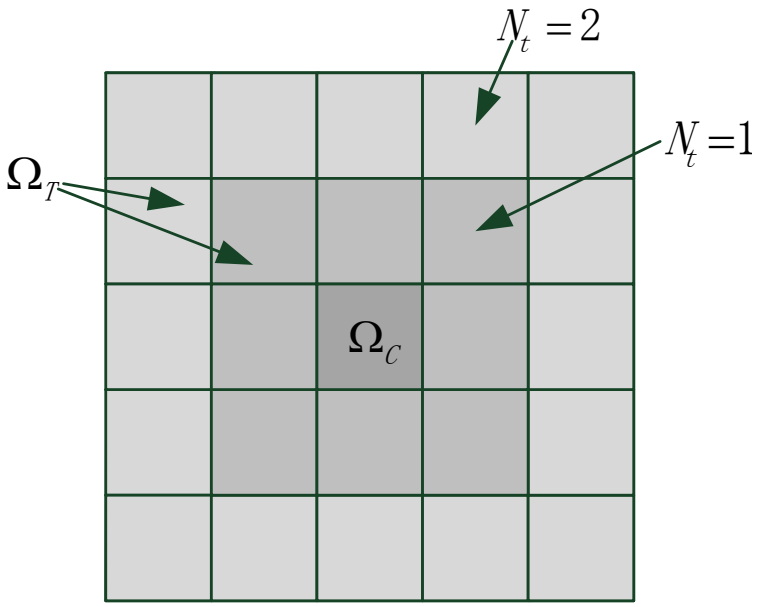

Figure 5.3: Interference area with $N_t = 2$.

5.3.2 Interference and signal-to-interference-plus-noise ratio

In cellular networks, the interference is caused by co-channel transmissions in the same cell and neighboring cells, which is called intra-cell interference and inter-cell interference, respectively. In V-D2D communications underlaying cellular networks, the interference is caused by not only cellular uplink transmission, but also D2D transmissions which reuse uplink resources. In this part, we consider intra-cell and inter-cell interference from both cellular uplink transmissions and V-D2D transmissions. For inter-cell interference, we consider the interference from N_t tiers of cells around the considered cell, as shown in Fig. 5.3. Usually considering $N_t = 1$ is sufficient to analyze the inter-cell interference, and the interference power from transmissions of even further areas can be considered as noise.

Denote the considered cellular coverage area by Ω_C, the area where inter-cell interference originates by Ω_T, and $\Omega_I = \Omega_C + \Omega_T$. Denote the sets of road segments in Ω_C, Ω_T, and Ω_I by $\mathcal{M}_\mathcal{C}$, $\mathcal{M}_\mathcal{T}$, and $\mathcal{M}_\mathcal{I}$, respectively. Consider a D2D/uplink transmission in road segment $r_i \in \mathcal{M}_\mathcal{C}$. The total interference to the D2D/uplink transmission can be expressed

by

$$\begin{aligned}\mathcal{I}_i &= \mathcal{I}_{\mathcal{D},i} + \mathcal{I}_{\mathcal{C},i} \\ &= \sum_{r_j \in \mathcal{M}_{\mathcal{I}} \setminus r_i} \mathbb{1}_{D,j} Z_{D,j} h d_{ji}^{-\gamma_D} + \mathbb{1}_{C,j} Z_{C,j} h d_{ji}^{-\gamma_C},\end{aligned} \tag{5.6}$$

where $Z_{D,i}$ (resp. $Z_{C,i}$) is the transmit power of V-D2D (resp. cellular uplink) transmission in road segment r_i. d_{ji} is the distance from the interferer to the receiver, and d_{j0} denotes the distance from the interferer to the eNB of Ω_C. For simplicity, when the interference to the V-D2D transmission is considered, d_{ji} is the distance between the middle points of r_j and r_i; when the interference to uplink transmission is considered, d_{j0} is the distance from the middle point of r_j to the location of eNB of Ω_C. $\mathbb{1}_{D,i}$ and $\mathbb{1}_{C,i}$ are indicator functions where $\mathbb{1}_{X,i} = 1$ if a transmission request exists in r_i and chooses mode X, and $\mathbb{1}_{X,i} = 0$ otherwise. Based on the vehicle density distribution and the mode selection strategy, $\mathbb{P}(\mathbb{1}_{D,i} = 1) = p_{T,i} p_{D,i}$. Furthermore, for the analysis tractability, we consider that cellular uplink scheduling is round-robin [135]. Therefore, when $|\mathcal{M}_{\mathcal{C}}|$ becomes larger, the probability that no transmission selects cellular mode gets smaller (i.e., $\prod_{r_i \in \mathcal{M}_{\mathcal{C}}} 1 - p_{T,i}(1 - p_{D,i})$ gets smaller), and $\mathbb{P}(\mathbb{1}_{C,i} = 1) \approx \frac{p_{T,i}(1-p_{D,i})}{\sum_{r_i \in \mathcal{M}_{\mathcal{C}}} p_{T,i}(1-p_{D,i})}$.

With the total interference $\mathcal{I}_i$ given in (5.6), the signal-to-interference-plus-noise ratio (SINR) of a D2D/uplink transmission in road segment $r_i \in \mathcal{M}_{\mathcal{C}}$ can be expressed by

$$\eta_i = \frac{\rho_0 h}{n_0 + \sum_{r_j \in \mathcal{M}_{\mathcal{I}} \setminus r_i} \mathbb{1}_{D,j} Z_{D,j} h d_{ji}^{-\gamma_D} + \mathbb{1}_{C,j} Z_{C,j} h d_{j0}^{-\gamma_C}}, \tag{5.7}$$

where n_0 is the noise power.

5.3.3 Performance metrics

V-D2D communications can improve the frequency spatial reuse, and therefore the spectrum efficiency and throughput can be increased. On the other hand, more interference is introduced, resulting in decreasing SINR for both D2D and cellular transmissions. Therefore, in this part, we consider two performance metrics, i.e., SINR outage probability and throughput, to analyze the performance of the V-D2D communications underlaying cellular network.

Given the SINR outage threshold ω, the SINR outage probability of the transmission

$$p_{oD,i}(\omega) = 1 - \exp(\frac{-\omega n_0}{\rho_0}) \prod_{r_j \in \mathcal{M}_{\mathcal{I}} \setminus r_i} \big(\frac{2 p_{T,j} P_{D_{m,j}}^{\frac{1}{\gamma_D}} \mathcal{H}([1, \frac{1}{\gamma_D}], [1 + \frac{1}{\gamma_D}], \beta)}{L \rho_0^{\frac{1}{\gamma_D}}} - \frac{p_{T,j} P_{D_{m,j}}^{\frac{2}{\gamma_D}} \mathcal{H}([1, \frac{2}{\gamma_D}], [1 + \frac{2}{\gamma_D}], \beta)}{L^2 \rho_0^{\frac{2}{\gamma_D}}}$$
$$+ 1 - p_{D,j} p_{T,j} \big) \cdot \frac{1}{\sum_{r_i \in \mathcal{M}_{\mathcal{C}}} p_{T,i}(1 - p_{D,i})} \sum_{r_j \in \mathcal{M}_{\mathcal{I}} \setminus r_i} \frac{p_{T,j}(1 - p_{D,j})}{(1 + s Z_{C,j} d_{ji}^{-\gamma_C})} \tag{5.8}$$

---

in r_i is

$$\begin{aligned} p_{o,i}(\omega) &= \mathbb{P}(\eta_i \leq \omega) \\ &= \mathbb{P}(h \leq \frac{\omega}{\rho_0}(n_0 + \mathcal{I}_{\mathcal{D},i} + \mathcal{I}_{\mathcal{C},i})) \\ &\overset{i}{=} 1 - \exp\{-\frac{\omega}{\rho_0}(n_0 + \mathcal{I}_{\mathcal{D},i} + \mathcal{I}_{\mathcal{C},i})\} \\ &\overset{ii}{=} 1 - \exp\{-\frac{\omega n_0}{\rho_0}\} \mathcal{L}_{\mathcal{D},i}(\frac{\omega}{\rho_0}) \mathcal{L}_{\mathcal{C},i}(\frac{\omega}{\rho_0}), \end{aligned} \tag{5.9}$$

where $\mathcal{L}_{\mathcal{X}}(\cdot)$ denotes the Laplace transform of the PDF of the random variable, when mode X is chosen, and $\mathcal{L}_{\mathcal{D},i}(\cdot)$ and $\mathcal{L}_{\mathcal{C},i}(\cdot)$ are calculated in Appendix 5.6.3. In (5.9), (i) follows since h is an exponential random variable with unit mean, and (ii) follows because the transmission modes in each road segment are independent. Then, a V-D2D transmission in r_i, the SINR outage probability $p_{oD,i}(\omega)$ is given in (5.8), where $\mathcal{H}(\cdot)$ is hypergeometric function, and $\beta = -\frac{\omega}{\rho_0} d_{ji}^{-\gamma_D} P_{D_{m,i}}$. Therefore, the average V-D2D SINR outage probability in Ω_C, denoted by $p_{oD}(\omega)$, can be calculated by

$$p_{oD}(\omega) = \frac{\sum_{r_i \in \mathcal{M}_{\mathcal{C}}} p_{T,i} p_{D,i} p_{oD,i}(\omega)}{\sum_{r_i \in \mathcal{M}_{\mathcal{C}}} p_{T,i} p_{D,i}}. \tag{5.10}$$

For cellular uplink transmissions, the interference is caused at the eNB of Ω_C. Therefore, for an arbitrary cellular uplink transmission, the SINR outage probability can also be calculated by (5.8), where d_{ji} is replaced by d_{j0}. Note that for integer value of γ_C and γ_D, (5.8) has closed-form expression.

Another important performance metric is the link/network throughput. Since the V-D2D communications introduce interference to the network, the throughput of the cellular uplink is degraded. However, at network level, the throughput can be enhanced by spatial spectrum reuse due to concurrent transmissions. The average link throughput in a unit

spectrum (or spectrum efficiency) when the transmitter is in r_i, denoted by σ_i, can be calculated based on the SINR outage probability:

$$\begin{aligned}\sigma_i &= \mathbb{E}[\log_2(1+SINR_i)] \\ &= \int_0^\infty \mathbb{P}(\log_2(1+SINR_i) > x)dx \\ &= \int_0^\infty \mathbb{P}(\eta_i > 2^x - 1)dx \\ &= \int_0^\infty 1 - p_{o,i}(2^x - 1)dx, \end{aligned} \tag{5.11}$$

where $p_{o,i}(\cdot)$ is the SINR outage probability given in (5.9). Therefore, the average total spectrum efficiency in a cellular coverage Ω_C can be calculated by

$$\sigma = \sum_{r_i \in \mathcal{M}_\mathcal{C}} p_{T,i}\big(p_{D,i}\sigma_{D,i} + \frac{1-p_{D,i}}{\sum_{r_i \in \mathcal{M}_\mathcal{C}} p_{T,i}(1-p_{D,i})}\sigma_{C,i}\big) \tag{5.12}$$

5.4 Evaluation

In this section, we conduct a simulation to validate the proposed analytical framework. In an urban area with grid-like road system, the length of road segment $L = 100$ m, and the side length of a cellular BS coverage area is set to $M = 10$ road segments. Each road segment has two lanes with bidirectional vehicle traffic. We use VANETMobisim [134] to generate the mobilities of vehicles. Speed limit is set to 50 km/h. The vehicle mobility is controlled by Intelligent Driver Model with Lane Changes (IDMLC) model, in which vehicle speed is based on movements of vehicles in neighborhood. Unless otherwise stated, we set the channel inversion threshold $\rho_0 = -80$ dBm, noise power $N_0 = -90$ dBm, the path-loss exponents $\gamma_C = \gamma_D = 4$, the SINR outage threshold $\omega = 2$, and $N_t = 1$ tier of cells where inter-cell interference is considered. All simulation results are plotted with 10% confidential intervals.

In the simulation, two arbitrary vehicles in the same road segment can request a transmission between each other. If more than two transmission requests happen in the same road segment, the cellular network randomly schedules one request with V-D2D transmission (called potential V-D2D transmission), and schedules the others to use traditional cellular transmissions, i.e., the transmitter-BS-receiver two-hop transmissions. A potential V-D2D transmission selects the D2D mode if the D2D selection condition (5.3) is satisfied;

otherwise, the cellular mode is selected. Note that only one cellular uplink transmission can be scheduled in one time and sub-channel.

Fig. 5.4 shows the average SINR outage probability in the considered area Ω_C, including V-D2D transmissions and cellular uplink transmissions, with respect to (w.r.t.) the SINR outage threshold ω, and varied values of ρ_0 and φ. Straightforwardly, the SINR outage probability increases with the increase of the outage threshold ω. Different vehicular services and applications may require different data rates, which correspond to different SINR requirements. Thus, the results of Fig. 5.4 indicate that for data-craving applications, such as high-quality video streaming, the SINR outage probability could be higher, which can be an important design concern of the V-D2D communications underlaying cellular network. Fig. 5.4(a) shows the impact of the channel inversion threshold ρ_0 on the SINR outage probability. ρ_0 influence the SINR in two different ways. On one hand, with a smaller value of ρ_0, the V-D2D/cellular transmitters can use a smaller power, and thus cause less interference to each other; on the other hand, the received signal power $\rho_0 h$ is also smaller. In the simulated scenario, the latter, i.e., the impact on the received signal power dominates, and thus the SINR outage probability increases with the decrease of ρ_0. Note that the conclusion may vary with different VANETs topology patterns and topology parameters L and M, the analysis of which is considered one of our future works. Fig. 5.4(b) shows the impact of the bias factor φ on the SINR outage probability. With a larger value of φ, more transmission requests will choose D2D mode, which in turn causes more interference, and results in higher SINR outage probability.

Fig. 5.5 shows the SINR outage probability w.r.t. the bias factor φ. One important observation is that the SINR outage probability increases monotonously with φ. Different from ρ_0, φ does not impacts the received signal power, but influence the interference in the following ways. First, a higher value of φ leads to a higher D2D selecting probability according to (5.4), and thus more concurrent transmissions. Second, with a higher value of φ, it is more likely for V-D2D transmission to use a higher transmit power based on (5.5). Therefore, a higher value of φ will lead to a higher level of interference, and thus result in a higher average SINR outage probability. However, a higher average SINR outage probability does not necessarily indicate a lower cell throughput, which will be discussed later. When φ surpasses a certain value, most of V-D2D transmissions can use the possibly maximum transmit power, i.e., $P_{D_{m,i}} = \min\left(P'_{D_m}, \varphi\rho_0 d_{C,i}^{\gamma_C}\right) = P'_{D_m}$, and consequently further increasing φ will have little impact on the SINR outage probability, as shown in Fig. 5.5 where $\varphi > 0.9 \times 10^{-3}$.

Fig. 5.6 shows the throughput performance of the V-D2D underlaying cellular network w.r.t. the bias factor φ. The throughput is presented in the form of spectrum efficiency, and thus the unit is bits/s/Hz. It can be seen that a larger value of channel inversion threshold

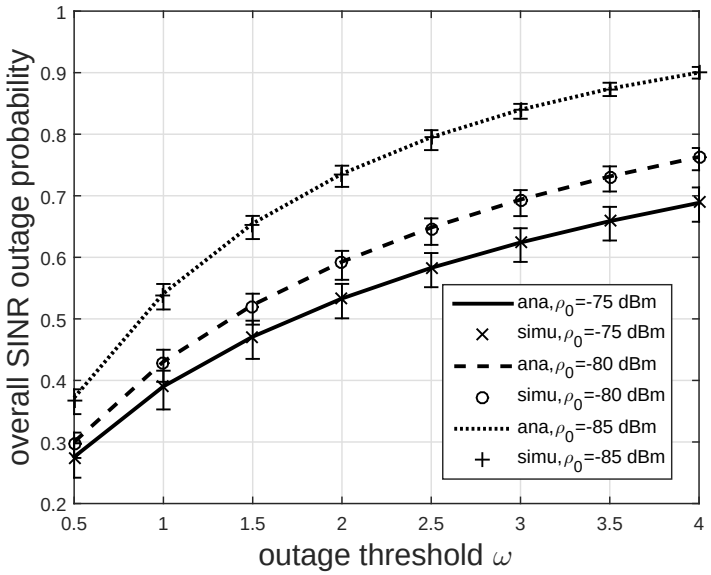

(a) Varied channel inversion threshold ρ_0.

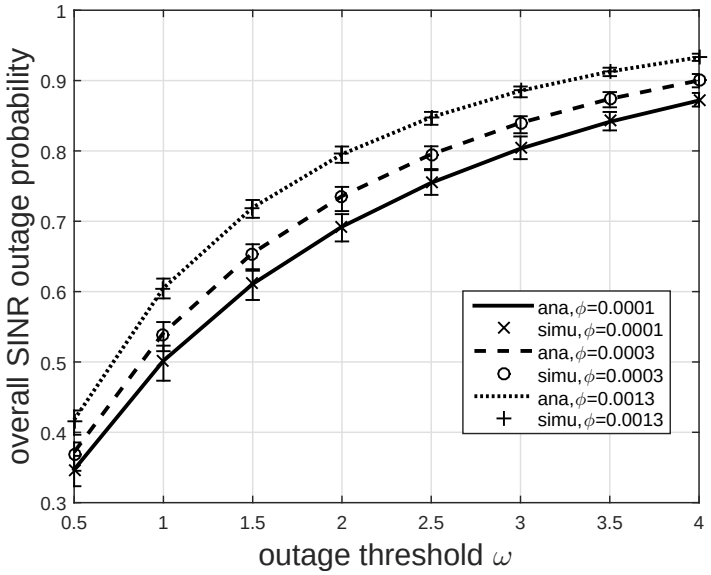

(b) Varied bias factor φ.

Figure 5.4: SINR outage probability w.r.t. ω.

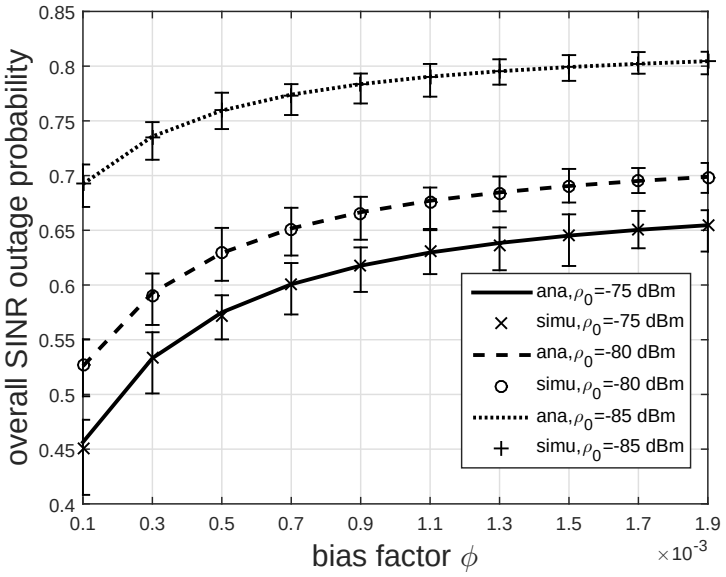

Figure 5.5: SINR outage probability w.r.t. φ.

ρ_0 leads to a higher throughput due to a higher SINR, as discussed in Fig. 5.4(a). In Fig. 5.6(a), we consider the average throughput of the cellular uplink transmission, i.e., $\sigma_C = \sum_{r_i \in \mathcal{M}_\mathcal{C}} \frac{p_{T,i}(1-p_{D,i})}{\sum_{r_i \in \mathcal{M}_\mathcal{C}} p_{T,i}(1-p_{D,i})} \sigma_{C,i}$, which reflects the cellular uplink throughput from the perspective of the network operator. As shown in the figure, the cellular uplink throughput decreases with the increase of φ. This is because with a larger φ, both D2D selecting probability and D2D transmission power increase, resulting in a larger interference at the BS. The SINR of the cellular uplink transmissions thus decreases, leading to a lower throughput. Different from Fig. 5.5, even when φ is large, there is still an obvious decrease of the cellular uplink throughput with the increase of φ. This is because the throughput of cellular uplink is mainly influenced by the D2D transmissions in the road segments close to the BS. When φ is large, the transmit power of these transmissions still increases with φ, as $P_{D_{m,i}} = \min\left(P'_{D_m}, \varphi\rho_0 d_{C,i}^{\gamma_C}\right) = \varphi\rho_0 d_{C,i}^{\gamma_C}$, which causes more interference at the BS. Fig. 5.6(b) shows the total average throughput in a cellular coverage area, including all V-D2D transmissions and the cellular uplink transmission. By comparing to Fig. 5.6(a), it is shown that V-D2D communications can greatly boost the spectral efficiency of the cellular networks. Also, for different values of channel inversion threshold ρ_0, the bias factor φ impacts the throughput in different ways. For the cases of $\rho_0 = -75$ dBm and $\rho_0 = -80$ dBm, the total throughput increases from $\varphi = 0.1 \times 10^{-3}$ to 0.3×10^{-3}, but decreases

slightly with the further increase of φ. This is because when φ is small, the interference is low, and with the increase of φ, there are more concurrent V-D2D transmissions, leading to larger total throughput. However, when φ is relatively large, the interference becomes the dominating factor, and thus the increase of φ leads to a decrease of total throughput. For the case of $\rho_0 = -85$ dBm, the total throughput increases with φ even when φ is larger than 0.3×10^{-3}. The reason is that when ρ_0 is small, the transmit power is small according to the channel inversion model, and thus the interference is small. Therefore, as the value of φ increases, more concurrent transmissions lead to a higher throughput. Compared with the results of Fig. 5.5, it can be seen that though the increase of φ increase the SINR outage probability, it can influence the total throughput in varied ways.

5.5 Summary

In this chapter, we have theoretically studied the performance of V-D2D underlaying cellular networks. We have modeled the urban road system and the vehicle density distribution, and employed channel inversion model and biased channel quality based mode selection to control the transmit power and mode selection of vehicular users. Two performance metrics, SINR outage probability and throughput, have been theoretically analyzed. Simulation has been conducted, which validates our analysis, and shows the impact of design parameters on the performance metric. Results in this chapter can be applied to obtain the performance of a V-D2D underlaid cellular network given the design parameters, and provide valuable guidance for network operators when deploying the future networks.

5.6 Appendix

5.6.1 Upper bound of interference

Consider an arbitrary D2D transmission in road segment r_i. According to the mode selection, D2D mode is selected if $\varphi d_{D,i}^{-\gamma_D} \geq d_{C,i}^{-\gamma_C}$. Then, we have $d_{D,i}^{\gamma_D} \leq \varphi d_{C,i}^{\gamma_C}$, and the D2D transmit power $\mathbb{P}_{D,i} = \rho_0 d_{D,i}^{\gamma_D} \leq \varphi \rho_0 d_{C,i}^{\gamma_C}$. Therefore, the interference at the eNB from the D2D transmission is given by

$$I_{D,i}^{C} = \mathbb{P}_{D,i} d_{C,i}^{-\gamma_C} \leq \varphi \rho_0. \tag{5.14}$$

From (5.14), we can see that the interference from any D2D transmission to the cellular uplink transmission is upper bounded by $\varphi \rho_0$.

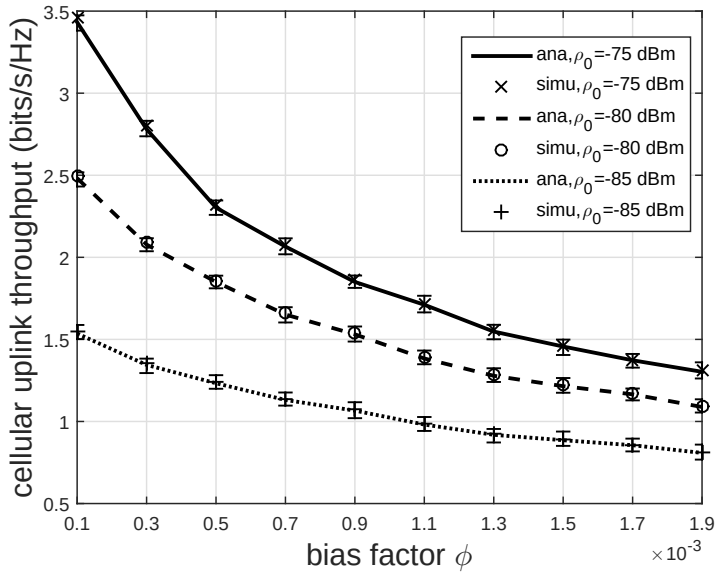

(a) Cellular uplink throughput.

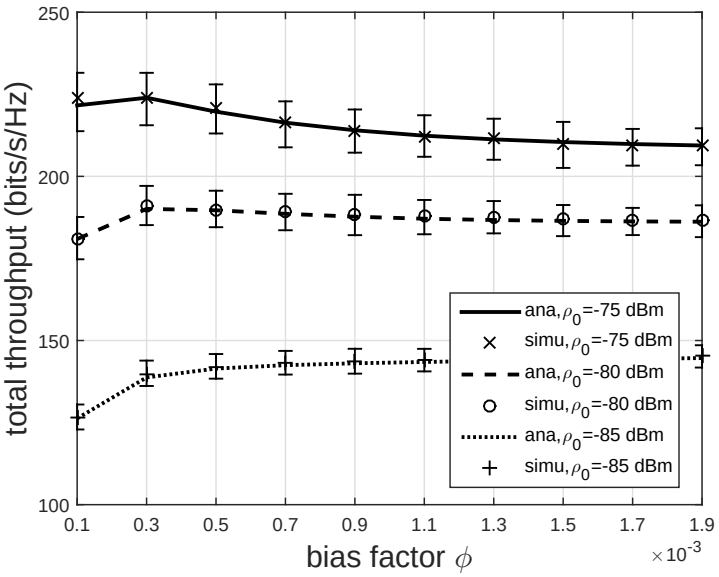

(b) Total throughput.

Figure 5.6: Throughput performance w.r.t. φ.

$$\mathcal{L}_{\mathcal{I}_{\mathcal{DD},i}}(s) \overset{\gamma=4}{=} \prod_{r_j \in \mathcal{M}_{\mathcal{I}} \setminus r_i} p_{T,j}\Big\{ - \frac{d_{ji}^2 \arctan(\frac{\sqrt{sx}}{d_{ji}^2})}{L^2\sqrt{\rho_0 s}}\Big\} + \frac{\sqrt{2}}{4} \frac{\frac{d_{ji}}{s^{\frac{1}{4}}} \ln(\frac{\sqrt{x}+\sqrt{2}x^{\frac{1}{4}}\frac{d_{ji}}{s^{\frac{1}{4}}}+\frac{d_{ji}^2}{\sqrt{s}}}{\sqrt{x}-\sqrt{2}x^{\frac{1}{4}}\frac{d_{ji}}{s^{\frac{1}{4}}}+\frac{d_{ji}^2}{\sqrt{s}}})}{L\rho_0^{\frac{1}{4}}}$$
$$+ \frac{\sqrt{2}}{2} \frac{\frac{d_{ji}}{s^{\frac{1}{4}}} \arctan \frac{\sqrt{2}x^{\frac{1}{4}}}{\frac{d_{ji}}{s^{\frac{1}{4}}}} + 1}{L\rho_0^{\frac{1}{4}}} + \frac{\sqrt{2}}{2} \frac{\frac{d_{ji}}{s^{\frac{1}{4}}} \arctan \frac{\sqrt{2}x^{\frac{1}{4}}}{\frac{d_{ji}}{s^{\frac{1}{4}}}} - 1}{L\rho_0^{\frac{1}{4}}} + 1 - p_{D,j}p_{T,j} \quad (5.13)$$

5.6.2 Lemma 1

Given D2D mode is selected, the D2D transmit power $Z_{D,i}$ is $Z_{D,i} = \{P_{D,i} : \varphi d_{D,i}^{-\gamma_D} \geq d_{C,i}^{-\gamma_C}\} = \{P_{D,i} : \rho_0 d_{D,i}^{\gamma_D} \leq \varphi\rho_0 d_{C,i}^{\gamma_C}\} = \{P_{D,i} : P_{D,i} \leq \varphi P_{C,i}\}$. Therefore, the PDF of $Z_{D,i}$ can be obtained by

$$\begin{aligned} f_{Z_{D,i}}(x) &= f_{P_{D,i}|P_{D,i}\leq\varphi P_{C,i}}(x) \\ &= \frac{f_{P_{D,i}}(x)}{\mathbb{P}(P_{D,i} \leq \varphi P_{C,i})} \\ &= \frac{1}{p_{D,i}}\Big(\frac{2x^{\frac{1}{\gamma_D}-1}}{\gamma_D L \rho_0^{\frac{1}{\gamma_D}}} - \frac{2x^{\frac{2}{\gamma_D}-1}}{\gamma_D L^2 \rho_0^{\frac{2}{\gamma_D}}}\Big), \end{aligned} \quad (5.15)$$

where $P_{D,i}$ is obtained in (5.4), and $f_{P_{D,i}}(x)$ can be derived from the PDF of D2D distance d_D in (5.1) and the fact that $P_{D,i} = \rho_0 d_{D,i}^{\gamma_D}$.

5.6.3 Laplace transforms of $\mathcal{I}_{\mathcal{C}}$ and $\mathcal{I}_{\mathcal{D}}$

First we consider the interference from all V-D2D transmissions to a V-D2D transmission in road segment r_i, denoted by $\mathcal{I}_{\mathcal{DD},i}$. The Laplace transform of the PDF of $\mathcal{I}_{\mathcal{DD},i}$, denoted

by $\mathcal{L}_{\mathcal{I}_{\mathcal{DD},i}}(s)$ can be calculated by

$$\begin{aligned}
&\mathcal{L}_{\mathcal{I}_{\mathcal{DD},i}}(s)\\
&= \mathbb{E}[e^{-s\sum_{r_j\in\mathcal{M}_{\mathcal{I}}\setminus r_i}\mathbb{1}_{D,j}Z_{D,j}hd_{ji}^{-\gamma_D}}]\\
&= \mathbb{E}[\prod_{r_j\in\mathcal{M}_{\mathcal{I}}\setminus r_i} e^{-s\mathbb{1}_{D,j}Z_{D,j}hd_{ji}^{-\gamma_D}}]\\
&= \prod_{r_j\in\mathcal{M}_{\mathcal{I}}\setminus r_i} \mathbb{E}[e^{-s\mathbb{1}_{D,j}Z_{D,j}hd_{ji}^{-\gamma_D}}]\\
&= \prod_{r_j\in\mathcal{M}_{\mathcal{I}}\setminus r_i} p_{D,j}p_{T,j}\mathbb{E}[e^{-sZ_{D,j}hd_{ji}^{-\gamma_D}}] + 1 - p_{D,j}p_{T,j}\\
&= \prod_{r_j\in\mathcal{M}_{\mathcal{I}}\setminus r_i} \frac{2p_{T,j}P_{D_{m,j}}^{\frac{1}{\gamma_D}}\mathcal{H}([1,\frac{1}{\gamma_D}],[1+\frac{1}{\gamma_D}],\beta)}{L\rho_0^{\frac{1}{\gamma_D}}}\\
&- \frac{p_{T,j}P_{D_{m,j}}^{\frac{2}{\gamma_D}}\mathcal{H}([1,\frac{2}{\gamma_D}],[1+\frac{2}{\gamma_D}],\beta)}{L^2\rho_0^{\frac{2}{\gamma_D}}} + 1 - p_{D,j}p_{T,j}
\end{aligned} \tag{5.16}$$

where $\mathcal{H}([\cdot],[\cdot],v)$ is hypergeometric function, and $\beta = -sd_{ji}^{-\gamma_D}\mathbb{P}_{D_{m,j}}$. Note that for integer values of γ_C and γ_D, (5.16) has closed-form expression. For example, when $\gamma_C = \gamma_D = 4$, $\mathcal{L}_{\mathcal{I}_{\mathcal{DD},i}}(s)$ is shown in (5.13), where $x = \mathbb{P}_{D_{m,j}}$.

The interference from all cellular uplink transmissions in Ω_I to a V-D2D transmission in road segment r_i is denoted by $\mathcal{I}_{\mathcal{CD},i}$. Similarly, the Laplace transform of the PDF of $\mathcal{I}_{\mathcal{CD},i}$, denoted by $\mathcal{L}_{\mathcal{I}_{\mathcal{CD},i}}(s)$ can be calculated by

$$\begin{aligned}
&\mathcal{L}_{\mathcal{I}_{\mathcal{CD},i}}(s)\\
&= \mathbb{E}[e^{-s\sum_{r_j\in\mathcal{M}_{\mathcal{I}}\setminus r_i}\mathbb{1}_{C,j}Z_{C,j}hd_{ji}^{-\gamma_C}}]\\
&= \mathbb{E}[\prod_{r_j\in\mathcal{M}_{\mathcal{I}}\setminus r_i} e^{-s\mathbb{1}_{C,j}Z_{C,j}hd_{ji}^{-\gamma_C}}]\\
&= \sum_{r_j\in\mathcal{M}_{\mathcal{I}}} \mathbb{P}(\mathbb{1}_{C,j}=1)\mathbb{E}[e^{-sZ_{C,j}hd_{ji}^{-\gamma_C}}]\\
&= \frac{1}{\sum_{r_i\in\mathcal{M}_{\mathcal{C}}} p_{T,i}(1-p_{D,i})} \sum_{r_j\in\mathcal{M}_{\mathcal{I}}\setminus r_i} \frac{p_{T,j}(1-p_{D,j})}{(1+sZ_{C,j}d_{ji}^{-\gamma_C})}.
\end{aligned} \tag{5.17}$$

When considering the interference to a cellular uplink transmission in road segment r_i, the calculation of $\mathcal{I}_{\mathcal{DC},i}$ and $\mathcal{I}_{\mathcal{CC},i}$ is similar to (5.16) and (5.17), by replacing d_{ji} with the distances from the road segments in $\mathcal{M}_{\mathcal{I}}$ to the BS of Ω_C.

Chapter 6

Conclusions and Future Work

In this chapter, we summarize the main concepts and results presented in this thesis and highlight future research directions.

6.1 Conclusions

In this thesis, we have investigated different methods to efficiently exploit opportunistic spectrum bands for vehicular communications. Based on the analysis and discussion provided, we present the following remarks.

- Utilizing opportunistic spectrum bands for VANETs can be an efficient and cost-effective solution to the problem of spectrum scarcity in VANETs. Through techniques such as cognitive radio, WiFi, and D2D communication, the opportunities in both licensed and unlicensed spectrum bands can be explored to support the mobile data services of vehicular users. However, different from other networks, the unique features of VANETs, such as the high vehicle mobility, impose many challenges in analyzing the spectrum opportunity and efficiently exploiting it. On the other hand, these features can even improve the spectrum utilization if proper schemes are designed.
- We studied three main techniques to explore and exploit opportunistic spectrum bands, i.e., CR, WiFi, and D2D communication, respectively. In CR-VANETs, licensed spectrum bands, such as TV white spaces, are theoretically analyzed in terms of channel availability for vehicular users. Following the channel availability, an

efficient and fair spectrum access scheme is proposed based on game theory. In vehicular WiFi offloading, intermittent WiFi access opportunities on unlicensed bands are utilized for providing Internet data services to moving vehicles. In V-D2D communications, we have shown that the total spectrum efficiency and throughput of the cellular network can be greatly boosted by the underlaid proximate V-D2D communications. The opportunistic spectrum bands under investigation are basically a small portion of the whole wireless spectrum. With the soaring number of connected vehicles and exponentially increasing demands of mobile data services, we believe that opportunistic spectrum will play an increasingly important role in offering cost-effective data pips for VANETs.

- The study in this thesis plays an vital role in understanding the performance of VANETs when applying opportunistic spectrum bands for V2V and V2I communication. This understanding can in turn provide important insights and guidance for spectrum access and network design and deployment. Specifically, for vehicular users, using the results of the study, combined with their own knowledge such as speed and scheduling moving route, the critical information about different spectrum bands, such as availability, supporting QoS, even costs, can be obtained, which could be essential criterions for selecting the best spectrum to access. For content providers (as an example, car manufacturers), knowing the performance and cost of different data pipes for content dissemination can reduce the cost while preserving QoS. For network operators, the knowledge of the network performance and the impact of the design parameters can assist the network deployment and optimization, without the need for time-consuming large-scale simulations.

6.2 Future Research Directions

In this thesis, we focus on performance study and protocol design of VANETs utilizing opportunistic spectrum bands, through CR, WiFi, and D2D communications, respectively. Our future work includes designing more efficient spectrum utilization schemes, extending spectrum bands to exploit, investigate integrated opportunistic communication framework, extensive simulation validations through real-world maps and trace, and further exploring the implication on network design and operations. Despite existing studies on opportunistic spectrum utilization of VANETs, many issues remain unclear. For example, when considering a more complex mobility pattern of vehicles, and more general PU activity models, the channel availability in CR-VANETs could be more difficult to study. Moreover, exploiting opportunistic spectrum bands often involves economic concerns, such as

the pricing strategies of CRNs and D2D underlaid network, and the cost/QoS tradeoff issues. Currently, there are little works investigating these topics for VANETs. We conclude the thesis by providing several thoughts of our future research directions.

- Analysis of the opportunistic spectrum utilization in a more general network environment. The spectrum availability depends on the movement of vehicles. In this thesis we employed the grid-like street patterns, and modeled the vehicle mobility in a simplified form where the vehicle mobility can be represented by maximum/minimum speed, and turning probabilities at intersections. In addition, in CR-VANETs, we consider the PU activity model by an ON-OFF model. Straightforwardly, when a more general network environment is under consideration, such as more complex street patterns and inhomogeneous vehicle densities, the analysis should be more difficult. Moreover, we also plan to design spectrum access schemes considering the generalized network conditions, and the QoS requirements of varied data services/applications.

- Extend spectrum bands to exploit, in order to further relieve the spectrum scarcity. TVWS have been proposed for unlicensed access due to the current underutilization and good propagation properties. The availability of local TVWS channels change over time and location. Therefore, to enable effective vehicular access, a first challenge is efficiently plan the TVWS networks, e.g., deploying the TVWS access points. Providing a TVWS network, another challenge to deliver vehicular data services is to design efficient vehicular access scheme considering the vehicle mobility and the different QoS requirements of applications. We plan to solve these challenges in the future work.

- Investigate on integrated opportunistic communication framework for VANETs. An integrated framework that can effectively incorporate all kinds of available opportunistic spectrum is required for VANETs, so that VUs can adaptively access different spectrums. First, due to the movement of vehicles, the availability of the opportunistic transmission spectrums is changing spatially and temporally, which may lead to different availability of different spectrum. Thus, better knowledge of the spectrum availability will lead to better utilization of the opportunistic spectrums. Second, the targets and requirements of accessing different spectrums are varying. For licensed spectrum, the target is to use the vacant bands to improve the communication performance as well as to offload the cellular network, while avoiding or minimizing the interference to primary transmissions. For WiFi access, the spectrum bands are free to use, and the target is to maximize the utility considering cost and user satisfac-

tion (e.g., delay), and to improve the offloading performance given the deployed WiFi network.

References

[1] D. Hadaller, S. Keshav, T. Brecht, and S. Agarwal, "Vehicular opportunistic communication under the microscope," in *Proc. of ACM MobiSys*, Puerto Rico, 2007.

[2] "Spectrum management." [Online]. Available: https://en.wikipedia.org/wiki/Spectrum_management

[3] "Tiger/line shapefiles." [Online]. Available: http://www.census.gov/geo/maps-data/data/tiger-data.html

[4] G. Karagiannis, O. Altintas, E. Ekici, G. Heijenk, B. Jarupan, K. Lin, and T. Weil, "Vehicular networking: A survey and tutorial on requirements, architectures, challenges, standards and solutions," *IEEE Communications Surveys & Tutorials*, no. 99, pp. 1–33, 2011.

[5] H. Omar, W. Zhuang, and L. Li, "VeMAC: A tdma-based mac protocol for reliable broadcast in VANETs," *IEEE Trans. on Mobile Computing*, vol. 12, no. 9, pp. 1724–1736, 2013.

[6] T. Luan, L. Cai, J. Chen, X. Shen, and F. Bai, "Engineering a distributed infrastructure for large-scale cost-effective content dissemination over urban vehicular networks," *IEEE Trans. on Vehicular Technology*, vol. 63, no. 3, pp. 1419–1435, 2014.

[7] O. Trullols-Cruces, M. Fiore, and J. Barcelo-Ordinas, "Cooperative download in vehicular environments," *IEEE Trans. on Mobile Computing*, vol. 11, no. 4, pp. 663–678, 2012.

[8] J. Kenney, "Dedicated short-range communications (dsrc) standards in the united states," *Proceedings of the IEEE*, vol. 99, no. 7, pp. 1162–1182, 2011.

[9] H. Moustafa and Y. Zhang, *Vehicular networks: techniques, standards, and applications*. Auerbach publications, 2009.

[10] F. Bai and B. Krishnamachari, "Exploiting the wisdom of the crowd: localized, distributed information-centric VANETs," *IEEE Communications Magazine*, vol. 48, no. 5, pp. 138–146, 2010.

[11] R. Lu, X. Lin, T. Luan, X. Liang, and X. Shen, "Pseudonym changing at social spots: An effective strategy for location privacy in VANETs," *IEEE Trans. on Vehicular Technology*, vol. 61, no. 1, pp. 86–96, 2012.

[12] "KPMG's global automotive executive survey." [Online]. Available: http://www.kpmg.com/GE/en/IssuesAndInsights/ArticlesPublications/Documents/Global-automotive-executive-survey-2012.pdf

[13] M. Ramadan, M. Al-Khedher, and S. Al-Kheder, "Intelligent anti-theft and tracking system for automobiles," *International Journal of Machine Learning and Computing*, vol. 2, no. 1, 2012.

[14] J. Lin, S. Chen, Y. Shih, and S. Chen, "A study on remote on-line diagnostic system for vehicles by integrating the technology of OBD, GPS, and 3G," *World Academy of Science, Engineering and Technology*, vol. 56, p. 56, 2009.

[15] H. Hartenstein and K. Laberteaux, "A tutorial survey on vehicular ad hoc networks," *IEEE Communications Magazine*, vol. 46, no. 6, pp. 164–171, 2008.

[16] L. Cheng, B. E. Henty, D. D. Stancil, F. Bai, and P. Mudalige, "Mobile vehicle-to-vehicle narrow-band channel measurement and characterization of the 5.9 ghz dedicated short range communication (dsrc) frequency band," *IEEE J. Selected Area in Communications*, vol. 25, no. 8, pp. 1501–1516, 2007.

[17] W. Viriyasitavat., F. Bai., and O. K. Tonguz, "Dynamics of network connectivity in urban vehicular networks," *IEEE J. Selected Areas in Communications*, vol. 29, pp. 515–533, 2011.

[18] K. Liu, M. Li, Y. Liu, X.-Y. Li, M. Li, and H. Ma, "Exploring the hidden connectivity in urban vehicular networks," in *Proc. IEEE ICNP*, Japan, 2010, pp. 243–252.

[19] S. Yousefi, E. Altman, R. El-Azouzi, and M. Fathy, "Analytical model for connectivity in vehicular ad hoc networks," *IEEE Trans. on Vehicular Technology*, vol. 57, no. 6, pp. 3341–3356, 2008.

[20] G. H. Mohimani, F. Ashtiani, A. Javanmard, and M. Hamdi, "Mobility modeling, spatial traffic distribution, and probability of connectivity for sparse and dense vehicular ad hoc networks," *IEEE Trans. on Vehicular Technology*, vol. 58, no. 4, pp. 1998–2007, 2009.

[21] M. Wada, T. Yendo, T. Fujii, and M. Tanimoto, "Road-to-vehicle communication using led traffic light," in *Proc. IEEE Intelligent Vehicles Symposium*, USA, 2005, pp. 601–606.

[22] S. Iwasaki, C. Premachandra, T. Endo, T. Fujii, M. Tanimoto, and Y. Kimura, "Visible light road-to-vehicle communication using high-speed camera," in *Proc. IEEE Intelligent Vehicles Symposium*, Netherlands, 2008, pp. 13–18.

[23] C. B. Liu, B. Sadeghi, and E. W. Knightly, "Enabling vehicular visible light communication (v2lc) networks," in *Proc. ACM VANET*, USA, 2011, pp. 41–50.

[24] "Car Connectivity Consortium, MirrorLink." [Online]. Available: http://www.mirrorlink.com/

[25] *BMW ConnectedDrive*. [Online]. Available: http://www.bmw.com/com/en/insights/technology/connecteddrive/2013/index.html

[26] "GM OnStar." [Online]. Available: https://www.onstar.com/us/en/home.html

[27] V. Bychkovsky, B. Hull, A. Miu, H. Balakrishnan, and S. Madden, "A measurement study of vehicular Internet access using in situ Wi-Fi networks," in *Proc. of ACM MobiCom*, USA, 2006.

[28] A. E2213-03, *Standard specification for telecommunications and information exchange between roadside and vehicle systems5 GHz band dedicated short range communications (DSRC) medium access control (MAC) and physical layer (PHY) specifications*, Std., 2003.

[29] J. Yin, T. ElBatt, G. Yeung, B. Ryu, S. Habermas, H. Krishnan, and T. Talty, "Performance evaluation of safety applications over dsrc vehicular ad hoc networks," in *Proc. ACM VANET*, USA, 2004.

[30] D. Jiang and L. Delgrossi, "Ieee 802.11 p: Towards an international standard for wireless access in vehicular environments," in *Proc. IEEE VTC*, Singapore, 2008, pp. 2036–2040.

[31] V. Taliwal, D. Jiang, H. Mangold, C. Chen, and R. Sengupta, "Empirical determination of channel characteristics for dsrc vehicle-to-vehicle communication," in *Proc. ACM VANET*, USA, 2004, pp. 88–88.

[32] F. Yu and S. Biswas, "Self-configuring tdma protocols for enhancing vehicle safety with dsrc based vehicle-to-vehicle communications," *IEEE J. Selected Areas in Communications*, vol. 25, no. 8, pp. 1526–1537, 2007.

[33] S. Zeadally, R. Hunt, Y.-S. Chen, A. Irwin, and A. Hassan, "Vehicular ad hoc networks (vanets): status, results, and challenges," *Springer Telecommunication Systems*, vol. 50, no. 4, pp. 217–241, 2012.

[34] B. Chen and M. Chan, "Mobtorrent: A framework for mobile internet access from vehicles," in *Proc. of IEEE INFOCOM*, Brazil, 2009.

[35] A. J. Ghandour, K. Fawaz, and H. Artail, "Data delivery guarantees in congested vehicular ad hoc networks using cognitive networks," in *Proc. of IEEE IWCMC*, Turkey, 2011.

[36] N. Lu, T. Luan, M. Wang, X. Shen, and F. Bai, "Capacity and delay analysis for social-proximity urban vehicular networks," in *Proc. of IEEE INFOCOM*, USA, 2012.

[37] "The 1000x mobile data challenge." [Online]. Available: http://www.qualcomm.com/media/documents/files/web_1000x-mobile-data-challenge.pdf

[38] "Connected Car Industry Report 2014." [Online]. Available: http://blog.digital.telefonica.com/connected-car-report-2014/

[39] A. Asadi, Q. Wang, and V. Mancuso, "A survey on device-to-device communication in cellular networks," *IEEE Communications Surveys & Tutorials*, vol. 16, no. 4, pp. 1801–1819, 2014.

[40] A. B. Flores, R. E. Guerra, E. W. Knightly, P. Ecclesine, and S. Pandey, "IEEE 802.11 af: a standard for TV white space spectrum sharing," *IEEE Communications Magazine*, vol. 51, no. 10, pp. 92–100, 2013.

[41] C. R. Stevenson, G. Chouinard, Z. Lei, W. Hu, S. J. Shellhammer, and W. Caldwell, "IEEE 802.22: the first cognitive radio wireless regional area network standard," *IEEE Communications Magazine*, vol. 47, no. 1, pp. 130–138, 2009.

[42] I. Akyildiz, W. Lee, M. Vuran, and S. Mohanty, "Next generation/dynamic spectrum access/cognitive radio wireless networks: a survey," *Computer Networks*, vol. 50, no. 13, pp. 2127–2159, 2006.

[43] S. Huang, X. Liu, and Z. Ding, "Opportunistic spectrum access in cognitive radio networks," in *Proc. of IEEE INFOCOM*, USA, 2008.

[44] N. Zhang, N. Lu, N. Cheng, J. W. Mark, and X. S. Shen, "Cooperative spectrum access towards secure information transfer for CRNs," *IEEE J. Selected Areas in Communications*, vol. 31, no. 11, pp. 2453–2464, 2013.

[45] N. Zhang, H. Zhou, K. Zheng, N. Cheng, J. W. Mark, and X. Shen, "Cooperative heterogeneous framework for spectrum harvesting in cognitive cellular network," *IEEE Communications Magazine*, vol. 53, no. 5, pp. 60–67, 2015.

[46] R. Urgaonkar and M. Neely, "Opportunistic scheduling with reliability guarantees in cognitive radio networks," in *Proc. of IEEE INFOCOM*, USA, 2008.

[47] D. Niyato, E. Hossain, and P. Wang, "Optimal channel access management with QoS support for cognitive vehicular networks," *IEEE Trans. on Mobile Computing*, vol. 10, no. 5, pp. 573–591, 2011.

[48] N. Cheng, N. Zhang, N. Lu, X. Shen, J. Mark, and F. Liu, "Opportunistic Spectrum Access for CR-VANETs: A Game-Theoretic Approach," *IEEE Trans. on Vehicular Technology*, vol. 63, no. 1, pp. 237–251, 2014.

[49] R. Gass, J. Scott, and C. Diot, "Measurements of in-motion 802.11 networking," in *Proc. of IEEE WMCSA*, USA, 2006.

[50] J. Eriksson, H. Balakrishnan, and S. Madden, "Cabernet: vehicular content delivery using WiFi," in *Proc. of ACM MobiCom*, USA, 2008.

[51] T. H. Luan, X. Ling, and X. Shen, "MAC in motion: impact of mobility on the MAC of drive-thru Internet," *IEEE Trans. on Mobile Computing*, vol. 11, no. 2, pp. 305–319, 2012.

[52] N. Cheng, N. Lu, N. Zhang, X. Shen, and J. W. Mark, "Opportunistic WiFi offloading in vehicular environment: a queueing analysis," in *Proc. of IEEE GLOBECOM*, USA, 2014.

[53] K. Doppler, M. Rinne, C. Wijting, C. Ribeiro, and K. Hugl, "Device-to-device communication as an underlay to lte-advanced networks," *IEEE Communications Magazine*, vol. 47, no. 12, pp. 42–49, 2009.

[54] N. Golrezaei, A. F. Molisch, and A. G. Dimakis, "Base-station assisted Device-to-Device communications for high-throughput wireless video networks," in *Proc. of IEEE ICC*, Canada, 2012.

[55] L. Lei, Z. Zhong, C. Lin, and X. Shen, "Operator controlled device-to-device communications in LTE-advanced networks," *IEEE Wireless Communications*, vol. 19, no. 3, pp. 96–104, 2012.

[56] B. Kaufman and B. Aazhang, "Cellular networks with an overlaid device to device network," in *Proc. of Asilomar Conference on Signals, Systems and Computers*, USA, 2008.

[57] N. Cheng, H. Zhou, L. Lei, N. Zhang, Y. Zhou, X. Shen, and F. Bai, "Performance analysis of vehicular device-to-device underlay communication," *IEEE Trans. on Vehicular Technology*, submitted.

[58] N. Zhang, N. Cheng, A. T. Gamage, K. Zhang, J. W. Mark, and X. Shen, "Cloud assisted hetnets toward 5g wireless networks," *IEEE Communications Magazine*, vol. 53, no. 6, pp. 59–65, 2015.

[59] N. Zhang, N. Lu, R. Lu, J. Mark, and X. Shen, "Energy-efficient and trust-aware cooperation in cognitive radio networks," in *Proc. of IEEE ICC*, Canada, 2012.

[60] S. Haykin, "Cognitive radio: brain-empowered wireless communications," *IEEE J. Sel. Areas Commun.*, vol. 23, no. 2, pp. 201–220, 2005.

[61] F. Berggren, O. Queseth, J. Zander, B. Asp, C. Jönsson, P. Stenumgaard, N. Kviselius, B. Thorngren, U. Landmark, and J. Wessel, "Dynamic spectrum access," *Tech. Rep, Royal Institute of Technology Communication and System Department*, 2004.

[62] F. C. C. (FCC), "Notice of proposed rule making and order," Tech. Rep., 2003.

[63] F. Ian, Y. Won, and R. Kaushik, "CRAHNs: cognitive radio ad hoc networks," *ACM Ad Hoc Networks*, vol. 7, no. 3, pp. 810–836, 2009.

[64] T. Yucek and H. Arslan, "A survey of spectrum sensing algorithms for cognitive radio applications," *IEEE Communications Surveys & Tutorials*, vol. 11, no. 1, pp. 116–130, 2009.

[65] A. De Domenico, E. C. Strinati, and M. Di Benedetto, "A survey on MAC strategies for cognitive radio networks," *IEEE Communications Surveys & Tutorials*, vol. 14, no. 1, pp. 21–44, 2012.

[66] D. Cabric, S. M. Mishra, and R. W. Brodersen, "Implementation issues in spectrum sensing for cognitive radios," in *Proc. Asilomar conference on Signals, systems and computers*, 2004.

[67] C. hun Ting, S. Sai, K. Hyoil, and G. Kang, "What and how much to gain by spectrum agility?" *IEEE J. Selected Areas in Communications*, vol. 25, no. 3, pp. 576–588, 2007.

[68] Z. Qing, T. Lang, S. Ananthram, and C. Yunxia, "Decentralized cognitive MAC for opportunistic spectrum access in ad hoc networks: a POMDP framework," *IEEE J. Selected Area in Communications*, vol. 25, no. 3, pp. 589–600, 2007.

[69] H. Kim and K. G. Shin, "Efficient discovery of spectrum opportunities with mac-layer sensing in cognitive radio networks," *IEEE Trans. on Mobile Computing*, vol. 7, no. 5, pp. 533–545, 2008.

[70] Z. Ji and K. Liu, "Cognitive radios for dynamic spectrum access-dynamic spectrum sharing: A game theoretical overview," *IEEE Communications Magazine*, vol. 45, no. 5, pp. 88–94, 2007.

[71] L. Cao and H. Zheng, "Distributed spectrum allocation via local bargaining." in *Proc. IEEE SECON*, 2005, pp. 475–486.

[72] J. Huang, R. A. Berry, and M. L. Honig, "Auction-based spectrum sharing," *Mobile Networks and Applications*, vol. 11, no. 3, pp. 405–418, 2006.

[73] C. Cordeiro, K. Challapali, D. Birru, and N. Sai Shankar, "Ieee 802.22: the first worldwide wireless standard based on cognitive radios," in *New Frontiers in Dynamic Spectrum Access Networks, 2005. DySPAN 2005. 2005 First IEEE International Symposium on*, 2005, pp. 328–337.

[74] P. Bahl, R. Chandra, T. Moscibroda, R. Murty, and M. Welsh, "White space networking with wi-fi like connectivity," *ACM SIGCOMM Computer Communication Review*, vol. 39, no. 4, pp. 27–38, 2009.

[75] S. Deb, V. Srinivasan, and R. Maheshwari, "Dynamic spectrum access in dtv whitespaces: design rules, architecture and algorithms," in *Proceedings of the 15th annual international conference on Mobile computing and networking*, 2009, pp. 1–12.

[76] L. Yu, C. Liu, W. Zhu, S. Hua, and W. Wang, "Bandwidth efficient and rate-adaptive video delivery in tv white space," *EEE Trans. Circuits and Systems for Video Technology*, vol. 24, no. 9, pp. 1605–1619, 2014.

[77] W. Kim, M. Gerla, S. Oh, K. Lee, and A. Kassler, "CoRoute: a new cognitive anypath vehicular routing protocol," *Wiley Journal on Wireless Communications and Mobile Computing*, vol. 11, no. 12, pp. 1588–1602, 2011.

[78] M. Di Felice, R. Doost-Mohammady, K. Chowdhury, and L. Bononi, "Smart radios for smart vehicles: cognitive vehicular networks," *IEEE Vehicular Technology Magazine*, vol. 7, no. 2, pp. 26–33, 2012.

[79] M. Pan, P. Li, and Y. Fang, "Cooperative communication aware link scheduling for cognitive vehicular networks," *IEEE J. Sel. Areas Commun.*, vol. 30, no. 4, pp. 760–768, 2012.

[80] A. Al-Ali, Y. Sun, M. DiFelice, J. Paavola, and K. Chowdhury, "Accessing spectrum databases using interference alignment in vehicular cognitive radio networks," *IEEE Trans. on Vehicular Technology*, vol. 64, no. 1, pp. 263–272, 2015.

[81] X. Wang and P. Ho, "A novel sensing coordination framework for cr-vanets," *IEEE Trans. on Vehicular Technology*, vol. 59, no. 4, pp. 1936–1948, 2010.

[82] H. Li and D. K. Irick, "Collaborative spectrum sensing in cognitive radio vehicular ad hoc networks: Belief propagation on highway," in *Proc. of IEEE VTC-Spring*, China, 2010.

[83] D. Marco, R. Kaushik, and B. Luciano, "Analyzing the potential of cooperative cognitive radio technology on inter-vehicle communication," in *Proc. of the IEEE Wireless Day*, Italy, 2010.

[84] "Tv fool coverage maps." [Online]. Available: http://www.tvfool.com/

[85] R. Doost-Mohammady and K. R. Chowdhury, "Design of spectrum database assisted cognitive radio vehicular networks," in *Proc. of IEEE CROWNCOM*, Sweden, 2012, pp. 1–5.

[86] S. Pagadarai, A. M. Wyglinski, and R. Vuyyuru, "Characterization of vacant UHF TV channels for vehicular dynamic spectrum access," in *Proc. of IEEE VNC*, Japan, 2009.

[87] S. Chen, R. Vuyyuru, O. Altintas, and A. M. Wyglinski, "On optimizing vehicular dynamic spectrum access networks: Automation and learning in mobile wireless environments." in *Proc. of IEEE VNC*, 2011.

[88] K. Tsukamoto, Y. Omori, O. Altintas, M. Tsuru, and Y. Oie, "On spatially-aware channel selection in dynamic spectrum access multi-hop inter-vehicle communications," in *Proc. of IEEE VTC-Fall*, USA, 2009.

[89] C. Yang, Y. Fu, Y. Zhang, S. Xie, and R. Yu, "Energy-efficient hybrid spectrum access scheme in cognitive vehicular ad hoc networks," *IEEE Communications Letters*, vol. 17, no. 2, pp. 329–332, 2013.

[90] A. Aijaz, H. Aghvami, and M. Amani, "A survey on mobile data offloading: technical and business perspectives," *IEEE Wireless Communications*, vol. 20, no. 2, pp. 104–112, 2013.

[91] K. Lee, J. Lee, Y. Yi, I. Rhee, and S. Chong, "Mobile data offloading: how much can WiFi deliver?" *IEEE/ACM Trans. on Networking*, vol. 21, no. 2, pp. 536–550, 2013.

[92] S. Singh, H. Dhillon, and J. Andrews, "Offloading in heterogeneous networks: modeling, analysis, and design insights," *IEEE Trans. on Wireless Communications*, vol. 12, no. 5, pp. 2484–2497, 2012.

[93] S. Dimatteo, P. Hui, B. Han, and V. O. Li, "Cellular traffic offloading through WiFi networks," in *Proc. of IEEE MASS*, Spain, 2011.

[94] J. Ott and D. Kutscher, "Drive-thru Internet: IEEE 802.11b for automobile," in *Proc. of IEEE INFOCOM*, China, 2004.

[95] N. Lu, N. Zhang, N. Cheng, X. Shen, J. W. Mark, and F. Bai, "Vehicles Meet Infrastructure: Towards Capacity-Cost Tradeoffs for Vehicular Access Networks," *IEEE Trans. on Intelligent Transportation Systems*, vol. 14, no. 3, pp. 1266–1277, 2013.

[96] Y. Go, Y. Moon, G. Nam, and K. Park, "A disruption-tolerant transmission protocol for practical mobile data offloading," in *Proc. of ACM MobiOpp*, Switzerland, 2012.

[97] Y. Choi, H. W. Ji, J.-y. Park, H.-c. Kim, and J. A. Silvester, "A 3W network strategy for mobile data traffic offloading," *IEEE Communications Magazine*, vol. 49, no. 10, pp. 118–123, 2011.

[98] "List of US cities and counties with large scale WiFi networks." [Online]. Available: http://www.scribd.com/doc/32622309/7-June-2010-List-of-Muni-Wifi-Cities

[99] J. Ott and D. Kutscher, "The "drive-thru" architecture: WLAN-based Intenet access on the road," in *Proc. of IEEE VTC*, Italy, 2004.

[100] P. Deshpande, X. Hou, and S. R. Das, "Performance comparison of 3G and metro-scale WiFi for vehicular network access," in *Proc. of ACM SIGCOMM Internet Measurement Conference*, Australia, 2010.

[101] "Multiband Atheros driver for WiFi." [Online]. Available: http://www.madwifi.org/

[102] A. Balasubramanian, R. Mahajan, and A. Venkataramani, "Augmenting mobile 3G using WiFi," in *Proc. of ACM MobiSys*, USA, 2010.

[103] P. Deshpande, A. Kashyap, C. Sung, and S. R. Das, "Predictive methods for improved vehicular WiFi access," in *Proc. of ACM MobiSys*, Poland, 2009.

[104] X. Hou, P. Deshpande, and S. R. Das, "Moving bits from 3G to metro-scale WiFi for vehicular network access: An integrated transport layer solution," in *Proc. of IEEE ICNP*, Canada, 2011.

[105] Z. Zheng, P. Sinha, and S. Kumar, "Sparse WiFi deployment for vehicular internet access with bounded interconnection gap," *IEEE/ACM Trans. on Networking*, vol. 20, no. 3, pp. 956–969, 2012.

[106] Y.-D. Lin and Y.-C. Hsu, "Multihop cellular: A new architecture for wireless communications," in *Proc. of IEEE INFOCOM*, Israel, 2000, pp. 1273–1282.

[107] T. Peng, Q. Lu, H. Wang, S. Xu, and W. Wang, "Interference avoidance mechanisms in the hybrid cellular and device-to-device systems," in *Proc. of IEEE PIMRC*, Japan, 2009.

[108] Y. Pei and Y.-C. Liang, "Resource allocation for device-to-device communications overlaying two-way cellular networks," *IEEE Trans. on Wireless Communications*, vol. 12, no. 7, pp. 3611–3621, 2013.

[109] A. Asadi and V. Mancuso, "On the compound impact of opportunistic scheduling and D2D communications in cellular networks," in *Proc. of ACM MSWiM*, Spain, 2013, pp. 279–288.

[110] R. Zhang, X. Cheng, L. Yang, and B. Jiao, "Interference-aware graph based resource sharing for device-to-device communications underlaying cellular networks," in *Proc. of IEEE WCNC*, China, 2013.

[111] A.-H. Tsai, L.-C. Wang, J.-H. Huang, and T.-M. Lin, "Intelligent resource management for Device-to-Device (D2D) communications in heterogeneous networks," in *Proc. of IEEE WPMC*, China, 2012.

[112] S. Xu, H. Wang, T. Chen, Q. Huang, and T. Peng, "Effective interference cancellation scheme for Device-to-Device communication underlaying cellular networks," in *Proc. of IEEE VTC*, Canada, 2010.

[113] X. Xiao, X. Tao, and J. Lu, "A QoS-aware power optimization scheme in OFDMA systems with integrated device-to-device (D2D) communications," in *Proc. of IEEE VTC-fall*, USA, 2011.

[114] M. Jung, K. Hwang, and S. Choi, "Joint mode selection and power allocation scheme for power-efficient device-to-device (D2D) communication," in *Proc. of IEEE VTC-Spring*, Japan, 2012.

[115] M. Belleschi, G. Fodor, and A. Abrardo, "Performance analysis of a distributed resource allocation scheme for D2D communications," in *Proc. of IEEE GLOBECOM*, USA, 2011, pp. 358–362.

[116] T. H. Luan, X. Shen, F. Bai, and L. Sun, "Feel bored? join verse! engineering vehicular proximity social networks," *IEEE Trans. on Vehicular Technology*, vol. 64, no. 3, pp. 1120–1131, 2015.

[117] X. Cheng, L. Yang, and X. Shen, "D2D for intelligent transportation systems: A feasibility study," *IEEE Trans. on Intelligent Transportation Systems*, vol. 16, no. 4, pp. 1784–1793, 2015.

[118] W. Sun, E. G. Strom, F. Brannstrom, Y. Sui, and K. C. Sou, "D2d-based v2v communications with latency and reliability constraints," in *Proc. of IEEE GLOBECOM*, USA, 2014.

[119] Y. Ren, F. Liu, Z. Liu, C. Wang, and Y. Ji, "Power control in d2d-based vehicular communication networks," *IEEE Trans. on Vehicular Technology*, vol. 64, no. 12, pp. 5547–5562, 2015.

[120] S. Kostof and R. Tobias, *The city shaped*. Thames and Hudson London, 1991.

[121] A. Siksna, "The effects of block size and form in north american and australian city centres," *Urban Morphology*, vol. 1, pp. 19–33, 1997.

[122] J. Lee, R. Mazumdar, and N. Shroff, "Joint resource allocation and base-station assignment for the downlink in CDMA networks," *IEEE/ACM Trans. on Networking*, vol. 14, no. 1, pp. 1–14, 2006.

[123] Y. Liu, L. Cai, and X. Shen, "Spectrum-aware opportunistic routing in multi-hop cognitive radio networks," *IEEE J. Sel. Areas Commun.*, vol. 30, no. 10, pp. 1958–1968, 2012.

[124] A. Min, K. Kim, J. Singh, and K. Shin, "Opportunistic spectrum access for mobile cognitive radios," in *Proc. of IEEE INFOCOM*, China, 2011.

[125] X. Zhang, H. Su, and H. Chen, "Cluster-based multi-channel communications protocols in vehicle ad hoc networks," *IEEE Wireless Communications*, vol. 13, no. 5, pp. 44–51, 2006.

[126] Z. Han, D. Niyato, W. Saad, T. Başar, and A. Hjørungnes, *Game theory in wireless and communication networks: theory, models, and applications*. Cambridge University Press, 2011.

[127] L. Blumrosen and S. Dobzinski, "Welfare maximization in congestion games," *IEEE J. Selected Area in Communications*, vol. 25, no. 6, pp. 1224–1236, 2007.

[128] L. M. Law, J. Huang, and M. Liu, "Price of anarchy for congestion games in cognitive radio networks," *IEEE Trans. on Wireless Communications*, vol. 11, no. 10, pp. 3778–3787, 2012.

[129] R. Jain, D. Chiu, and W. Hawe, "A quantitative measure of fairness and discrimination for resource allocation in shared computer systems," *DEC research report TR-301*, 1984.

[130] W. L. Tan, W. C. Lau, O. Yue, and T. H. Hui, "Analytical models and performance evaluation of drive-thru internet systems," *IEEE J. Selected Areas in Communications*, vol. 29, no. 1, pp. 207–222, 2011.

[131] D. Fiems, T. Maertens, and H. Bruneel, "Queueing systems with different types of server interruptions," *European Journal of Operational Research*, vol. 188, no. 3, pp. 838–845, 2008.

[132] J. Abate, G. L. Choudhury, and W. Whitt, "An introduction to numerical transform inversion and its application to probability models," pp. 257–323, 2000.

[133] S. K. Bose, *An introduction to queueing systems*. Springer, 2001.

[134] J. Härri, F. Filali, C. Bonnet, and M. Fiore, "VanetMobiSim: Generating Realistic Mobility Patterns for VANETs," in *Proc. of ACM VANET*, USA, 2006.

[135] H. ElSawy, E. Hossain, and M.-S. Alouini, "Analytical modeling of mode selection and power control for underlay d2d communication in cellular networks," *IEEE Trans. on Communications*, vol. 62, no. 11, pp. 4147–4161, 2014.

[136] N. Lu, T. Luan, M. Wang, X. Shen, and F. Bai, "Bounds of asymptotic performance limits of social-proximity vehicular networks," *IEEE/ACM Trans. on Networking*, vol. 22, no. 3, pp. 812–825, 2014.

[137] G. S. Thakur, P. Hui, and A. Helmy, "Modeling and characterization of vehicular density at scale," in *Proc. IEEE INFOCOM*, Italy, 2013.

[138] M. Botsov, M. Klugel, W. Kellerer, and P. Fertl, "Location dependent resource allocation for mobile device-to-device communications," in *Proc. IEEE WCNC*, Turkey, 2014.

[139] C. Xu, L. Song, Z. Han, Q. Zhao, X. Wang, X. Cheng, and B. Jiao, "Efficiency resource allocation for device-to-device underlay communication systems: a reverse iterative combinatorial auction based approach," *IEEE J. Selected Areas in Communications*, vol. 31, no. 9, pp. 348–358, 2013.

[140] H. ElSawy, E. Hossain, and M. Haenggi, "Stochastic geometry for modeling, analysis, and design of multi-tier and cognitive cellular wireless networks: A survey," *IEEE Communications Surveys & Tutorials*, vol. 15, no. 3, pp. 996–1019, 2013.

[141] C.-H. Yu, K. Doppler, C. B. Ribeiro, and O. Tirkkonen, "Resource sharing optimization for Device-to-Device communication underlaying cellular networks," *IEEE Trans. on Wireless Communications*, vol. 10, no. 8, pp. 2752–2763, 2011.

List of Publications

Book/Book Chapter

[B1]. **N. Cheng**, and X. Shen,"Opportunistic Spectra Utilization in Vehicular Communication Networks," Springer, 2015.

[B2]. N. Zhang, **N. Cheng**, N. Lu, H. Zhou, J.W. Mark, and X. Shen,"Opportunistic Spectrum Access in Multi-Channel Cognitive Radio Networks,"
Multimedia Over Cognitive Radio Networks: Algorithms, Protocols, and Experiments, CRC Press, 2014.

Journal Papers

[J1]. **N. Cheng**, H. Zhou, L. Lei, N. Zhang, Y. Zhou, X. Shen, and F. Bai, "Performance analysis of vehicular device-to-device underlay communication,"
IEEE Trans. on Vehicular Technology, submitted.

[J2]. **N. Cheng**, N. Lu, N. Zhang, T. Yang, X. Shen, and J.W. Mark, "Vehicle-Assisted Device-to-Device Data Delivery for Smart Grid,"
IEEE Transactions on Vehicular Technology, to appear.

[J3]. **N. Cheng**, N. Lu, N. Zhang, X. Zhang, X. Shen, and J.W. Mark, "Opportunistic WiFi Offloading in Vehicular Environment: A Game-Theory Approach,"
IEEE Transactions on Intelligent Transportation System, to appear.

[J4]. H. Omar, K. Abboud, **N. Cheng**, A. Gamage, W. Zhuang, 'A Survey on High Efficiency Wireless Local Area Networks: Next Generation WiFi,"
IEEE Communications Surveys & Tutorials, to appear.

[J5]. H. Zhou, **N. Cheng**, N. Lu, L. Gui, D. Zhang, Q. Yu, F. Bai, X. Shen, "WhiteFi Infostation: Engineering Vehicular Media Streaming with Geolocation Database,"
IEEE Journal on Selected Areas in Communications, to appear.

[J6]. L. Lei, Y. Kuang, **N. Cheng**, X. Shen, Z. Zhong, C. Lin, "Delay-Optimal Dynamic Mode Selection and Resource Allocation in Device-to-Device Communications - Part I: Optimal Policy,"
IEEE Transactions on Vehicular Technology, to appear.

[J7]. L. Lei, Y. Kuang, **N. Cheng**, X. Shen, Z. Zhong, C. Lin, "Delay-Optimal Dynamic Mode Selection and Resource Allocation in Device-to-Device Communications - Part II: Practical Algorithm,"
IEEE Transactions on Vehicular Technology, to appear.

[J8]. Y. Zhou, **N. Cheng**, N. Lu, and X. Shen, "Multi-UAV Aided Vehicular Networks: Challenges and Solutions",
IEEE Vehicular Technology Magazine, vol.10, no.4, pp.36-44, 2015.

[J9]. T. Yang, H. Liang, **N. Cheng**, R. Deng, and X. Shen, "Efficient Scheduling for Video Transmission in Maritime Wireless Communication Network,"
IEEE Transactions on Vehicular Technology, Vol. 64, No. 9, pp. 4215-4229, 2015.

[J10]. **N. Cheng**, N. Lu, N. Zhang, X. Shen, and J.W. Mark, "Vehicular WiFi Offloading: Challenges and Solutions,"
Vehicular Communications (Elsevier), Vol. 1, No. 1, pp. 13-21, 2014.

[J11]. N. Lu, **N. Cheng**, N. Zhang, X. Shen, J.W. Mark, and Fan Bai, "Wi-Fi Hotspot at Signalized Intersection: Cost-Effectiveness for Vehicular Internet Access,"
IEEE Transactions on Vehicular Technology, to appear.

[J12]. T. Yang, Z. Zheng, H. Liang, R. Deng, **N. Cheng**, and X. Shen, "Green Energy and Content Aware Data Transmission in Maritime Wireless Communication Network,"
IEEE Transactions on Intelligent Transportation System, Vol. 16, No. 2, pp. 751-762, 2015.

[J13]. N. Lu, **N. Cheng**, N. Zhang, X. Shen, and J.W. Mark, "Connected Vehicles: Solutions and Challenges,"
IEEE Internet of Things Journal, Vol. 1, No. 4, pp. 289-299, 2014.

[J14]. N. Lu, N. Zhang, **N. Cheng**, X. Shen, J.W. Mark, and F. Bai, "Vehicles Meet Infrastructure: Towards Capacity-Cost Tradeoffs for Vehicular Access Networks," **IEEE Transactions on Intelligent Transportation Systems**, Vol. 14, No. 3, pp. 1266-1277, 2013.

[J15]. N. Zhang, **N. Cheng**, N. Lu, H. Zhou, X. Shen, and J.W. Mark, "Risk-aware Cooperative Spectrum Access for Multi-Channel Cognitive Radio Networks," **IEEE Journal on Selected Areas in Communications**, Vol, 32, No. 3, pp. 516-527, 2014.

[J16]. **N. Cheng**, N. Zhang, N. Lu, X. Shen, J.W. Mark, and F. Liu, "Opportunistic Spectrum Access for CR-VANETs: A Game Theoretic Approach," **IEEE Transactions on Vehicular Technology**, Vol. 63, Issue 1, pp. 237-251, 2014.

[J17]. N. Zhang, N. Lu, **N. Cheng**, J.W. Mark, and X. Shen, "Cooperative Spectrum Access Towards Secure Information Transfer for CRNs," **IEEE Journal on Selected Areas in Communications**, Vol. 31, No. 11, pp. 2453-2464, 2013.

Conference Papers

[C1]. **N. Cheng**, N. Lu, N. Zhang, X. Shen, and J.W. Mark, "Opportunistic WiFi Offloading in Vehicular Environment: A Queueing Analysis," **GLOBECOM 2014** — IEEE Global Communications Conference, Austin, TX, USA, 2014. (**Best Paper Award**)

[C2]. H. Zhou, **N. Cheng**, N. Zhang, S. Wu, L. Gui, Q. Yu, X. Shen, and F. Bai, "Enabling Efficient and Wide-Coverage Vehicular Content Distribution over TV White Spaces," **WCSP 2015** — IEE International Conference on Wireless Communications and Signal Processing, Nanjing, Jiangsu, China, 2015. (**Best Paper Award**)

[C3]. L. Lei, H. Wang, X. Shen, **N. Cheng**, Z. Zhong, "Flow-Level Performance of Device-to-Device Underlaid OFDM Cellular Networks," **ICCC 2015** — IEEE International Conference on Computer and Communications, Chengdu, Sichuan, China, 2015. (**Best Paper Award**)

[C4]. T. Yang, **N. Cheng**, C. Yu, H. Feng, X. Shen, "Knowing who and when to deliver: An Optimal Stopping method for Maritime Data Scheduling,"
ICC 2015 — IEEE International Conference on Communications, accepted.

[C5]. N. Zhang, **N. Cheng**, N. Lu, H. Zhou, J.W. Mark, and X. Shen, "Cooperative Cognitive Radio Networking for Opportunistic Channel Access,"
GLOBECOM 2013 — IEEE Global Communications Conference, Atlanta, USA, 2013.

[C6]. **N. Cheng**, N. Lu, N. Zhang, X. Shen, and J.W. Mark, "Vehicle-Assisted Data Delivery for Smart Grid: An Optimal Stopping Approach,"
ICC 2013 — IEEE International Conference on Communications, Budapest, Hungary, 2013.

[C7]. N. Lu, **N. Cheng**, N. Zhang, X. Shen, and J.W. Mark, "VeMail: A Message Handling System Towards Efficient Transportation Management,"
WCNC 2013 — IEEE Wireless Communications and Networking Conference, Shanghai, China, 2013.

[C8]. N. Zhang, N. Lu, **N. Cheng**, J.W. Mark, and X. Shen, "Cooperative Networking Towards Secure Communications for CRNs,"
WCNC 2013 — IEEE Wireless Communications and Networking Conference, Shanghai, China, 2013.

[C9]. N. Zhang, N. Lu, **N. Cheng**, J.W. Mark, and X. Shen, "Towards Secure Communications in Cooperative Cognitive Radio Networks",
ICCC 2013 — IEEE/CIC International Conference on Communications in China, Xi'An, China, 2013.

Vita

Nan Cheng received the B.Sc. and M.Sc. degrees from Tongji University, Shanghai, China, in 2009 and 2012, respectively, both in electrical engineering. He is currently working toward the Ph.D. degree with the Department of Electrical and Computer Engineering, University of Waterloo, Waterloo, ON, Canada. His current research interests include resource allocation, performance analysis, and heterogeneous communications for vehicular networks.